THE PHYSICS AND CHEMISTRY OF SOLAR NEBULA SHOCK WAVES: APPLICATIONS TO CHONDRULE FORMATION

by

Fred John Ciesla

A Dissertation Submitted to the Faculty of the

DEPARTMENT OF PLANETARY SCIENCES

In Partial Fulfillment of the Requirements
For the Degree of

DOCTOR OF PHILOSOPHY

In the Graduate College

THE UNIVERSITY OF ARIZONA

2 0 0 3

UMI Number: 3089936

UMI®
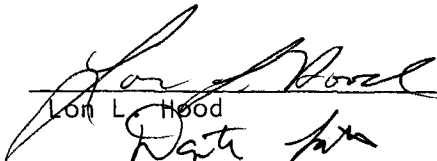
THE UNIVERSITY OF ARIZONA ®
GRADUATE COLLEGE

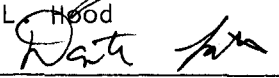As members of the Final Examination Committee, we certify that we have

read the dissertation prepared by Fred John Ciesla

entitled The Physics and Chemistry of Solar Nebula Shock Waves:
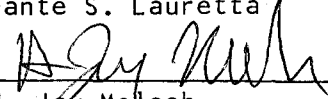
   Applications to Chondrule Formation

and recommend that it be accepted as fulfilling the dissertation

requirement for the Degree of Doctor of Philosophy

Lon L. Hood	Date 4/24/03
Dante S. Lauretta	Date 4/24/03
H. Jay Melosh	Date 4/24/03
William Hubbard	Date 4/24/03
William Boynton	Date 4/24/03
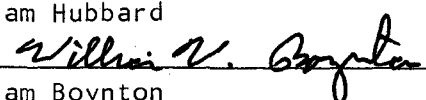
Final approval and acceptance of this dissertation is contingent upon
the candidate's submission of the final copy of the dissertation to the
Graduate College.

I hereby certify that I have read this dissertation prepared under my
direction and recommend that it be accepted as fulfilling the dissertation
requirement.

Dissertation Director Lon Hood   Date 5/6/03

STATEMENT BY AUTHOR

This dissertation has been submitted in partial fulfillment of requirements for an advanced degree at The University of Arizona and is deposited in the University Library to be made available to borrowers under rules of the library.

Brief quotations from this dissertation are allowable without special permission, provided that accurate acknowledgment of source is made. Requests for permission for extended quotation from or reproduction of this manuscript in whole or in part may be granted by the head of the major department or the Dean of the Graduate College when in his or her judgment the proposed use of the material is in the interests of scholarship. In all other instances, however, permission must be obtained from the author.

SIGNED: _____

Acknowledgements

This thesis would not have been possible without the support, encouragement, friendship, and love of a number of people. Unfortunately, space limits do not allow me to thank everyone who deserves it, and if you feel left out, I hope you can forgive me.

First of all, I must thank Lon Hood who was my advisor throughout the time I worked on this project. He pioneered the shock wave model for chondrule formation and supported me on his grant from the NASA Origins program. Also, Dante Lauretta served as a secondary advisor, helping me to understand meteorites and offering suggestions such as the investigation that led to Chapter 6 of this thesis. Thank you both for taking the time to teach me about how science is done.

I'd also like to thank all of the friends I've made at the University of Arizona who helped me get through the years of pain and frustration as well as joy and excitement. In particular, I want to thank David O'Brien and Jason Barnes for being great officemates. We created an environment where we could bounce ideas off of one another or ask for help on a particular math or prgramming problem. And we had the couch. I lived with Terry Hurford for most of the time I was a graduate student and not only was he the best roommate I ever had, but also the best friend. Thank you for everything, Terry–grad school would have been so much more difficult without you.

Lastly, I'd like to thank Carmen and Bob Henley for welcoming me into their family and encouraging me from Day 1. Wendy and Vinny Ciesla did nothing but support and love me for the 26.5 years leading up to this thesis, and they instilled in me the work ethic that I applied to this project and will apply to the rest of my career. And Nina, I love you so much. Thank you for putting up with me, helping me, and loving me. I can't imagine where I'd be without you.

TABLE OF CONTENTS

LIST OF FIGURES

LIST OF TABLES

ABSTRACT

Chondrules are a major component of primitive meteorites and are thought to be among the first solids to have formed in the solar system. However, the circumstances around the formation of chondrules have remained a mystery for the 200 years that chondrules have been known to exist. In this work, a model is developed to show that shock waves in the nebula could have been responsible for the complex thermal processing that chondrules are thought to have experienced. By studying different sizes of shock waves, it is shown that for shock waves to have been the dominant chondrule producing mechanism in the nebula, the shocks would have to be large (> 1000 km) in size. Such shocks may be linked to the formation or evolution of Jupiter within the solar nebula. In addition, the thermal evolution of chondrules by shock waves can explain the geometric properties of compound chondrules if these objects formed by the collisions of molten chondrules. Finally, for the first time, the case of a shock wave passing through an icy region of the solar nebula is studied. It is found that such a situation may have produced conditions that would allow silicates to be hydrated on very short time scales, explaining the presence of phyllosilicates in the accretionary rims around chondrules in CM chondrites.

CHAPTER 1

Introduction

Chondritic meteorites represent samples of the leftover building blocks of our solar system. Except for the most volatile elements, their elemental compositions closely match that of the sun and, thus, are believed to come from bodies which have remained relatively unaltered since the solar system formed. Therefore, understanding the makeup of these meteorites, and by extension, their parent bodies, will provide insights to the processes which were taking place during the birth of our solar system.

Chondrules, for which the chondritic meteorites are named, are major components of these meteorites (up to 80% by volume). Chondrules are silicate spheres which measure between 0.1 and 1 mm in diameter, and have evidence of being molten at some point in their histories. The popular theory, though not unanimous, is that chondrules formed in the solar nebula before being incorporated into their respective parent bodies. Our current understanding for how chondrules formed is as follows:

1. Dust grains condensed from the solar nebula as it cooled.

2. These dust grains collided and grew in size to form fractal aggregates.

3. These dust grains experienced some flash heating event which brought them from a relatively low temperature (<650 K because of the presence of primary troilite (Wasson, 1996)) to a peak temperature of 1700–2400 K (Connolly *et al.*, 1998).

4. Once these peak temperatures were reached, the particles cooled at rates between 10 and 1000 K/hr during the time of crystal growth. These rates are fast compared to the time that they would cool if radiating to free space, but slow compared to nebular cooling time scales.

5. As these particles cooled, or after they returned to their original temperatures, some accreted fine-grained rims composed of dust that was suspended in the nebula.

6. Some chondrules were recycled (repeated this process).

7. The chondrules and their rims were then accreted into larger bodies which became planetesimals.

Each of these particular stages in chondrule evolution will be discussed below. More complete reviews of chondrule formation can be found in Hewins (1997, and references therein) and Jones *et al.* (2000).

1.1 Location of Chondrule Formation

The location of chondrule formation has been debated for some time and can be thought of as having two possibilities: the solar nebula and on a parent body. Both locations have been argued, and neither is without its flaws. While the solar nebula is the most commonly accepted location, it is worth giving a brief review of the evidence for this interpretation. For detailed reviews see Taylor *et al.* (1983), Grossman (1988), or Boss (1996).

The oldest objects identified in the solar system are calcium-aluminum rich inclusions (CAIs), which have been dated to be 4.5672 +/- 0.0006 billion years old (Amelin *et al.*, 2002). Evidence from extinct radio-nuclides had suggested that chondrules formed 2-3 million years after the formation of CAIs, and no objects have been identified as being older (e.g. Swindle *et al.*, 1996, and references therein). This

has been supported by Pb-Pb dating of CAIs and chondrules by Amelin *et al.* (2002) who found that chondrules are 2.5 +/- 1.2 million years younger than CAIs. These radiometric ages imply that chondrules formed at a time before the solar nebula had dispersed (Podosek and Cassen, 1994). In addition, if chondrules formed on planetary bodies (e.g. by impacts) then their formation would likely have lasted much longer, and possibly still continue today.

When the oxygen isotopes of chondrules are plotted on a three isotope graph, they fall on a line with a slope greater than 0.52. A slope of 0.52 is what would be expected for mass-dependent isotope fractionation, and is what is found for a planetary body such as the Earth, moon, the parent body of the HED meteorites (Vesta, e.g. Drake (1979))) and the parent body of the SNC meteorites (Mars, e.g. Treiman *et al.* (2000)) (Clayton and Mayeda, 1983). Thus it is doubtful that planetary scale igneous processes could have been the sources of the melts from which chondrules formed. For the scenario where chondrules formed in the solar nebula, the data has been interpreted to be the result of oxygen isotope exchange between the chondrules and ^{16}O rich nebular gas (Clayton, 1981).

Finally, the spherical shape of chondrules implies that their shapes were controlled by the surface tension of a melt and could not have been incorporated into a solid body before crystallizing. If chondrules were molten for minutes to hours as has been inferred, they must have floated in gas or space for that period of time. This would not likely be the case if they formed on the surfaces of large planetary bodies, though this does not rule out collisions among small bodies.

Among the problems with chondrule formation due to collisions between small bodies is the lack of evidence for there being a "target planetesimal" (Taylor *et al.*, 1983). Melts that form in impacts would be of the same composition as the material that collided. Thus, the absence of objects composed of obvious target material would have to suggest that either all such planetesimals experienced collisions or are absent from our meteorite collection. Also, there is evidence that some chondrules experienced multiple events (as some relic crystals) (Wasson, 1996) or

igneous rims (Rubin, 2000), which may be difficult to form in impact melts.

The conclusion that chondrules formed while free-floating in the nebula is not accepted by all researchers (Sanders, 1996; Kitamura and Tsuchiyama, 1996). While a planetary or impact origin for chondrules has been argued for, these theories tend to have more difficulties than those that have chondrules forming in the solar nebula (Taylor *et al.*, 1983; Grossman, 1988; Boss, 1996). The goal of this work is to see if shock waves in the solar nebula can reconcile some of those problems associated with nebular formation models.

1.2 Initial Temperature of Chondrule Precursors

The initial temperature of chondrule precursors has been inferred from the minerals found within them that are believed to be primary, that is, those minerals that were contained within the precursors and survived the heating process. Particularly, many chondrules contain primary S (FeS), Na (Na_2O), and K (K_2O) in their centers and mesostases (Jones, 1990; Rubin, 2000). These three elements represent the most volatile major elements found in chondrules, and therefore help to constrain the thermal evolution of chondrules.

Particularly, for chondrules to contain primary troilite, it is believed that they must have originally been at temperatures below ~ 650 K (Wasson, 1996), where troilite would be incorporated into solids under standard solar nebula conditions. Thus, most models of chondrule formation have assumed that precursors were originally at some temperature below this, and this is the assumption made in this work as well. In reality, chondrule formation likely occurred over a range of distances from the sun in the solar nebula, and thus the initial temperature for chondrule precursors would not be a single value. Any model for chondrule formation should work for a range of initial temperatures.

Lauretta *et al.* (2001), while studying the behavior of S during the chondrule formation event, demonstrated that the temperature where sulfur would form troilite and be incorporated into solids can vary substantially over a range of possible conditions (concentration of solids and ambient pressure) in the solar nebula. Thus, it is possible that the initial temperature of the precursors was above 650 K, provided the nebular pressure and/or concentration of solids were above the canonical solar nebular values. It remains to be determined how plausible such a scenario would be prior to a chondrule forming event.

1.3 Duration of Heating and Cooling Rates

The duration and intensity of heating for chondrules cannot fully be divorced from a consideration of their cooling rates. In fact, the thermal histories of chondrules are sometimes discussed in terms of the length of time they were molten or in relation to their peak temperature over the time during which they were above their ambient temperature (Rubin, 2000; Jones *et al.*, 2000). The reason for this is because the inferred cooling rates for chondrules are based on studies whose results vary with the degree of heating the chondrules (or the chondrule environment) experienced. These thermal histories of chondrules have been deduced through studies of chondrule textures, volatile elements which survived the chondrule forming event, and the degree of melting which chondrules experienced (presence of relict grains).

Chondrule textures have been shown to be strongly dependent on the number of nucleation sites present within the chondrule melt from which crystals can grow as the melt cools (Lofgren, 1996). Porphyritic chondrules, which make up ~80% of all chondrules (Gooding and Keil, 1981), are formed when chondrules begin to cool with a significant amount of nucleation sites as compared to non-porphyritic (i.e. barred or radial) chondrules. A larger number of nucleation sites will survive provided the intensity of heating is low or if the temperature of the chondrule does not climb above its liquidus for long periods of time. This is why it

is thought that most chondrules experienced "flash heating," that is, experienced a short heating duration as opposed to a long one. This case is strengthened by the fact that volatile elements (S, Na, K) were retained by chondrules during the chondrule formation process. Wasson (1993) found that at a temperature of 1780 K, a 1 millimeter diameter chondrule would lose all of its Na in less than 30 seconds, though this time could be increased if the oxygen fugacity was significantly above the solar value (Tsuchiyama *et al.*, 1981).

The maximum (peak) temperatures reached by chondrules have been estimated by comparing synthetic chondrules produced in laboratories with real ones found in meteorites. Such temperatures can only be considered as estimates due to the fact that two chondrules of different compositions or having different distributions of grain sizes may exhibit different textures despite being exposed to the same heating conditions (Lofgren, 1996). The estimated range of chondrule peak temperatures is 1800 to 2200 K (Jones *et al.*, 2000), though temperatures as high as 2400 K have been suggested (Connolly *et al.*, 1998). If the peak temperature of a chondrule is high but maintained for only a short period of time, it may develop a similar texture as a chondrule which reached a lower peak temperature but was maintained at the temperature for a relatively long time (Jones *et al.*, 2000).

The cooling rates of chondrules during the time when they were molten also play a role in determining their textures. These, too, were initially studied by comparing the textures of synthetic chondrules cooled from a melt to those found in primitive meteorites (other methods have also been applied to further constrain the rates). A large number of experiments have been done which have considered a range of initial conditions for the original melt. These studies have been able to put some, although far from hard, constraints on the cooling histories of chondrules. Lofgren (1996) argued that chondrules with similar thermal histories could develop different textures if their initial grain sizes, or some other features, are slightly different and likewise similar textures in two chondrules could be developed even if they had very different thermal histories.

Thus, while the heating and cooling of chondrules have been studied in detail, there is a wide range of thermal histories that are believed to possibly lead to the observed chondrule textures and chemical zoning profiles. What can definitely be said is that the chondrules were brought from their initial temperatures to their peak temperatures, which were just below or slightly above their liquidus temperatures, on very short time scales (seconds to minutes). They then cooled on time scales which were short when compared to nebular time scales, but long when compared to the rate at which they would cool if radiating to free space. The cooling rates were likely between 10s to 1000s of Kelvin per hour as crystals grew. This cooling continued down to the ambient temperature of the nebula (Jones *et al.*, 2000).

1.4 Compound Chondrules

Some objects in meteorites have been identified as compound chondrules: two individual chondrules that have fused together. These objects were originally interpreted to be the result of collisions among plastic chondrules, and, thus, from the frequency of compounds the number density of chondrules during formation could be estimated (Gooding and Keil, 1981). Other authors have argued that the length of time during which chondrules were susceptible to collisions (the time during which they were molten) would be too short to account for the high frequency of compounds (Wasson *et al.*, 1995). These authors suggested an alternative method for formation where porous aggregates melted onto a preexisting chondrule, forming a secondary. Experiments and observations of pyroclastic melts argue that collisions were responsible for the formation of compounds, though the model of Wasson *et al.* (1995) has not been completely ruled out (Connolly *et al.*, 1994b; Lofgren and Hanson, 1997). Thus, whatever process was responsible for chondrule formation must account for the production of compound chondrules.

1.5 Chondrule Rims

Many chondrules are surrounded by fine-grained rims (FGRs) which consist of silicates, metal, and sulfides. These rims are thought to be dust particles that accreted onto the chondrules before parent body formation. The rims around some chondrules are found to get thicker with increasing size of the chondrules, which has been interpreted as evidence that chondrules, and their rims, formed close to where the final parent body formed (Morfill *et al.*, 1998). Other authors have argued this based on the chemical composition of the meteoritic components (Wood, 1985).

In some carbonaceous chondrites, particularly the CM meteorites, the FGRs contain phyllosilicate minerals, such as serpentine, which contains structural OH. While some authors have argued that these phyllosilicates are due to the reaction of liquid water with the rims on the parent body (Browning *et al.*, 2000), others argue that the phyllosilicates had to have formed prior to parent body formation (Metzler *et al.*, 1992; Lauretta *et al.*, 2000).

1.6 Summary

Chondrule ages, chemistry, and physical properties are consistent with their formation taking place in the solar nebula, the cloud of gas and dust from which our solar system formed. Had these objects never been observed, it is likely that models of the solar nebula would not have predicted their existence. The abundance of chondrules in primitive meteorites suggests that energetic events processed, perhaps multiple times, a majority of the solids in the inner part of the solar nebula. Thus chondrules provide the only clues to what these events were, how they operated, and how they affected the evolution of the solar nebula. This chapter presented a review of the properties of chondrules and the inferences that have been made from these properties about how these chondrules evolved. These properties will be important to keep in mind when evaluating the shock wave model for chondrule

formation.

CHAPTER 2

The Solar Nebula

As discussed in the previous chapter, chondrules provide insight into processes that occurred within the solar nebula and determined how it evolved. In order to fully understand the information chondrules provide, a general understanding of the solar nebula as a whole is needed. Over the last few years, thanks to increased modeling capabilities and detailed observations of disks around other stars, a greater understanding of the solar nebula has been achieved. The general picture is described below.

2.1 Formation and Evolution

The Milky Way is filled with clouds of gas and dust which engulf vast regions of space between the stars. It is from molecular clouds such as these that objects like our sun, and by extension the planets around them, form. These clouds are initially supported against gravity by the pressure of the gas within them, but if the pressure increases somewhere in the cloud, it may begin to collapse. The process which triggered the collapse of the molecular cloud from which our solar system formed is thought to be a supernova (Boss and Vanhala, 2000). Not only could the shock wave produced in the interstellar medium due to an exploding star trigger the collapse of the molecular cloud, but it may have injected a number of short lived radionuclides into that cloud. The evidence of such nuclides within solar system objects indicates that they must have been injected and incorporated into those bodies over time scales of less than a few million years (see Swindle *et al.*, 1996;

Wood, 2000b, and references therein).

As material from the cloud from which our solar system formed fell inward (toward the center of the cloud), most of it gathered in a dense ball at the center, the proto-sun. However, some of the material had too much angular momentum to fall to the center, and instead settled into orbits around the proto-sun. Due to the drastic increase in pressure associated with this collapse, the gas temperature would rise from $\sim$10 K to $\sim$1000s K. The hottest portion was the inner ball which eventually became hot enough to initiate hydrogen fusion and became the sun. The disk of material around the proto-sun was the solar nebula.

The evolution of the nebula can be broken up into two regimes (Wood, 1996). The first is a highly energetic stage as material from the interstellar region where the sun formed fell onto either the proto-sun or solar nebula. Much of the infall energy was converted to heat, and such evolution has been inferred by the infrared excesses observed around young stars (Wood, 1996). This stage of stellar evolution is thought to last less than 10^6 years (Beckwith *et al.*, 1990).

The second stage of evolution represents the time when the nebula still circled the sun, but the infall of interstellar material had ceased. It is during this stage that the nebula began to cool allowing solids to condense out of the gas and accrete into large objects. This is the latest stage at which the giant planets could have formed. This stage is thought to have lasted on the order of 10^7 years (Podosek and Cassen, 1994).

During the lifetime of the solar nebula, there are many processes that act to erode or consume it. If the disk is viscous (see below), angular momentum can be transferred within it, causing material to fall onto the star or move outwards from it. Other processes, such as photo-evaporation by UV light from a nearby star may remove the gas in the outer nebula (Hollenbach *et al.*, 2000). Whatever the exact cause or causes were, the gas in the nebula was removed leaving the giant planets and a debris disk full of solids which eventually formed the terrestrial

planets, asteroids, and Kuiper Belt.

2.2 Structure of the Nebula

As discussed above, the solar nebula evolved over its lifetime, and therefore its properties such as its mass, angular momentum, temperature structure, and pressure structure evolved as well. The ages of chondrules found by Amelin *et al.* (2002) suggests that chondrules formed during the quiescent (later) stage of nebular evolution, and thus it is the properties of the nebula at this time that are important to this work. Studies have looked at minor aspects of nebular evolution, such as the temperature structure or dynamics of solids within the nebular gas, but a complete model for the nebula has not been developed. Here, general properties of the nebula are discussed and some early fundamental work, along with some recent work, is reviewed.

2.2.1 Nebular Mass

The lowest mass that the nebula could have had would be the mass needed to form all of the planets, asteroids, and comets which orbit the sun. Weidenschilling (1977) calculated the minimum mass needed in a nebula to form all of the planets, provided they came from a gas of solar composition (therefore added hydrogen, helium, and other light elements back to the nebula in amounts determined by the composition of the planets). The total mass of the nebula determined in this manner is somewhere between 0.01 and 0.1 times the mass of the sun, where the range comes from uncertainty in the compositions of the giant planets. However, models for giant planet formation via gas accretion onto a solid core in a minimum mass nebula suggest that the time scale for Jupiter to form would be comparable to the expected lifetime of the nebula (Pollack *et al.*, 1996). While such a scenario is plausible, it requires that the nebula persisted for more than 10^7 years.

Thus, it has been proposed that the nebula was more massive than predicted by Weidenschilling (1977). Studies of giant planet formation by gravitational instabilities (Boss, 2000, 2002; Mayer *et al.*, 2002) have assumed disk masses between 0.08 and 0.1 times the mass of the sun. These values represent the mass contained between 4 and 20 AU in the nebula, and therefore cannot be directly compared to that of Weidenschilling (1977), who reported the nebular mass contained within 36 AU. Depending on how the nebular mass density varied with distance from the sun, which is relatively unconstrained (Cassen, 1994), the gravitational instability models assume nebular masses up to 3 times that of the minimum mass nebula.

The solar nebula is thought to have evolved through a wide range of masses, as it was likely more massive early on during its formation, and lost mass to accretion onto the sun. While the exact mass evolution of the solar nebula is unknown, values ranging from 0.01 to 0.3 solar masses have been used.

2.2.2 Pressure and Temperature Structures

The predominately gaseous nature of the solar nebula allows it to be studied with the same tools and methods as those used to study planetary atmospheres. As discussed by Wood (2000a), this idea is what drove some of the pioneering work in solar nebula studies, such as that by Lewis (1972). In this work, the nebular pressure and temperature are assumed to have an adiabatic relationship in the radial direction, as the Earth's atmosphere does in the vertical direction. While the observed density profile of solid bodies in the solar system follows the same trend as the equilibrium products which would condense out of such an adiabatic nebula, this structure was unlikely. Firstly, as discussed by Wood (2000a), the nebular gas was not supported radially by pressure alone, as an adiabatic atmosphere is, but also by angular momentum. Secondly, the nebula described by Lewis (1972) does not evolve with time. It represents just a possible snap shot at an unspecified time.

Since the work of Lewis (1972), a number of more detailed models describing

the pressure and temperature structure of the nebula have been developed. These models have treated the nebula as a "viscous accretion disk" (Wood and Morfill, 1988; Cassen, 1994, 2001). In these disks, the viscosity of the disks drives their evolution. Material closer to the sun orbits with a greater velocity than material further away. The resulting shear heats the gas and causes angular momentum to be exchanged. This angular momentum exchange causes the faster moving (inner) gas to slow down and fall inwards while the slower moving (outer gas) speeds up and migrates outwards.

The viscosity of the disk was likely enhanced by turbulence in the gas driven by temperature gradients (Wood and Morfill, 1988). Turbulence creates a viscosity, ν, in the nebula quantified by (Wood and Morfill, 1988):

$$\nu = K\ \alpha\ c\ H \tag{2.1}$$

where K $\sim$ 1, c is the local speed of sound, H is the nebular scale height, and α is a dimensionless parameter which quantifies the strength of turbulence in the gas. Assumed values for α range from 10^{-10} to $1/3$ (Wood and Morfill, 1988; Cuzzi *et al.*, 2001). Given such a nebula, the pressure and temperature structure can be derived by assuming hydrostatic equilibrium above the nebular midplane, and by balancing energy and momentum fluxes (Morfill, 1985).

2.2.3 Nebula Structure Used in this Work

As just described, the structure of the solar nebula can be derived using the basic physical ideas of energy and momentum balance. This structure, however will depend strongly on the assumed initial parameters, including the value chosen for α, the accretion rate onto the sun, and the dependence of nebular opacity with temperature Wood (2000a). It is beyond the scope of this work to review all published considerations, especially with the large uncertainties associated with the assumptions.

The general results of studies of solar nebula structure are important for this work, however, especially the particular values of pressure and temperature that would have existed during chondrule formation. As reviewed by Wood (2000a), models predict that over the lifetime of the nebula, the asteroid belt region could have experienced temperatures between 150 to 1000 K, with cooler temperatures being expected after the sun had ceased to accrete material. This same region would have reached pressures between 10^{-4} and 10^{-7} bars, again with lower pressures being expected after the sun had stopped accreting material.

It is unclear exactly what the conditions of the nebula were in this region during chondrule formation (though, as discussed in Chapter 1, some inferences have been made). This is due to the uncertainty of the exact stage of evolution the nebula was in during chondrule formation. The work presented here does not explore all possible scenarios, but rather presents models using reasonable assumptions of the state of the nebula during chondrule formation. These assumptions are discussed when used, and a detailed discussion of this work and how it depends on these assumptions is presented in the Conclusions chapter.

2.3 Evolution of Solids in the Solar Nebula

The solid objects found in the solar system and their components went through many stages of processing before their formation was complete. These different stages have been studied in detail, but due to the complexities involved, it is generally assumed that each stage ends before the next begins. For example, many of the solids in the nebula formed by condensing out of the nebular gas as it cooled. These objects then grew over time due to collisions and sticking to form the first planetesimals. In this planetesimal building stage, the nebula is often assumed to be filled, uniformly, with micrometer-sized dust (Weidenschilling, 2000). Such treatments allow the general ideas of accretion and coagulation to be studied and reduces the problem to something that can be studied in reasonable time scales. However, it

does neglect some possibly important effects. For example, as solids formed in the nebula, they would become the dominant source of its opacity. Therefore, the solids would control the thermal structure of the nebula, which in turn would determine which, and how many, solid species would form. Thus, solids likely existed and began to coagulate while other solids were still forming. This does not invalidate the work done, but rather demonstrates how difficult it is to build a comprehensive model for the evolution of solids in the nebula.

Nonetheless, much has been learned through these studies about how solids formed and grew into the objects found in the solar system today. As mentioned, many of the solids in the solar system originally formed as the nebula cooled and the more refractory species condensed out of the nebular gas. In the terrestrial planet region of the nebula, the solids were composed mostly of rock and metals, while further out in the nebula ices were also incorporated into the solids. In the inner part of the nebula, the average ratio of the mass density of condensable material to nebular gas is thought to be about 0.005. When water ice condenses as well, the ratio increases to be 0.01.

In the absence of gas, solid particles would have orbited the sun in Keplerian orbits. However, the gas in the nebula, due to the radial pressure gradient, orbited the sun at slightly less than Keplerian speeds. The resulting drag on the solids due to this velocity differential, caused them to spiral inwards towards the sun (Adachi *et al.*, 1976). This effect decreased as the solids began to coagulate and grow in size.

The solid particles in the nebula were also subjected to a gravitational force which pulled them towards the midplane of the nebula. In a low mass nebula, this gravitational force would just be a component of the gravitational force from the sun, though the gravity from the nebula itself would be important if it was more massive. This gravitational force would cause solid particles to settle towards the midplane, concentrating them at densities greater than the canonical solar value. This would result in an increased coagulation rate of the solids, and lead to more

rapid growth of planetesimals.

However, if the nebula was especially turbulent, then this settling of solids may have been limited. Turbulence may have been caused by convection due to the temperature gradient above the midplane (Cuzzi *et al.*, 2001) or due to the shear between the particle-rich midplane layer and the surrounding gas (Weidenschilling, 1988). In the case of shear induced turbulence, it may act as a self-regulating process such that it would prevent the concentration of solids at the midplane from reaching values much greater than 100 times the canonical value unless the solids began to accrete into large bodies (Weidenschilling, 2002). In the case of convective turbulence studied by Cuzzi *et al.* (2001), solids may be kept from settling to the midplane unless they either grew in size or got concentrated between convective cells at substantially high values. These authors found that such a nebula could create zones where the solids were enhanced by up to 10^5 times the canonical solar value. Once these objects made it to the midplane, they would begin to be accreted into planetesimals (Weidenschilling, 1988).

Thus, at any given time the concentration of solids could have ranged from the canonical solar value to many orders of magnitude above that. The occurrence of compound chondrules and fine-grained rims suggests that some episodes of chondrule formation took place in regions where the solids were concentrated above the solar value. The size distribution of these solids is not clear, although they likely were predominately chondrule sized objects and smaller.

2.4   Transient Processes

Thus far in the outline of solar nebular evolution, no episodes of heating which would have formed chondrules have been mentioned. As stated earlier, had chondrules never been observed, the processes which formed them may not have been predicted. Thus, they are clues to high energy mechanisms that would have been overlooked.

A large number of mechanisms for producing chondrules have been proposed. Currently, no mechanism is without its flaws, though some have more serious flaws than others. As a result, a number of these mechanisms have been dismissed, leaving only three that are currently being considered as plausibly forming chondrules. For detailed reviews of the advantages and disadvantages of the different proposed mechanisms, the reader is referred to Boss (1996), Jones *et al.* (2000), and Rubin (2000). Below the three mechanisms which are currently being considered by the meteoritic and astrophysical communities are reviewed.

2.4.1 Lightning

Lightning, as seen in terrestrial thunderstorms, represents a mechanism by which large amounts of energy are released over a very short period of time. As mentioned above, the gaseous nature of the nebula has led many to draw comparisons to planetary atmospheres. Thus, it was proposed that lightning in the solar nebula may have released energy quickly enough to flash heat the silicate particles nearby and form chondrules.

In order for lightning to occur, charges must be separated over large distances. In the atmosphere of the Earth, this is achieved by collisionally charging water particles in clouds and then allowing them to separate due to graviational forces. Once the electric field across this separation becomes strong enough, it ionizes the atmosphere between the charges, and a lightning bolt is released (Gibbard *et al.*, 1997).

A similar scenario for the solar nebula has been proposed. Collisions among dust or ice particles could occur which would allow charges to be exchanged, and then gravitational settling to the midplane would separate these charged particles. This possibility was investigated by Gibbard *et al.* (1997), who concluded that lightning would be very difficult to produce in the nebula. They argued that before significant charge separation would occur, the large conductivity of the nebular gas,

due to ionization from radioactive decay, would short circuit the charge build up. Desch and Cuzzi (2000) argued that grains could be charged through a process called *triboelectric charging*, which allows charges to be transferred in collisions among particles due to the differences in the contact potentials of the colliding materials. If these particles were then separated into large clumps (with solids concentrated at $\sim 10^4$ times the canonical solar value) as predicted by Cuzzi *et al.* (2001), then lightning may have been possible. However, these authors point out that such a charging mechanism has not been shown to operate between materials expected to make up chondrules, nor was it absolutely certain that the nebula would not short circuit the charge separation.

Even if lightning did exist in the nebula, it is not clear it could thermally process chondrules as outlined in Chapter 1. Horanyi *et al.* (1995) modeled the heating of silicate particles by lightning, and found that it could indeed rapidly heat such particles that had sizes equal to those of chondrules. However, the cooling rate of these particles would have been roughly 1000 K/s, over 3 orders of magnitude greater than what is expected for chondrules. These authors suggested that if this event took place in an optically thick region of the nebula, then the cooling rates may fall more in line with the experimentally determined rates. However, as shown in Hood and Ciesla (2001), in order for this to happen, with favorable assumptions, large volumes of the nebula would have to be enhanced with dust over the solar value by factors of 10^3 or higher, provided that chondrules are embedded in a cloud of dust. These are opposite to the conditions believed to be needed to produce lightning.

Thus, while lightning has long been considered a possible chondrule forming mechanism, it has serious shortcomings.

2.4.2 X-Wind

The X-wind model for chondrule formation is attractive because it is based on a theory which has been able to explain many observations of disks around young stars. In this model, as discussed by Shu *et al.* (1996), winds driven by the interaction of the accretion disk (the solar nebula) with the magnetosphere of the sun launch particles upwards out of the solar nebula. As they are launched upwards, following trajecotries which make the shape of an 'X' centered on the sun, the particles are exposed to an increased amount of electromagnetic radiation from the young star, which causes them to melt. The particles move through this radiation bath along a parabolic trajectory, falling back onto the disk where they are incorporated into planetesimals.

The particles that are launched in this model form in the disk and migrate inwards due to gas drag. Only when they get close to the sun do they get launched in the jets described above. An issue that the X-wind model has yet to explain is how the chondrule precursors manage to retain their primary volatiles throughout this process. As the precursors migrated close to the jets (located approximately 15 stellar radii away from the sun (Shu *et al.*, 1996)), the temperature of the nebula would rise well above 650 K, the temperature at which troilite is stable. Unless the solids moved through this hot region very quickly, this model would not be able to explain the presence of primary troilite or other volatiles.

Another issue associated with the X-wind model is that the conditions needed to heat chondrules to their melting points are not expected to normally be reached. Thus in order to melt magnesium-iron silicates the X-wind model requires special circumstances which are somewhat speculative (Shu *et al.*, 1997). In addition, it is unclear at what rate these silicates would cool after reaching their peak temperature.

Finally, there are a number of issues surrounding the plausibility and our understanding of the X-wind phenomena. A prediction of the X-wind models is that

there would be a large number of energetic particles near these jets that would allow the short-lived ^{26}Al to be created locally in the nebula, explaining the differences in ages between CAIs and chondrules. However, Amelin *et al.* (2002) has found that CAIs and chondrules formed millions of years apart, proving that a local source of ^{26}Al did not exist or at least was not significant. The fact that predictions of the X-wind model disagree with what is found in meteorites implies that our understanding of the X-wind model is incomplete.

Thus, the X-wind model also has a number of issues that still must be investigated and addressed before it can be considered a dominant chondrule formation mechanism.

2.4.3 Nebular Shocks

In recent years, shock waves have become the mechanism with the most support from the astrophysical and meteoritical communities for forming chondrules (Hewins, 1997). As this mechanism is the focus of this thesis, only the results up until 1999, when this project began, will be discussed. Over the last few years, a number of discoveries have added support for the shock wave model and a number have presented problems. Thus, recent work will be discussed as this work is presented and discussed in detail in the Conclusions chapter.

Hood and Horanyi (1991) proposed that shock waves within the nebula could have been responsible for processing silicates in a manner that formed chondrules. The idea can be described as follows. First, a gas dynamic shock wave passed through the solar nebula. As the nebular gas passed through the shock front, its temperature and density increased, but its velocity with respect to the shock front decreased. These properties changed as predicted by the Rankine-Hugoniot relations Landau and Lifshitz (1987). The solids that were suspended within the gas passed through the shock front unaffected. Thus, while upstream from the shock

the particles were in thermal and dynamical equilibrium with the gas (same temperature and no relative velocity), the two species were out of equilibrium immediately behind the shock front. As the solids sped through the slower moving gas, they gained thermal energy from the gas, but lost momentum due to gas drag. As the solids slowed to the speed of the gas, the energy input from collisions with the gas molecules decreased and the solids began to cool.

The scenario described above is very similar to the way that meteorites are heated in the Earth's upper atmosphere (Rizk *et al.*, 1991). It is from this area of study, along with treatments of the heating of particles in a cometary coma (Gombosi *et al.*, 1986), that the original equations used in the study of Hood and Horanyi (1991) were obtained. These authors showed that millimeter sized silicate grains can be heated to their melting temperatures on very short time scales, consistent with what had been inferred for chondrules, by shock waves moving through the asteroid belt region of the solar nebula at speeds of 5 to 7 km/s.

Hood and Horanyi (1993) investigated how shock waves would process millimeter-sized silicate spheres if they were contained in a large cloud of such particles. These authors thus improved upon their earlier work by no longer considering how a single particle would be processed in a shock wave, and instead considered how they would be heated if they were surrounded by similar particles. This would allow particles to be heated by the radiation from other particles in the nebula. These authors found that such a scenario required slightly weaker (slower moving) shock waves to melt the silicates than in their previous study.

In these two studies, the authors did not specify what the source of their shocks were, though they, and many authors since, speculated as to what the sources may be. Some possible mechanisms include shocks created by the supersonic accretion of material onto the solar nebula (Ruzmaikina and Ip, 1994; Hood and Kring, 1996); spiral density waves in the early, accretional stage of the solar nebula (Wood, 1996), a gravitational instability which grew to become Jupiter (Boss, 1998), and supersonic planetesimals moving through the nebular gas (Hood, 1998;

Weidenschilling *et al.*, 1998).

The lack of a definite shock source has proven to be the major fault in the shock wave model. While a number of possibilities have been suggested, they have not been fully tested. In addition, while shock waves are known to be capable of melting silicates in a manner consistent with how chondrules were thought to be melted, it remained to be seen if these same particles would cool at the rates chondrules are thought to have cooled. Thus, while shock waves are a promising theory, much still needs to be studied before they can be considered to be the dominant chondrule forming mechanism that operated in the solar nebula.

2.5 Summary

Because chondrules formed in the solar nebula, it is important to understand its structure and evolution before determining what additional information chondrules can provide about it. As such, the region of the solar nebula where chondrules formed could have experienced a wide range of temperatures and gas pressures and contained a concentration of solids that varied between the standard solar value and orders of magnitude higher. Thus, whatever formed chondrules likely operated under a wide range of conditions.

While a number of chondrule forming mechanisms have been proposed, none are without flaws. Of all the mechanisms, shock waves are considered the leading candidate among meteoriticists and astrophysicists, though a number of issues must still be addressed. In Chapter 3 of this thesis, a shock wave model for processing silicates in a particle-gas suspension is developed and applied to silicates within the solar nebula. In Chapter 4, this shock wave model is modified to consider small-scale shocks of the type that may be produced by supersonic planetesimals in the solar nebula. Chapter 5 investigates the frequency and properties of compound chondrules and discusses how they can be explained in the shock wave model. Chapter 6 presents a more detailed version of the shock wave model which

considers how silicates would be processed in icy regions of the solar nebula allowing for chondrules and hydrated rims (such as those found in CM chondrites) to be formed in the same event in the solar nebula. In the Conclusions chapter, this work is reviewed and discussed along with recent work by other authors.

CHAPTER 3

Shock Processing of a Particle-Gas Suspension

3.1 Introduction

Previous studies of chondrule formation in shock waves have shown that 1 mm diameter silicate particles can be heated in a manner which is consistent with the rates inferred for chondrules (Hood and Horanyi, 1991, 1993; Hood, 1998). These studies did not, however, consider in detail the behavior of the particles after heating to see if their cooling rates also matched those that have been inferred for chondrules. Also, in calculating the thermal and kinetic evolution of these spheres, it was often assumed that the energy and momentum transferred to the particle by the shocked gas was small compared to the total energy and momentum of the gas.

However, the cooling histories of chondrules have been studied in detail (Radomsky and Hewins, 1990; Lofgren, 1996; Yu and Hewins, 1998; Connolly *et al.*, 1998), and models for chondrule formation must reproduce these cooling rates in order to be considered viable. Because this requires extending the above models of gas-solid interactions behind a shock wave, it is necessary to consider in detail these interactions. Also, it has been argued that chondrules formed in regions of the nebula where solids were concentrated at or above the solar ratio Gooding and Keil (1981); Radomsky and Hewins (1990); Lauretta *et al.* (2001); Hood and Ciesla (2001). Thus, the assumption that the energy and momentum transferred to the solids from the shocked gas is small is not necessarily valid.

In the next section a new model for the processing of a particle-gas suspension by a shock wave is developed and applied to study the formation of chondrules

in the solar nebula. Different cases, believed to be plausible for the solar nebula, are then studied using this model. The results of these simulations and their implications for chondrule formation are then discussed.

3.2 The Model

The effects of a shock passing through a particle-gas suspension have been studied in some detail by Igra and Ben-Dor (1980). In their model, they consider a suspension initially in thermal and kinetic equilibrium (the particles and gas are at the same temperature and there is no relative velocity between the two species). Upon passage through the shock front, the temperature, velocity, and density of the gas change in a way given by the Rankine-Hugoniot relations. The particles, however, pass through the shock front unaffected. Immediately behind the shock front, there is a state of disequilibrium between high temperature-low velocity (with respect to the shock front) gas and low temperature-high velocity particles. Over some distance, termed the "relaxation zone", energy and momentum are exchanged between the two species until a new state of equilibrium is established. Due to these exchanges, the temperature of the gas is increased due to the loss of the particle kinetic energy.

Igra and Ben-Dor (1980) considered only the cases of shocks propagating through the lower terrestrial atmosphere, that is, at gas densities many orders of magnitude greater than expected for the solar nebula. In addition, these authors did not allow for phase transitions of the particles in the suspension nor did they account for the exchange of radiation between the particles. Therefore, in order to formulate a model for studying the effects of a shock wave processing solids in the solar nebula, several modifications are necessary.

Firstly, at the lower shocked gas number densities ($< 3 \times 10^{16}$ cm^{-3}) appropriate for the solar nebula, the assumption of free molecular flow (mean free path much greater than dust particle size) is valid. Gas-particle energy transfer

rates can therefore be calculated using analytic expressions that depend on the gas-particle relative velocity and the temperatures of the particles and the gas (Gombosi *et al.*, 1986; Hood and Horanyi, 1991). Secondly, because Igra and Ben-Dor (1980) considered a higher-density gas, the length of the relaxation zone was only on the order of a few meters. In this study, the distance over which equilibrium between the chondrules and gas is achieved can be on the order of thousands of kilometers. Thus, the radiation flux that a particle would be exposed to could vary significantly during its evolution and therefore a detailed consideration of how this flux changes with distance is required. While this was addressed in Hood and Horanyi (1993), a complete model should not make any assumptions about the temperatures of the particles, but rather should calculate a radiation flux based on their actual temperature profile, including the warming of the particles upstream from the shock. Thirdly, particles must be allowed to melt as they are heated and crystallize as they cool because of the fundamental importance of these processes in chondrule formation.

In order to formulate a chondrule formation model for the thermal and dynamical evolution of a particle-gas suspension during passage of an adiabatic shock wave, a series of simplifying assumptions must be adopted (following Igra and Ben-Dor 1980):

1. Solids are present in the suspension only as chondrules or chondrule precursors, i.e., no micron-sized dust is present ('precursor' refers to the solids upstream from the shock front, 'chondrule' to those downstream, and 'particle' will be used to refer to both);

2. The particles are rigid, chemically inert, identical spheres distributed uniformly throughout the gas;

3. Particles do not physically interact with each other except for the exchange of radiative energy and the total particle volume is negligible compared to the gas volume;

4. At large distances ahead of the shock, the chondrule precursors are in a state of thermal and dynamical equilibrium with the gas;

5. The temperature within each particle is uniform;

6. Particle weight and buoyancy forces are negligible and the particles are too large to experience Brownian motion in the gas.

7. The gas properties change across the shock front in a way given by the jump conditions:

$$\frac{T_2}{T_1} = \frac{[2\gamma M^2 - (\gamma - 1)][(\gamma - 1)M^2 + 2]}{[(\gamma + 1)^2 M^2]} \tag{3.1}$$

$$\frac{n_2}{n_1} = \frac{(\gamma + 1)M^2}{[(\gamma - 1)M^2 + 2]} \tag{3.2}$$

$$\frac{v_2}{v_1} = \frac{n_1}{n_2} \tag{3.3}$$

where T, n, and v represent the gas temperature, number density and velocity with respect to the shock front, the subscripts 1 and 2 represent the values immediately before and after the shock, respectively, γ is the ratio of specific heats of the nebular gas, and M is the ratio of the speed of the gas with respect to the shock front to the speed of sound in that gas immediately before passage through the front.

For the above assumptions, the steady-state equations of mass, momentum, and energy conservation, in a frame of reference moving with the shock front, may be written in the form (following Igra and Ben Dor 1980),

$$\frac{d}{dx}(n_{H_2} v_g) = -\eta_{H_2} \tag{3.4}$$

$$\frac{d}{dx}(n_H v_g) = 2\eta_{H_2} \tag{3.5}$$

$$\frac{d}{dx}(\rho_c v_c) = 0 \tag{3.6}$$

$$\frac{d}{dx}\left(\rho_g v_g^2\right) + \frac{dP}{dx} = -F_D \tag{3.7}$$

$$\frac{d}{dx}\left(\rho_c v_c^2\right) = F_D \tag{3.8}$$

$$\frac{d}{dx}\left[\left(C_v^{H_2}T_g + C_v^H T_g + \frac{1}{2}v_g^2\right)\rho_g v_g + P v_g\right] = -Q_{gc} - F_D v_c - Q_{gd} \tag{3.9}$$

$$\frac{d}{dx}\left[\left(C_c T_c + \frac{1}{2}v_c^2\right)\rho_c v_c\right] = Q_{gc} + Q_{cc} - Q_{cr} + F_D v_c \tag{3.10}$$

where x is the one-dimensional spatial coordinate, n_{H_2} and n_H are the number densities of molecular and atomic hydrogen, η_{H_2} is the rate at which hydrogen molecules dissociate, ρ_g and ρ_c are the respective mass densities of gas and particles in the suspension, v_g and v_c are the corresponding velocities with respect to the shock front, T_g and T_c are the corresponding temperatures, $C_v^{H_2}$, C_v^H and C_c are the corresponding specific heats (at constant volume for the gas species), P is gas pressure, F_D is the drag force per unit volume acting on the particles, Q_{gc} is the rate of energy transfer from the gas to the particles per unit volume due to gas drag and thermal collisions, Q_{gd} is the rate of energy lost from the gas due to the dissociation of hydrogen, Q_{cc} is the rate of radiative energy transfer to particles from other particles per unit volume, and Q_{cr} is the rate of energy loss by radiation from the particles per unit volume. Equations (3.4-6) are the continuity equations for the gas species and chondrules. Equations (3.7) and (3.8) represent the equations describing the exchange of momentum between the gas and chondrules, where the only exchange is due to the drag force arising from the different velocities between the two species. Equations (3.9) and (3.10) describe the evolution of energy for the gas and chondrules respectively. In (3.10), the last term on the right hand side represents the effect of gas drag on the rate of particle kinetic energy density change in a frame of reference moving with the shock front. In (3.9), an equal and opposite term is on the right hand side to account for the effect on the gas. Note that no radiation exchange terms appear in the gas energy equation (3.9). This will be discussed below.

Hydrogen molecules are assumed to dissociate through the reaction
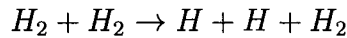
$$H_2 + H_2 \rightarrow H + H + H_2$$

with a forward reaction rate, $k^f_{H_2 H_2}$, and the backward reaction rate $k^b_{HHH_2}$, and the

reaction

$$H + H_2 \rightarrow H + H + H$$
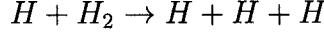
with a forward reaction rate, $k_{HH_2}^f$, and the backward reaction rate k_{HHH}^b. The values for these reaction rates were given by Iida *et al.* (2001). The total rate of hydrogen dissociation is then

$$\eta = k_{H_2H_2}^f n_{H_2} n_{H_2} - k_{HHH_2}^b n_{H_2} n_H n_H + k_{HH_2}^f n_H n_{H_2} - k_{HHH}^b n_H n_H n_H \qquad (3.11)$$

and the energy lost due to dissociation is:

$$Q_{gd} = E_{diss} n_{H_2} \left(k_{H_2H_2}^f n_{H_2} + k_{HH_2}^f n_H \right) \qquad (3.12)$$

where E_{diss}=4.48 ev is the binding energy of the hydrogen molecule.

In (3.7-10), the drag force per unit volume is expressed as (Igra and Ben-Dor, 1980):

$$F_D = -\frac{1}{2}\rho_g \left(v_c - v_g \right) |v_c - v_g| C_D \frac{\pi}{4} D^2 n_c \qquad (3.13)$$

where D is the particle diameter, n_c is the particle number density, and C_D is the drag coefficient. For the special case of perfectly elastic collisions of gas molecules and particles, the drag coefficient $C_D \simeq 2$ (Whipple, 1950). For more realistic conditions, C_D depends on the temperature of the gas and the relative velocity of the particles with respect to the gas (Gombosi *et al.*, 1986):

$$C_D = \frac{2}{3s} \left(\frac{\pi T_c}{T_g} \right)^{\frac{1}{2}} + \frac{2s^2 + 1}{s^3 \sqrt{\pi}} \exp\left(-s^2 \right) + \frac{4s^4 + 4s^2 - 1}{2s^4} \mathrm{erf}\,(s) \qquad (3.14)$$

where s is the ratio of the velocity of the chondrule with respect to the gas to the thermal velocity of the gas.

As noted above, the free molecular flow approximation is adopted, which is valid for millimeter-sized particles in a hydrogen dominated gas provided that the number density of gas molecules is less than about 3×10^{16} cm^{-3} (Hood and Horanyi, 1991). In this approximation, the rate of thermal energy transfer from the gas to the particles per unit volume is given by (Gombosi *et al.*, 1986):

$$Q_{gc} = \pi D^2 n_c \rho_g |v_c - v_g| \left(T_{rec} - T_c \right) C_H \qquad (3.15)$$

where T_{rec} is the adiabatic "recovery" temperature (defined as the particle temperature at which thermal heat transfer is zero) and is given by:

$$T_{rec} = T_{gas} \left(\frac{\gamma - 1}{\gamma + 1}\right) \left[\frac{2\gamma}{\gamma - 1} + 2s^2 - \left(\frac{1}{2} + s^2 + \frac{s}{\sqrt{\pi}} \exp\left(-s^2\right) \mathrm{erf}^{-1}(s)\right)^{-1}\right]$$

$$(3.16)$$

and C_H is the heat transfer function, or Stanton number, given by:

$$C_H = \frac{\gamma + 1}{\gamma - 1} \frac{k}{8\overline{m}s^2} \left[\frac{s}{\sqrt{\pi}} \exp\left(-s^2\right) + \left(\frac{1}{2} + s^2\right) \mathrm{erf}(s)\right] \qquad (3.17)$$

where γ is the ratio of the specific heats of the gas, k is Boltzmann's constant, and $\overline{m}$ is the mean molecular mass of the gas. Because there is more than one species in the gas, the energy transfer for each species is calculated and summed together to find the total amount of energy transfered to the solids.

As discussed earlier, previous treatments of radiation exchange among the chondrules by Hood and Horanyi (1993) considered only exchange of radiation between chondrules in a relatively small volume. A more correct treatment in this model would use principles of radiative transfer (Desch and Connolly, 2002) to find Q_{cc} and Q_{cr}. The details of this topic have been addressed in detail by many authors (Mihalas, 1970; Ozisik, 1977; Collison and Fix, 1991; Tanaka *et al.*, 1998). For the purposes of this work, all effects in the radiative transfer that are dependent on the frequency of the radiation are ignored and the typical "grey" case is considered.

The equation of transfer in this case is:

$$\mu \frac{dI}{d\tau} = I - S \qquad (3.18)$$

where I is defined as the specific intensity of the radiation at a given point in space, τ is a measure of optical depth into the suspension, S is the source function of the radiation from the particles, and μ is equal to $\cos\theta$ where θ is the angle between the direction the radiation is traveling and the normal to the surface that we are considering. The equation of transfer has a solution (Mihalas 1970):

$$
\begin{aligned}
I\left(\tau_1, \mu\right) = {} & I\left(\tau_2, \mu\right) e^{-\frac{(\tau_2-\tau_1)}{\mu}} + I\left(0, \mu\right) e^{-\frac{\tau 1}{\mu}} \\
& + \int_{\tau_1}^{\tau_2} S\left(t\right) e^{-\frac{t-\tau_1}{\mu}} \frac{dt}{\mu} + \int_0^{\tau_1} S\left(t\right) e^{-\frac{\tau_1-t}{\mu}} \frac{dt}{\mu}
\end{aligned} \tag{3.19}
$$

Here τ_1 represents the optical depth at which the specific intensity is calculated and τ_2 is the optical depth at the end of the region being considered ($\tau=0$ represents the distance upstream of the shock where the integration begins). Following Tanaka *et al.* (1998), the silicates (i.e., the chondrules) are considered as the only opacity source, and thus the source function is equal to the Planck function integrated over all frequencies (see below). In the case of a one-dimensional shock such as that considered here, integrating over all μ gives the specific intensity as a function of optical depth, or $\overline{I}\left(\tau\right)$.

Using (3.19), the specific intensity can be found at any point in the suspension, provided the temperature is known everywhere. At large distances in front of the shock, the chondrule precursors are assumed to be at the same temperature as the gas, and this dictates the first boundary condition. The second boundary condition makes the same assumption that the chondrules very far behind the shock are at a constant temperature equal to the initial temperature of the suspension, the exact position at which this temperature is re-established is found by the integrations. (The basis for this assumption is that, if this region of the nebula did not contain the shock, the temperature everywhere would be the same as determined by blackbody heating from the sun. Thus the shock represents a finite disturbance to this situation, where the thickness of the shock is greater than the distance it takes for the system to cool back down to its original temperature.) For the particles closer to the shock front, the temperature profile will vary with position. In this case, the integrations are calculated numerically.

Once $\overline{I}$ is known at a given position, the amount of radiative energy absorbed by the particles per unit volume per unit time can be found using equation

(1-18) of (Mihalas, 1970):

$$dE = \kappa \, \overline{I} \, d\omega \, dt \, \rho_c \, dA \, ds \tag{3.20}$$

This equation gives the amount of energy absorbed, dE, from a beam passing through a volume of cross section dA and length ds per time dt. The $d\omega$ represents the infinitesimal solid angle that the beam originates from and can be written $\sin\theta d\theta d\phi$, where θ is defined as above, and ϕ is the corresponding azimuthal angle. Using our definition from above for μ, we can write, for an azimuthally symmetric case:

$$d\omega = 2\pi d\mu \tag{3.21}$$

Thus Q_{cc}, which is the amount of energy absorbed per unit volume per unit time, can be defined as::

$$dQ_{cc} = \frac{dE}{dA \, ds \, dt} \tag{3.22}$$

This requires knowing the absorption coefficient, κ, for the particles, given by:

$$\kappa \quad = \quad \frac{\pi D^2 \varepsilon_{abs}}{4m_c} \tag{3.23}$$

where ε_{abs} is the frequency averaged absorptivity of the particles and m_c is the mass of a particle. This gives:

$$Q_{cc} \quad = \quad \int \rho_c \kappa \overline{I} \, (\tau) \, d\omega \tag{3.24}$$

Similarly, the amount of energy added to a beam of radiation is given by (Mihalas 1970):

$$dE = j \, d\omega \, dt \, \rho_c \, dA \, ds \tag{3.25}$$

This allows Q_{cr} to be defined as:

$$Q_{cr} = \int j \, \rho_c \, d\omega \tag{3.26}$$

If the particles are assumed to be in equilibrium with the radiation field, then

$$j = \kappa \int_0^\infty B_\nu \, (T) \, d\nu \tag{3.27}$$

where B_ν (T) is the Planck function. Thus:

$$Q_{cr} = 4\rho_c\kappa\sigma T^4 \tag{3.28}$$

Because the radiation calculations require knowledge of the temperature of the particles throughout the suspension, the temperatures of the chondrules are initially calculated after they pass through the shock front based on the other modes of heat transfer. The calculations are repeated, using the temperature profile from this first run to calculate the radiation flux through the suspension. This procedure is repeated until the temperatures of the particles do not change by more than 1 K.

The optical properties of the gas are ignored in this treatment, and thus radiative cooling due to rotational and vibrational transitions of molecules have been neglected. While these processes have been studied by previous authors (Ruzmaikina and Ip, 1994), in the future they should be considered in the context of a particle-gas suspension.

3.3 Model Results

A C program was written to numerically integrate the above equations using a Runge-Kutta adaptive stepsize method. For the cases studied in this paper, the following values were adopted (same as Hood 1998): a molecular hydrogen specific heat ratio of 7/5, a hydrogen molecular mass of 4×10^{-24} g (slightly greater than the mass of a hydrogen molecule so as to consider the effects of other species in the gas), a particle specific heat of 10^7 erg g^{-1} K^{-1}, a particle latent heat of melting of 4.5×10^9 erg g^{-1}, melting (and crystallization) takes place between 1400 and 1900 K (the latent heat of melting is divided and added to the heat capacity over this range), a vaporization temperature of 2100 K (though no runs will be presented where the chondrules begin to vaporize) and particle diameters of 0.1 cm. The particle wavelength averaged emissivities and absorptivities were assumed to be 0.9

following Hood and Horanyi (1993). The particle mass density was considered to be 3.3 g cm^{-3} (the same density as olivine). The atomic hydrogen specific heat ratio was assumed to be 5/3 and its mass was taken to be 2×10^{-24} g. In all of the simulations reported here the ambient nebula is assumed to be at a temperature of 400 K with a gas mass density upstream of the shock equal to 1×10^{-9} g cm^{-3} which gives a pressure of 1.4×10^{-5} atm (roughly appropriate for the asteroid belt region in a minimum mass nebula). In each case presented, shock velocities were chosen such that the chondrules were brought just above their liquidus temperatures (at increments of 0.5 km/s).

As discussed in Chapter 1, it is difficult to predict whether or not a given thermal history for silicate particles will produce textures and chemical zoning similar to those observed in real chondrules. Effects due to different grain size, thermal diffusion within the particle, initial composition and others that are known to affect the synthetic chondrules created in laboratories are neglected. For the purposes of this study, a shock wave is considered to form chondrules if it raises the silicate particles to peak temperatures between 1700 and 2400 K and the cooling rates are between 10 and 1000 K/hr as the silicates cool through the crystallization temperature range. This will be discussed further below.

3.3.1 Case 1: n_c = 1 m^{-3}, V_s = 7.0 km/s

The first case considered is that of a shock passing through the solar nebula with a chondrule precursor number density of 1 m^{-3} (solids-to-gas mass density ratio of $\sim$ 1.5, or roughly 300 times solar) far upstream of the shock. Gooding and Keil (1981) argued, based on their interpretations of compound and cratered chondrules, that chondrules formed in regions of the nebula with number densities between 1 and 10^6 chondrules per cubic meter. Thus, this case considers the lowest number density suggested by those authors. The shock velocity was chosen to be 7.0 km s^{-1} with respect to the velocity of the gas far upstream. Figure 3.1 shows the temperature of

the particles in the suspension as a function of time, with the chondrule precursors passing through the shock front at t=0. This figure only shows the time immediately around when the particles pass through the shock.

The precursors are significantly heated for approximately 5 minutes upstream of the shock, reaching a temperature of around 1640 K before crossing the shock front. Immediately behind the shock front, the chondrule temperature quickly rises (due to gas drag) to the peak temperature of 1960 K approximately 2 seconds later. At this point the relative velocity between the chondrules and the gas has decreased sufficiently so that the heating rate of the particles (due to both gas drag and radiation from other particles) is less than the radiative cooling rate, and the temperature decreases. The chondrules are fully crystallized again 90 seconds after crossing the shock front. They then continue to cool to the equilibrium temperature of 400 K roughly 40 minutes after passing through the shock front.

After reaching their peak temperature, the chondrules cool a total of ~1500 K in about 30 minutes. However, the cooling rate during the time period immediately after reaching their peak temperatures is much greater. Taking the instantaneous cooling rate when the chondrules are at 1400 K (an approximate lower temperature when most chondrules are assumed to be partially molten), the cooling rate is found to be roughly 20,000 K/hr, which is over an order of magnitude greater than the experimentally inferred cooling rates for chondrules (e.g. Radomsky and Hewins 1990). The cooling rate as a function of temperature while the particle is molten is shown in Figure 3.2. The cooling rates are too great to produce the textures observed in chondrules and for chemical zoning to take place.

Figure 3.3 shows the number density of the particles as a function of time. Immediately behind the shock, the number density increases most dramatically, increasing by a factor of 20 in the first minute after passing through the shock, before reaching a relatively constant value of ~100 m^{-3} after 20 minutes. This region, immediately behind the shock front when the chondrules are warm enough to be plastic, is where the collisions that formed compound chondrules would have

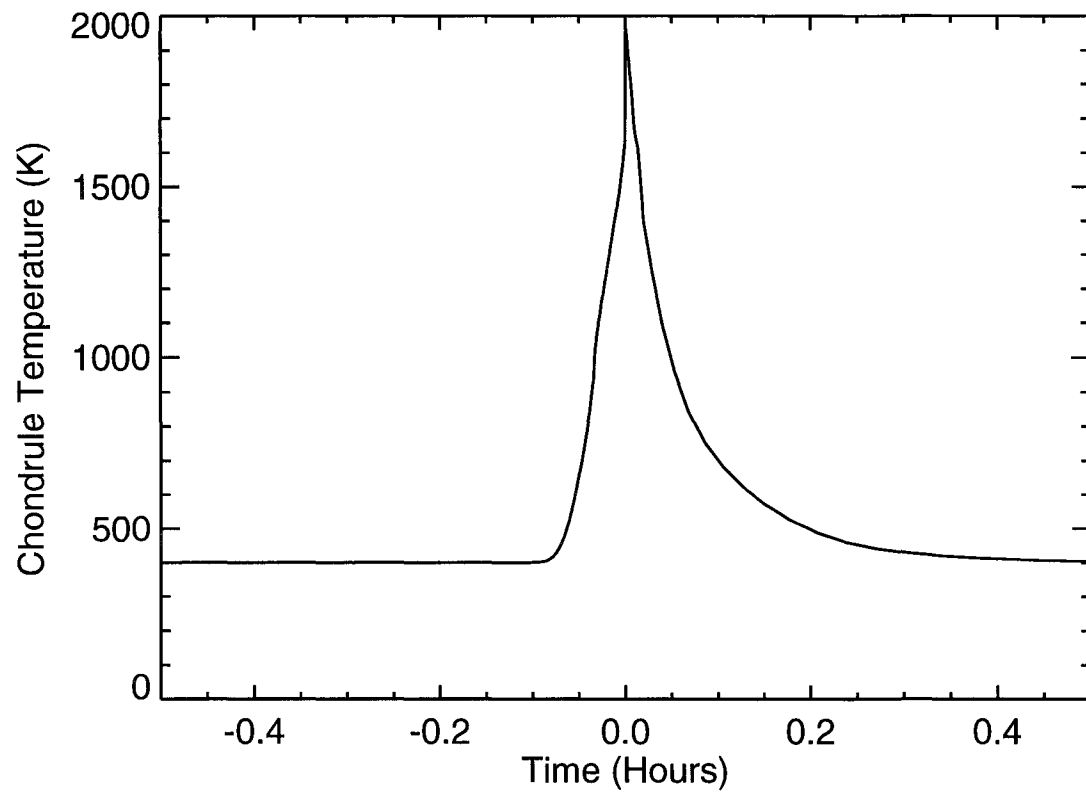Figure 3.1: This plot shows the thermal evolution of the particles as a function of time for the situation described in Case 1.
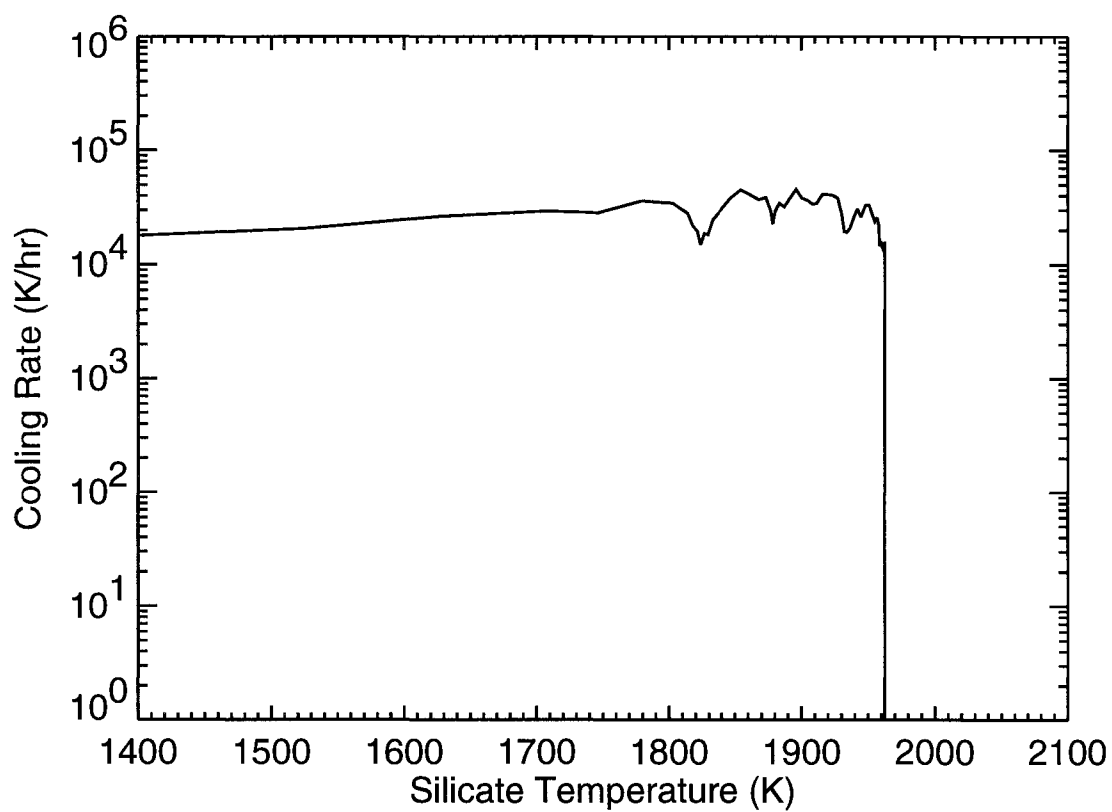
Figure 3.2: This plot shows the cooling rate of the particles as a function of particle temperature. In this model, crystallization takes place between 1400 and 1900 K. The cooling rates in this simulation for those temperatures are significantly higher than expected for chondrules.

taken place. Thus the resulting concentration of chondrules behind shock waves will determine the amount of compound chondrules which will form.

By comparing Figures 3.1 and 3.3, it can be seen that the temperature of the chondrules is linked to their density in the suspension. Because the number density of the particles increases by over two orders of magnitude behind the shock, one optical depth corresponds to a much smaller spatial distance (in this case, ≈ 3 km behind the shock versus 300 km upstream). The chondrules initially have a large velocity and therefore pass through many optical depths very quickly and thus are effectively shielded from the radiation of the warm particles immediately behind the shock. The cooling of the suspension is controlled mainly by energy transfer from the shock heated gas to the solids which in turn lose energy by thermal radiation. Without the solid particles, the gas would remain at the temperature given by the shock jump conditions (though cooling due to hydrogen dissociation would occur). As particles are added to the gas, the gas transfers heat energy to the particles through thermal collisions. These particles in turn radiate the heat to the cooler surroundings. This process becomes more efficient with increasing particle density. Therefore, a lower concentration of particles would lessen these effects. Thus, in this model, an initial particle density of 1 m^{-3} is too great to produce chondrules, because the cooling rates are too rapid.

3.3.2 Case 2: $n_c=$ 0.1 m^{-3} and V_s=8.0 km/s

The next case considered is for a particle number density of 0.1 m^{-3} (a gas to solid mass ratio of 0.15, or about 30 times solar) and a shock traveling at a velocity of 8.0 km/s with respect to the gas far upstream. Figure 3.4 shows the particle temperature profile for this case. Because the concentration of particles is lower in this case than the one previously examined, the radiation from particles behind the shock can travel further upstream. This results in a longer period of warming for the precursors, and in this case they are warmed for approximately 1 hour, reaching
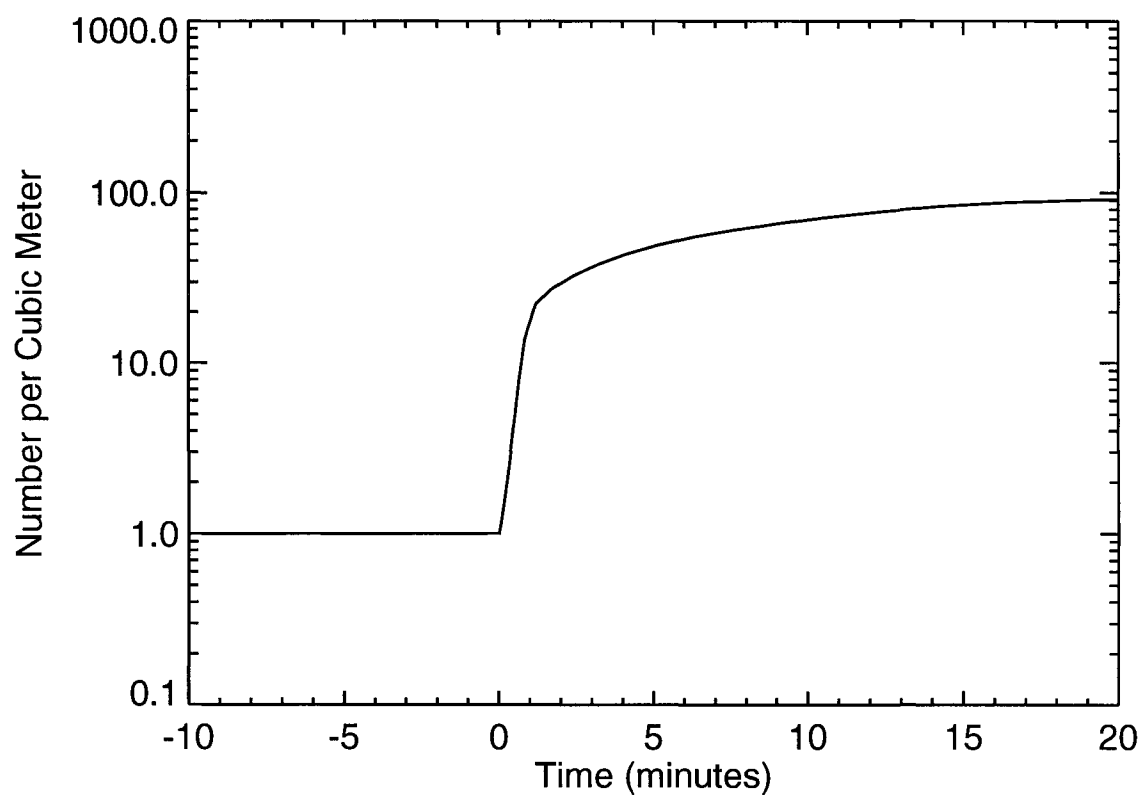
Figure 3.3: This plot shows how the number density of the particles change as a function of time when processed by a shock front. Shock waves spatially concentrate particles over very short time scales, possibly aiding in planetesimal formation.

a temperature of roughly 1407 K, before crossing the shock front. Approximately 1.5 seconds after crossing the shock front, the particles reach a peak temperature of 1970 K before beginning to cool.

The cooling rate of the particles in this simulation are shown in Figure 3.5. After reaching their peak temperature, the particles initially cool rapidly ($\sim 10^5$ K/hr) before approaching a more gradual cooling rate of 1000 K/hr before completely crystallizing. Thus, the peak temperature and the cooling rate of the particles in this simulation fit the criteria described above for forming chondrules. Figure 3.6 shows the number density of the particles in the same simulation.

3.3.3 Case 3: n_c=0.003 m^{-3} and V_s=8.0 km/s

Figure 3.7 shows the particle temperature profile for a suspension with a solar solids-to-gas ratio (mass ratio of 0.005 or ~ 0.003 chondrules m^{-3}). The chondrule precursors are warmed for over 30 hours, reaching a temperature of 1344 K immediately before crossing the shock front. They are then quickly brought to their peak temperature of 1935 K about 2 seconds after passing through the shock front. The chondrules then cool very rapidly over the next 2 minutes to a temperature of ~ 1460 K before reaching a more gradual cooling rate of 20 K hr^{-1} as shown in Figure 3.8. This value is consistent with the lower estimates of chondrule cooling rates. Figure 3.9 shows the increase in spatial density for the chondrules after passing through the shock.

3.4 Discussion

The goal of this work has been to study how millimeter-diameter, silicate particles would be processed by a shock wave passing through a suspension of particles and gas under conditions that may have existed in the solar nebula. By comparing the calculated evolution of the particles in this work to the inferred evolution
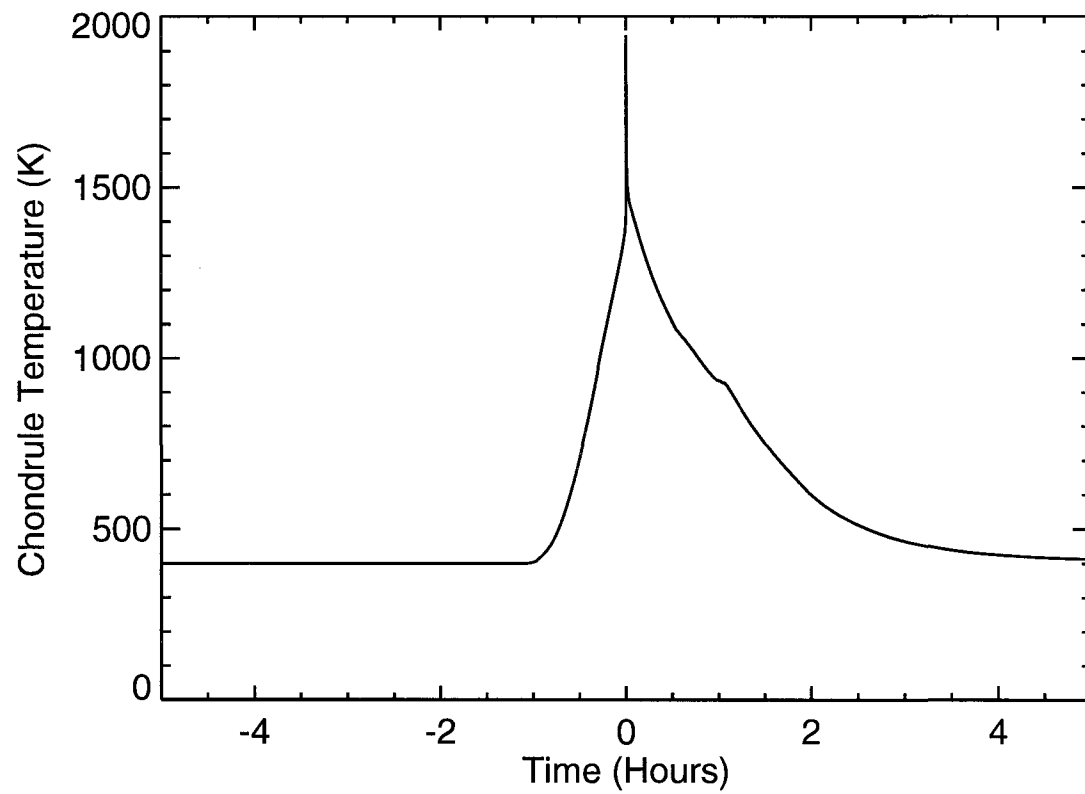
Figure 3.4: This plot shows the temperature profile as a function of time for Case 2. Due to the lower concentration of solid particles, radiation reaches further upstream of the shock allowing warming to take place for a longer period of time.
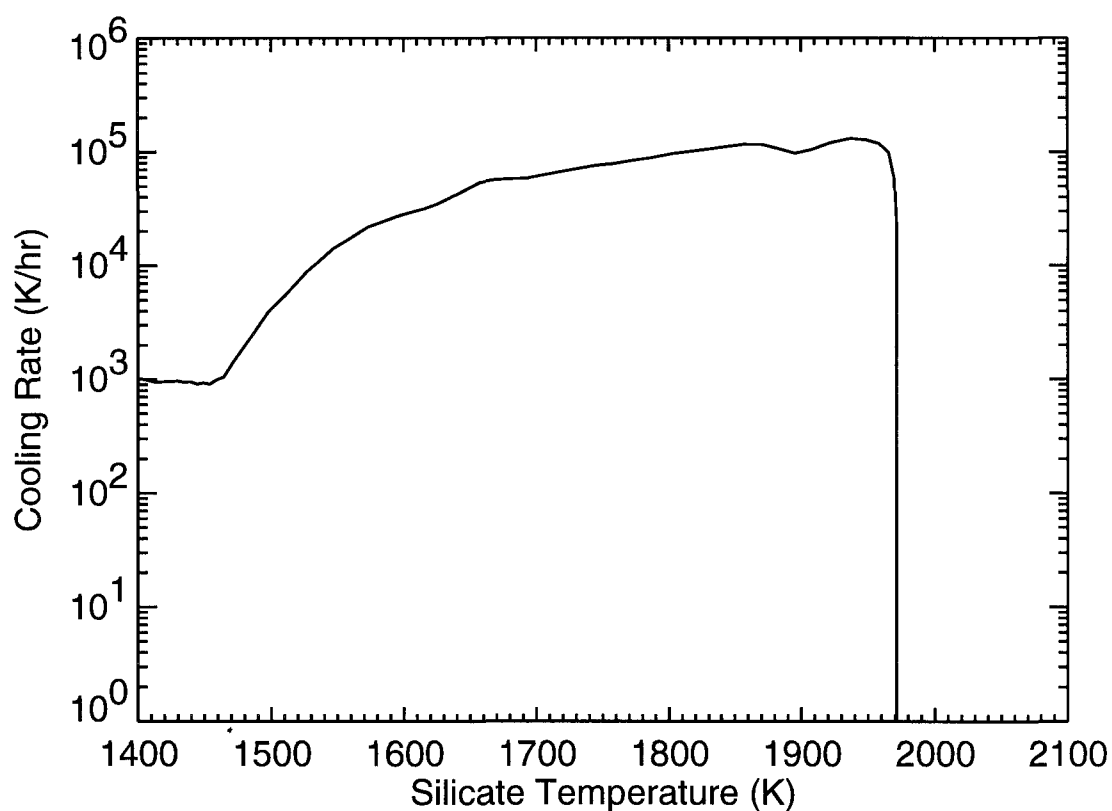
Figure 3.5: This plot shows the cooling rates of the particles in Case 2. As the particle temperature approaches the solidus (1400 K), the cooling rate is approximately 1000 K/hr, consistent with the upper limit of cooling rates inferred for chondrules.
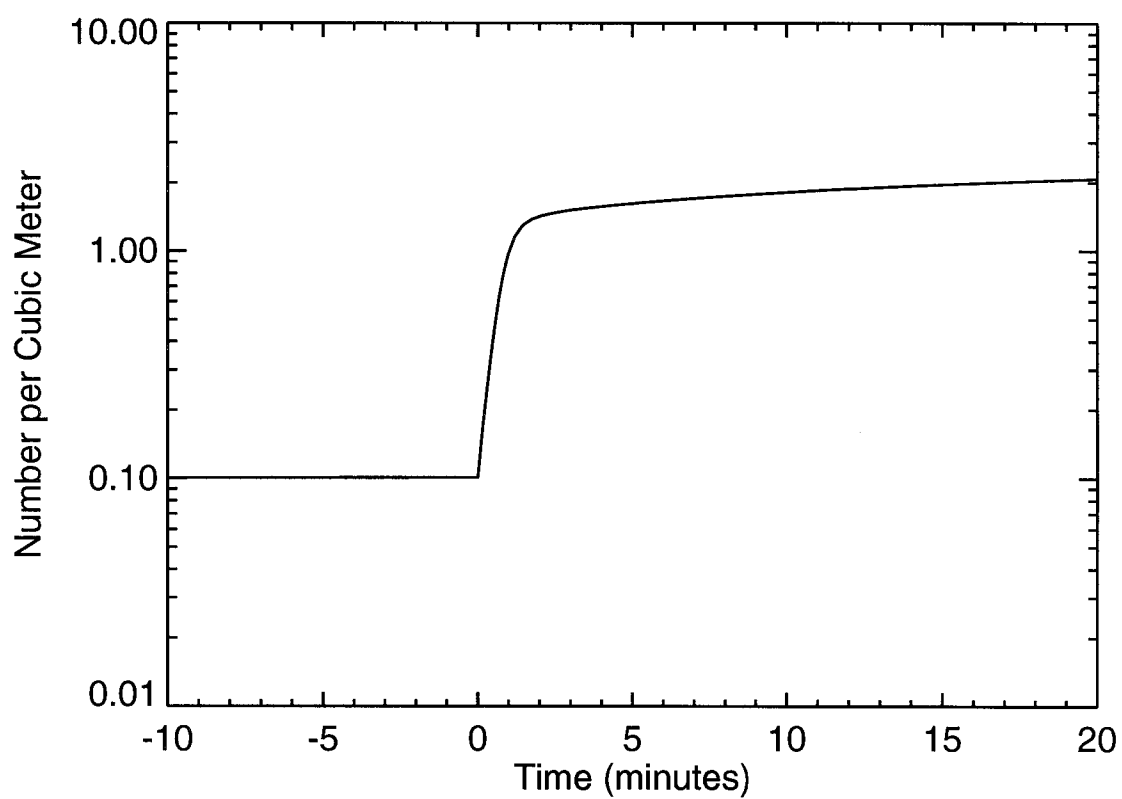
Figure 3.6: This plot shows the how the number density of the particles as a function of time for Case 2.
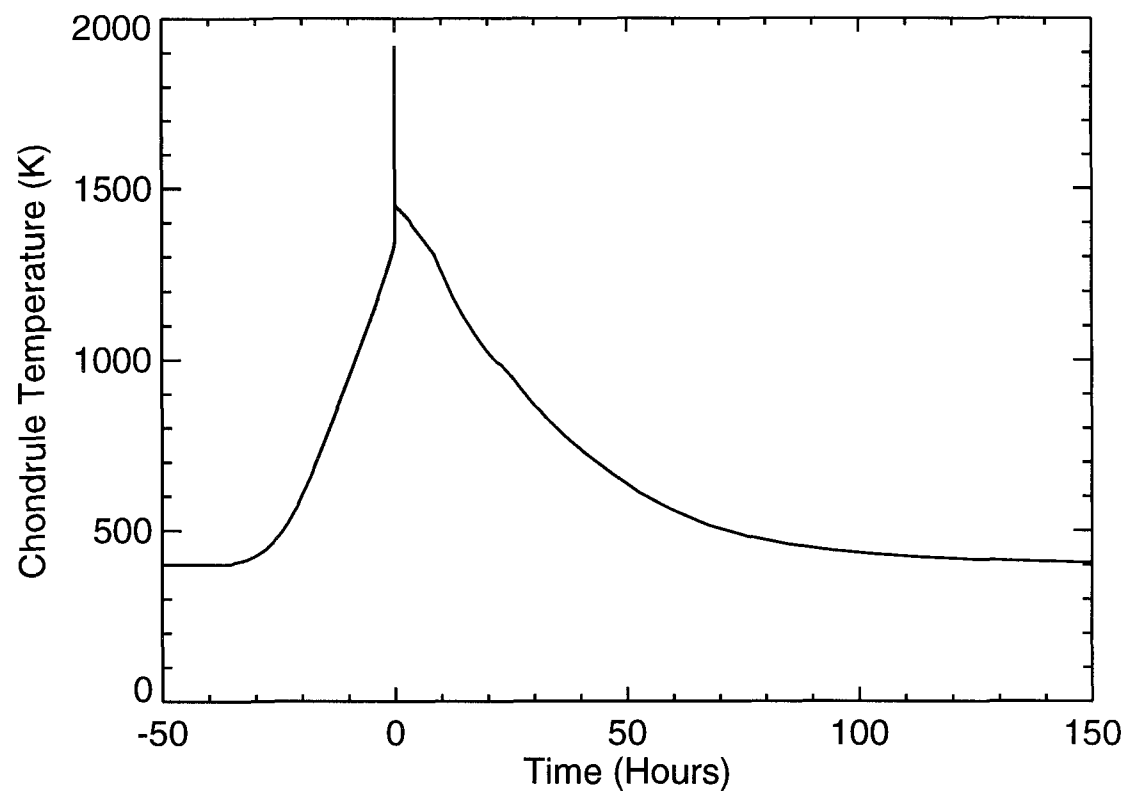
Figure 3.7: This plot shows the temperature profile of the particles for Case 3.
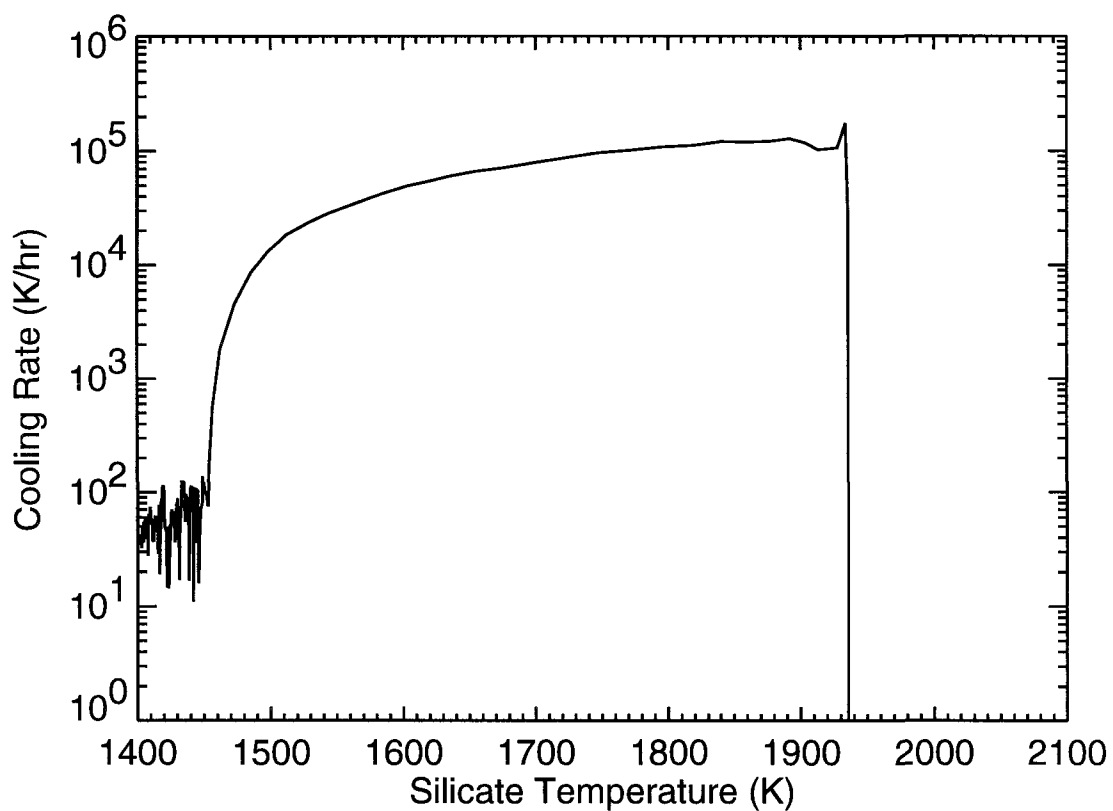
Figure 3.8: This plot shows the cooling rate of the particles as a function of temperature for Case 3. As the particles approach the solidus (1400 K), the cooling rate is approximately 20 K/hr, consistent with the lower end of cooling rates inferred for chondrules.

Figure 3.9: This plot shows the number density of the particles as a function of time for Case 3.

of chondrules, solar nebula shock waves can be evaluated as a chondrule forming mechanism. To do this, a set of equations that govern the energy and momentum transfer in a particle-gas suspension was presented and solved for a variety of plausible conditions appropriate for the solar nebula. In suspensions such as those studied here, there is a large amount of "feedback" that allows for the chondrules to be processed 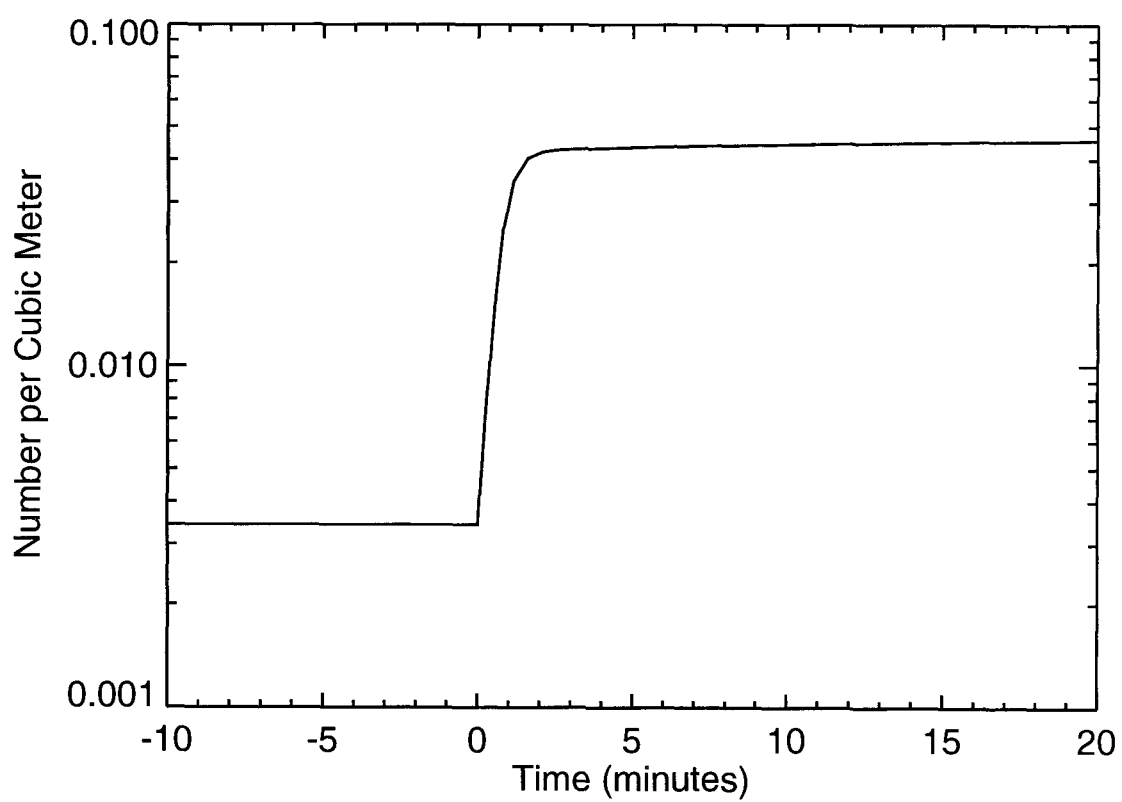by the gas and also allows the gas to be affected by the chondrules and their precursors. As the precursors are heated upstream from the shock (for a period of time that depends on the optical depth of the suspension) they will transfer energy to the gas by thermal conduction. Over this period of time, the gas will also be heated and can reach a relatively high temperature compared to its temperature at far distances upstream from the shock. Not only will the temperature rise, but because a pressure gradient develops due to the heating, the velocity of the gas with respect to the shock front will decrease. The changes in both of these properties are important in determining the jump conditions across the shock front. This effect is observed in all simulations, the magnitude depending on the spatial density of the particles.

The evolution of the suspension upstream of the shock as illustrated in these figures must be investigated. As stated in the introductory chapters, one of the constraints imposed on chondrules is that they were initially at low ($<$ 650 K) temperatures before being processed. This was inferred by the observed primary troilite found in many chondrules. As the chondrules approach the shock front in all of the cases studied, they are warmed significantly above their initial temperature. In all cases studied here, they reach temperatures $\sim$700 K above the condensation temperature of troilite, and therefore, would begin to lose troilite through vaporization. Thus, detailed studies of the kinetic vaporization of troilite for thermal processing of the type shown in this work is needed. This may constrain the amount of time that the chondrules are heated before entering the shock. This work has not considered the presence of dust ($\sim$1 μm particles), which may help to limit this preheating time by increasing the opacity upstream of the shock front.

An important result of this work is that the cooling rates that the chondrules experienced in these simulations were not constant with time. The experimentally inferred cooling rates of 10–1000 K hr^{-1} are based on experiments where melts were cooled linearly, that is, at a constant rate (Hewins, 1997). This likely was not the case; because chondrules radiate energy at a rate proportional to T_c^4 , all heat sources would have to sum up to the same relationship to prevent the cooling rate from resembling a power law function. Similar cooling histories were experimentally tested by Yu and Hewins (1998) and found to aid in retention of Na and S in type I chondrules. In their experiments, a wide variety of textures was produced that matched well with those of natural chondrules. These textures were dependent on the number of nucleation sites that remained as the samples started to cool, which depends on the peak temperatures reached by the chondrules. As discussed in Chapter 1, the textures which result for a chondrule forming event will depend on a number of issues. Due to the rapid heating above the solidus presented in these simulations ($\sim$seconds), it is likely that many nucleation sites would have survived, aiding in crystal growth of the type expected for porphyritic chondrules. For stronger shocks, higher peak temperatures would be reached, and therefore, more complete melting would be likely. Further testing of non-linear cooling of flash heated chondrules is needed to understand what cooling histories chondrules could have experienced.

In the cases presented, the cooling rates of the chondrules decreased with lower chondrule precursor number densities. There were two main factors that determined the cooling rates. First, the strongest sources of radiation in the simulation are the hot chondrules immediately behind the shock front. As the chondrules drift away from these radiation sources, the optical depth between them and the hot zone increases. Therefore the specific intensity of the radiation reaching them decreases as they drift from the shock front. This effect is greater for a higher concentration of particles. Second, the gas behind the shock is constantly transferring heat to the particles either by gas drag or by thermal collisions when the relative velocity is small. When the chondrules gain this energy, they radiate it away, effectively

cooling the gas. This effect is also more efficient with a higher concentration of particles.

These results may be consistent with som of the conclusions drawn by Gooding and Keil (1981). These authors observed that non-porphyritic chondrules exhibited more evidence for collisions than did porphyritic chondrules. Based on previous chondrule cooling studies, these authors assumed that porphyritic chondrules were plastic for a longer period of time than non-porphyritic chondrules and therefore formed in the regions of the nebula with a lower concentration of precursors. The simulations presented here support the conclusion that those chondrules which cooled more rapidly were formed in zones with high chondrule precursor number densities. (However, experiments such as those done by Yu and Hewins (1998) suggest that porphyritic chondrules may not have achieved as high a peak temperature or melted as completely as the non-porphyritic chondrules and the cooling rate played less of a role. Porphyritic chondrules therefore may not have been molten or plastic as long as the non-porphyritic chondrules were or may not have been as efficient at forming compounds. This will be discussed in more detail in Chapter 5.)

The spatial densities of chondrules discussed here were much lower than those predicted by Gooding and Keil (1981). Those authors argued that the number densities of chondrules during formation would be between 1 and 10^6 m^{-3} in order to account for the number of apparent collisions that took place while the chondrules were plastic. However, this was based on an assumed plasticity time for chondrules between 1 and 100 seconds. In this study, the silicates are calculated to be molten (above T_c=1400 K) for ~360 seconds in Case 2 and ~12,000 seconds in Case 3. Therefore, the longer time available for collisions would not require chondrules to be as spatially concentrated.

The chondrule precursor density will not only determine the time over which the suspension will cool, but also the length of the relaxation zone. This is intuitive as a given distance from the shock would correspond to a greater optical depth with

a higher concentration of chondrules. In the simulation with a chondrule precursor density of 1 m^{-3}, the suspension cooled to its original temperature over a distance of $\sim$ 1000 km. Due to the high cooling rates of the chondrules in this simulation, this is unlikely to have been representative of a chondrule forming event. When the precursor density decreased by a factor of 10 and the cooling rates agreed better with experimental estimates, the length of the relaxation zone was $\sim$ 7000 km. Since this simulation produced chondrules that corresponded to the higher end of the cooling rates, slower cooling rates would require even larger relaxation zones (the case with a solar solids to gas mass ratio required over 100,000 km before it relaxed to the original temperature). Therefore, under the assumptions and model parameters chosen here, nebular shocks must have been relatively large scale events in the nebula if they were responsible for chondrule formation. Spiral density waves (Wood, 1996) or gravitational instabilities (Boss, 2000) would be capable of producing shocks of this scale.

As discussed above and illustrated in Figures 3.3, 3.6, and 3.9, one of the consequences of a shock wave passing through a particle-gas suspension will be an increase in the spatial concentration of the resulting chondrules. The ultimate change in density will depend on the velocity of the shock and the initial densities of the precursors and gas. Shock waves themselves may therefore have served as a mechanism for spatially concentrating solids in the nebula and aiding in planetesimal formation. An investigation of how long such concentrations would persist is needed.

3.5 Summary

Not only do models of nebular shock waves show that they could have rapidly heated chondrules, but they also show that the cooling rates fall within the range that has experimentally inferred for chondrules. The cooling of the chondrules would not have been linear, but rather rapid at first before slowing to a more gradual rate.

This cooling behavior would enable the chondrules to retain many of their primary volatiles. In order to do this, though, the shock waves would have to be large (many thousands of kilometers) in extent. However, these types of shocks (graviational instabilities or spiral density waves) might only be formed in the early stages of nebular evolution. Amelin *et al.* (2002), through use of Pb-Pb dating, found that chondrule precursors formed at least 1.3 million years after CAIs formed. Because CAIs are believed to be the first solids formed in the solar nebula, this would imply chondrules formed in the more quiescent stage of nebular evolution, where spiral density waves and gravitational instabilities would likely not operate (Amelin *et al.*, 2002). In the next chapter, small shocks are investigated as possible sites of chondrule formation.

CHAPTER 4

Planetesimal Bow Shocks as Possible Sites for Chondrule Formation

4.1 Introduction

In Chapter 3 large scale shock waves were shown to be possible sites for chondrule formation. However, small shocks, such as those that would be formed by supersonic planetesimals in the solar nebula (Hood, 1998; Weidenschilling *et al.*, 1998), have been proposed as possibly being responsible for the formation of chondrules. In this chapter, this possibility is numerically tested.

Weidenschilling *et al.* (1998) found that planetesimals orbiting the sun in the asteroid belt region of the solar nebula could be trapped in resonances with Jupiter. These resonances would cause the eccentricity of these planetesimals to increase such that the relative velocity of the planetesimal with respect to the nebular gas would be between 5 and 10 km/s (Weidenschilling, personal communication).

Hood (1998) performed hydrodynamic simulations to investigate the characteristics of bow shocks which would be created by the passage of supersonic planetesimals in the solar nebula. Hood (1998) found that the distance over which the temperature and pressure of nebular gas were above their preshock values (the shock thickness) was approximately equal to the diameter of the planetesimal that created the shock. In addition, Hood (1998) found that the shocks created by such planetesimals would be strong enough to melt silicates on time scales consistent with how chondrules are thought to have formed. In this chapter, the model of Hood (1998) is extended to investigate whether planetesimal bow shocks could have thermally processed silicates in a manner similar to how chondrules are believed to have been

processed. In particular, the cooling rates of the silicates are investigated to see if those predicted in the model are consistent with those expected for chondrules.

4.2 Shock Model

The structure of the shock in the model used here is diagrammed in Figure 4.1. In the region upstream from the shock front, particles are heated by the radiation from the hot particles behind the shock front. These particles in turn heat the gas as the shock front approaches. Upon passing through the shock front, the gas properties change as given by the Rankine-Hugoniot relations (equations 3.1-3.3). The particles pass through the shock front unaffected and owing to energy and momentum exchange with the gas, are rapidly heated as their velocity with respect to the gas decreases. After reaching their peak temperatures, the particles begin to cool—rapidly at first, before reaching a slower, and roughly constant, rate (represented by the gentle slope immediately before the end of the shock in the diagram). Upon passing through the end of the shock, the gas properties immediately change back to what they were before crossing through the shock front. The particles again are unaffected when crossing through this region and exchange energy and momentum with the gas as the system relaxes back to its original state (same temperature and velocity as that far upstream from the shock). This immersion of the particles back in the cool gas serves to quench the particles, causing them to cool very rapidly.

In treating the system this way, a number of simplifying assumptions are made. In the simulations of Hood (1998), the gas properties began to relax back to their preshock state before traveling the full thickness of the shock. Also, the shocked region is assumed to be infinite in the directions perpendicular to the velocity of the shock. Both of these treatments likely lead to underestimating the cooling rates of the particles in our model.

The equations which govern the evolution of the system are the same as those used in Chapter 3 (equations 3.4-3.10). For the cases presented, the nebula
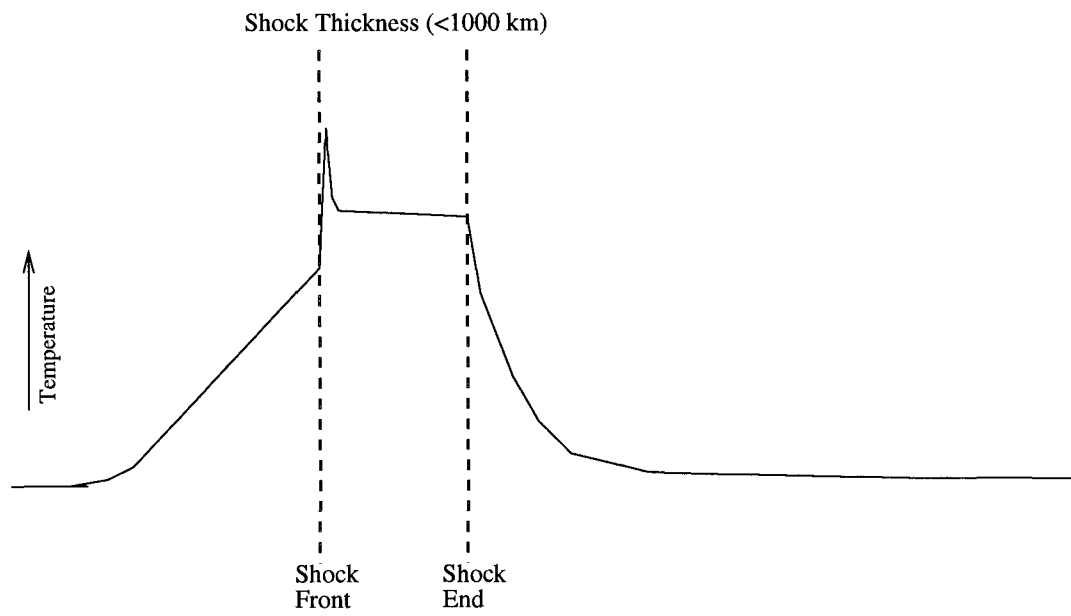
Shock Thickness (<1000 km)

Temperature

Shock
Front

Shock
End

Figure 4.1: The thermal profile of the bow shocks used in this model.

is assumed to originally be at some temperature, T_i far upstream of the shock which sets the forward boundary condition for the radiative transfer calculations. Far behind the shock (thousands of kilometers, determined by the integration), the suspension returns to this same original temperature, and therefore the end boundary condition for the radiative transfer is the same.

4.3 Results

In all cases presented here, the region of the nebula under consideration has an initial temperature of 500 K and a hydrogen molecule number density of 2.5×10^{14} g cm^{-3}, for a total pressure of $\sim 2 \times 10^{-5}$ bars. (A higher temperature is used here than in Chapter 3 in order to provide favorable assumptions for slow cooling rates–a higher initial temperature will increase the intensity of the radiation that the particles are exposed to. The fact that favorable assumptions are made is important for the conclusions of this chapter). The properties of the silicate particles are the same as those used in Chapter 3.

Below the results of model runs using various planetesimal properties and nebular conditions are presented and used to evaluate planetesimal bow shocks as possible chondrule forming sites. In these cases, the thermal evolution of the millimeter sized silicates are calculated and compared to the inferred evolution of chondrules which reached peak temperatures between 1700 and 2400 K (Connolly *et al.*, 1998; Jones *et al.*, 2000) and cooled at rates below ~ 1000 K hr^{-1} (Jones *et al.*, 2000). In the calculations presented, melting and crystallization were assumed to take place between 1400 and 1900 K to account for noncongruent melting of the chondrules, and this is therefore the temperature range of interest for the cooling rates.

Because Hood (1998) showed that planetesimal bow shocks would be capable of melting silicates on short time scales, this chapter focuses on the cooling histories of the silicates. Thus, the results of the simulations are presented in a

manner similar to that done in Figures 3.3, 3.6, and 3.9. The reason for this is to show the cooling rates of the particles as a function of their temperature. On each diagram, a grey box is plotted where cooling profiles must pass in order to be similar to chondrule cooling histories. The cooling profiles for each case are presented, when they begin cooling from their peak temperature (where the profile intersects the x-axis) and cool rapidly at first, before settling to a more gradual cooling rate. If the gradual cooling occurs while the temperature of the silicates is within the crystallization range and those cooling rates are below 1000 K/hr for some significant range of temperatures ($\sim$50 K or more), then these cooling profiles are considered to be consistent with those of chondrules.

4.3.1 Shock Size

The first set of cases considered the effects of the shock thickness on the thermal histories of silicates. The shock thicknesses considered were 50 km (solid line), 100 km (dashed line), and 1000 km (dotted line) and their cooling profiles are shown in Figure 4.2. In these cases, the shock wave was assumed to move at 8 km s^{-1} (a middle value according to those predicted by Weidenschilling), all solids were in the form of chondrule precursors and suspended at the canonical mass ratio with respect to the gas (gas/solids mass ratio of 0.005). In general, the cooling rates decreased as the temperature decreases. The points on the graph where the cooling rates increase drastically for the 50 and 100 km cases represent the points where the particles exit the thickness of the shock and are immersed in cool gas once again.

As can be seen, none of the cooling profiles pass through the region of the graph thought to be necessary to form chondrules. In all cases presented here, the cooling rates are too high, and thus would not form chondrules. It should be noted that the case which produces the lowest cooling rates is the 1000 km case which suggests that the heated, shocked gas is needed to keep chondrules warm as they crystallize.
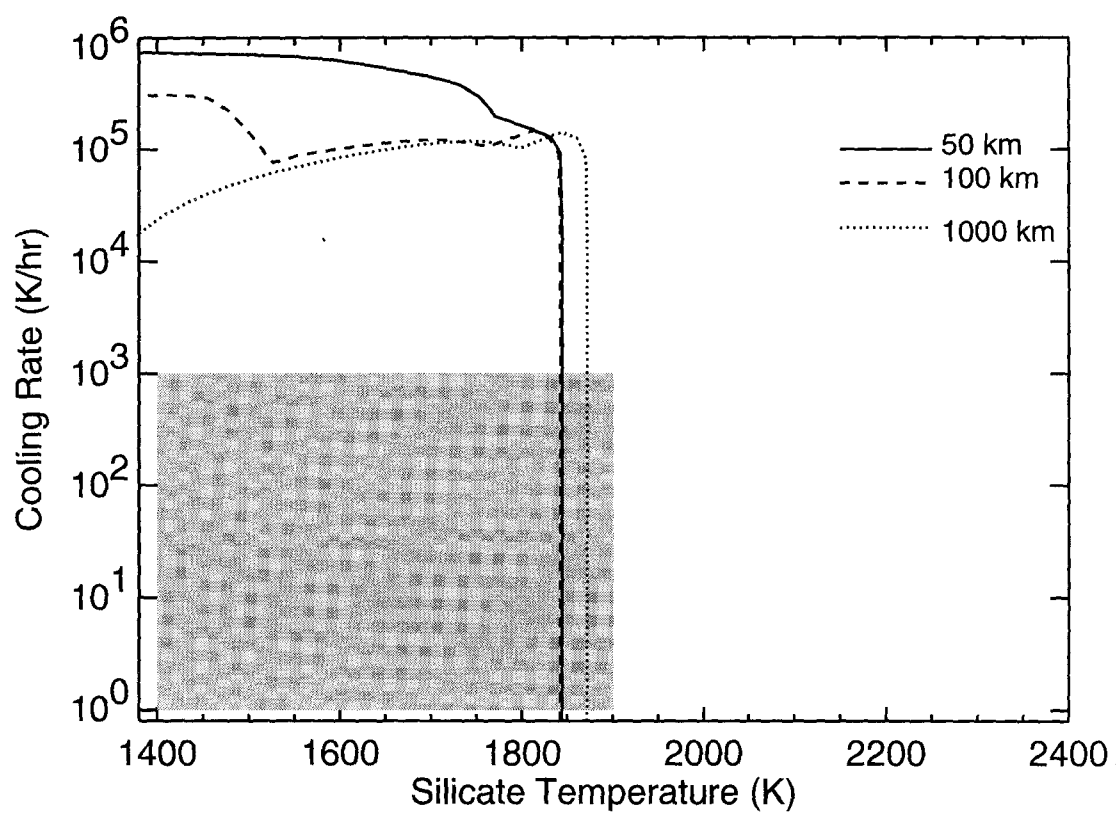
Figure 4.2: The cooling histories of chondrule-sized particles being processed by shocks of various thicknesses in the absence of dust.

4.3.2 Shock Size with Dust

The next set of cases investigated are similar to the last, except the presence of dust is considered. In these cases, the mass of the solids are distributed as 75% as chondrules and 25% as micron-sized dust particles as was done by Desch and Connolly (2002). The dust particles have all the same properties as the chondrules, except the wavelength averaged emissivity of the dust had a value of 0.1 (similar to Desch and Connolly (2002)). This lower value follows the general trend of small particles being unable to radiate photons whose wavelengths are longer than the particle's diameter. The results of these simulations are shown in Figure 4.3 for shock thicknesses of 50 km (solid line), 100 km (dashed line), and 1000 km (dotted line).

In these cases, the peak temperatures of the chondrules are significantly higher than in those presented above. This is due to the feedback of the dust particles with the gas immediately behind the shock front. This feedback causes the gas to maintain higher temperatures initially, allowing the chondrules to heat more rapidly. Despite these increased peak temperatures, the cooling rates of the chondrules are still very rapid, in all cases being approximately 10^4 K/hr as the particles cool through their solidus temperature.

It should be noted that the dust particles in these simulations are not allowed to vaporize. This was done so that the effects of increased nebular opacity could be studied. In these simulations, the dust particles reached temperatures of 2500 K, and, in reality, would likely have vaporized. This dust would in turn increase the density of the gas, and possibly aid in keeping the chondrules warm while they were in the shock wave.
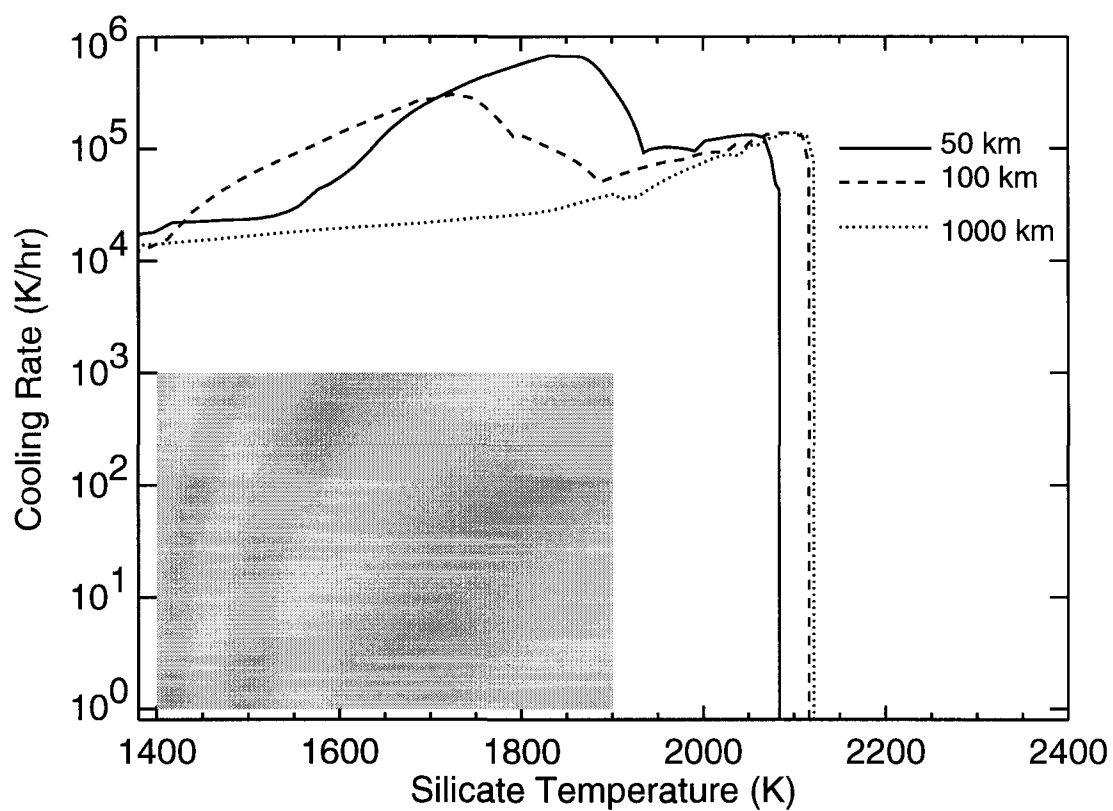
Figure 4.3: The cooling histories of chondrule-sized particles being processed by shocks of various thicknesses with dust present
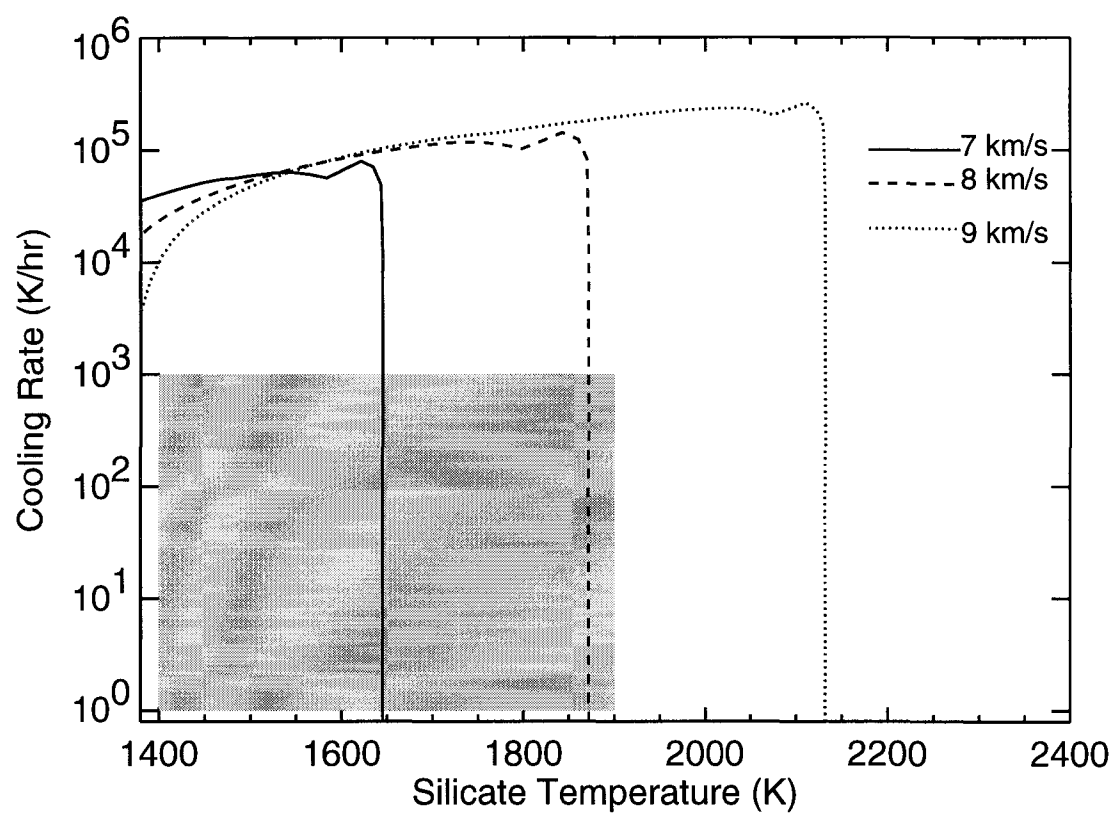
Figure 4.4: The cooling histories of chondrule-sized particles being processed by 1000 km-thick shocks of various speeds.

4.3.3 Shock Velocity

Figure 4.4 shows the cooling profiles resulting from 1000 km thick shocks moving through a nebula where solids were concentrated at the solid ratio with respect to the gas, and all solids were in the form of chondrules. In these cases, we considered shocks moving at speeds of 7 km/s (solid line), 8 km/s (dashed line) and 9 km/s (dotted line).

As would be expected, higher velocity shocks led to higher peak temperatures due to the more intense gas drag that would result behind the shock front. The cooling profiles for each case are very similar, with the 9 km/s case having the slowest cooling rate at the solidus temperature. This is because the nebular gas would be at a higher temperature than in the other cases, allowing more heat to be transferred to the particles at this temperature. Again, all of these cases produce cooling rates that are too rapid to form chondrules.

4.3.4 Chondrule Concentration

Figure 4.5 shows the cooling profiles resulting from 1000 km thick shocks moving through a nebula at 8 km/s where solids are concentrated at the solar value (solid line), 10 times solar (dashed line) and 100 times solar (dotted line). In the solar case, the cooling rates of the particles are too rapid through the crystallization range to form chondrules, as is true for the case of 100 times enhancement.

The 10 times enhancement case, however, has a region where the cooling rates are slightly higher than 100 K/hr. This region from ~1420 to 1500 K represents that gradual cooling region identified in the shock profile (Figure 4.1) above. The solar case also experiences a slow cooling rate region; however, this region is well below where crystallization takes place. The enhancement of the solids provides more feedback between the particles and the gas, allowing higher temperatures to be reached, and therefore, the slow cooling regime of the particles moves into the
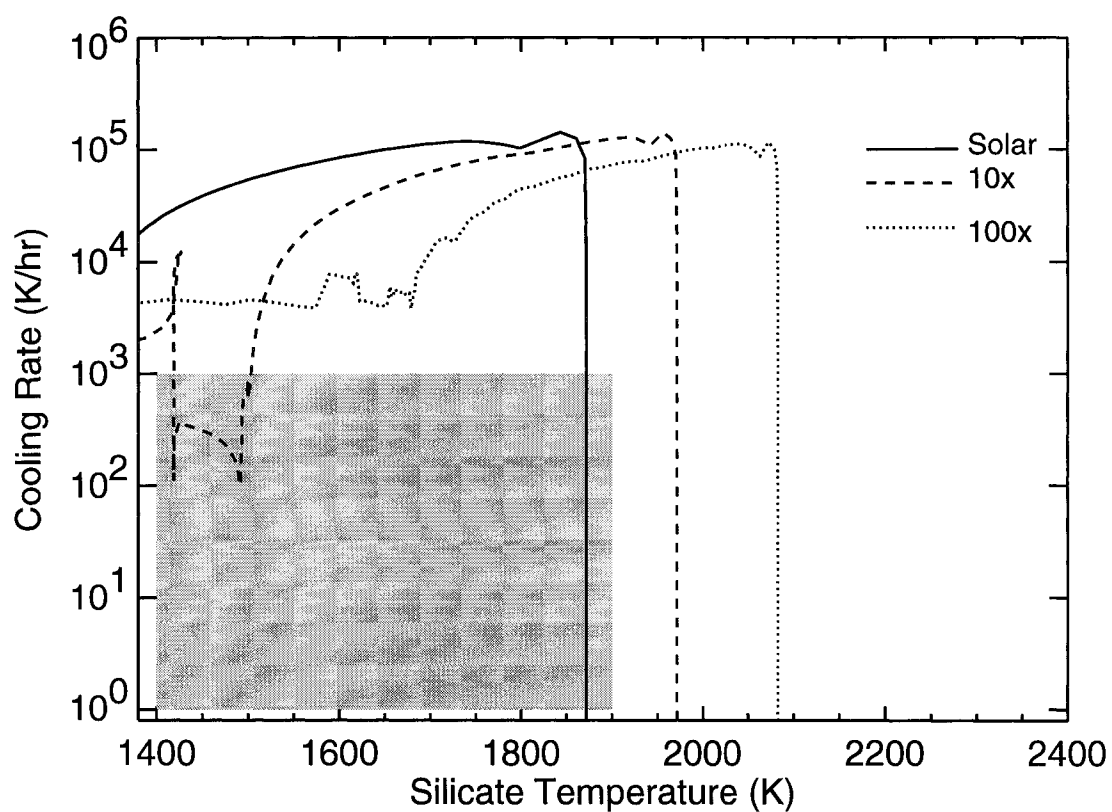
Figure 4.5: The cooling histories of chondrule-sized particles concentrated at different values, being processed by 1000 km-thick shocks in the absence of dust.

crystallization range. In the 100 times enhancement case, the feedback is even more dramatic, allowing this relatively slower cooling to begin at $\sim$1700 K. However, as was found previously, higher concentrations of particles cause more rapid cooling, and therefore the cooling rate in this case is still too rapid to form chondrules.

4.4 Discussion

In all of the cases presented here except for one, the cooling rates of the particles here were much too rapid to be consistent with what has been inferred for chondrules. There was one set of cases where the predicted cooling histories of the chondrules matched those inferred for chondrules; however, it required specific conditions in the nebula. It should also be remembered that the assumptions made in this model favored slow cooling rates for the particles. A more complex model, which accounts for three-dimensional radiative transfer and relaxation (cooling and expansion) of the gas prior to reaching the end of the shock, would likely predict more rapid cooling rates than those found here.

Comparing the results of this chapter with those in the previous chapter shows that the thermal histories of particles in large scale shock waves ($>$ a few 1000 km) more closely resemble those of chondrules than those in smaller scale shocks ($<$1000 km). Planetesimals larger than 1000 km would likely not be trapped in resonances with Jupiter and attain supersonic speeds, and thus chondrule forming shock waves may have been generated in some other manner. A discussion of how chondrule forming shocks could be generated is presented in the Conclusions chapter of this work.

4.5 Summary

In this chapter, the planetesimal bow shock model for chondrule formation was quantitatively tested to see if such shocks could have thermally processed chondrule-sized particles in a manner that was consistent with how chondrules are thought to have been processed. In most of the cases presented here, despite favorable assumptions, the cooling rates for the particles are much higher than expected for chondrules. Thus, large scale shock waves, such as those considered in the previous chapter, are probably needed to form chondrules. If chondrules formed by shock waves, the shock waves were probably greater than 1000 km in thickness. These large shocks would allow the shock heated gas to keep the chondrules warm as they crystallized.

CHAPTER 5

Compound Chondrules

5.1 Introduction

Studies of chondrules in thin-section and by removal as whole pieces from meteorites have shown that some chondrules are aggregates composed of two chondrules fused together. These compound chondrules have been interpreted by some as evidence that during the time when they were molten, chondrules were susceptible to collisions (Gooding and Keil, 1981). Some of these collisions resulted in chondrules sticking to one another, or, in some cases, one chondrule completely enveloping another. Understanding these collisional histories, it was argued, would lead to a better understanding of the environment in which chondrules formed and provide greater insight into what was taking place in the solar nebula during the early part of solar system formation.

An alternative formation mechanism for compound chondrules was proposed by Wasson (Wasson *et al.*, 1995). These authors suggested that compound chondrules were formed when porous aggregates around a primary chondrule were flash heated and melted to form the secondary chondrule. These authors did not favor the collisional model because they felt chondrules would remain plastic for only tens of seconds or less and argued that collisions would be too infrequent during this period. While the porous aggregate model cannot be dismissed, recently it has been shown that formation by shock waves would allow chondrules to remain plastic for sufficiently long periods of time (1000s of seconds) for the proper fraction of chondrules to collide (Chapter 3, Desch and Connolly, 2002).

Distinguishing which of the two mechanisms was responsible for the formation of compound chondrules would provide insights into how all chondrules formed. Thus it is important to fully understand all of the properties of compound chondrules and try to explain those properties in the context of a chondrule formation model.

In one of the first detailed studies of compound chondrules, Gooding and Keil (1981) examined over 1600 chondrules in thin-section to find the distribution of chondrule textural types and the frequency of compounds. They also examined 216 whole chondrules removed from meteorites. Their study found that 4% of all chondrules exist as compound chondrules, and that compound chondrules are more common among non-porphyritic (those that completely melted or cooled more rapidly) chondrules than porphyritic chondrules. Therefore, Gooding and Keil (1981) argued that non-porphyritic chondrules formed in regions of the nebula that had a higher density of precursors than did porphyritic chondrules. However, if the thermal histories of chondrules matches those studied by Yu and Hewins (1998) as was found in some shock wave models (Chapter 3, Desch and Connolly, 2002), then chondrule textures are determined more by peak temperatures and/or nucleation sites in the melts than by cooling rates. Thus non-porphyritic chondrules may have been susceptible to collisions for slightly longer times than porphyritic chondrules, or because they reached higher temperatures (more molten states) and were less rigid and more efficient at forming compound chondrules. This issue will be discussed below.

Wasson *et al.* (1995) performed a more comprehensive study by analyzing $\approx$10,000 chondrules in 79 cm^2 of ordinary chondrite thin-sections. In addition to characterizing all of the compounds they identified, these authors concluded that 2.4% of all chondrules are compounds. The reason for the different results of Gooding and Keil (1981) and Wasson *et al.* (1995) has been unclear, though the latter authors suggest it may be due to the fact that they did not include chondrules less than 40 μm in diameter in their statistics. Currently, this value of 2.4% is the

accepted frequency of compound chondrules (Hewins, 1997).

It has been shown that because thin-sections only sample a random slice of a chondrule, the uncertainties in where the cut intersects the chondrule can lead to biases in determining the chondrule size distribution (Eisenhour, 1996). Gooding and Keil (1981) and Wasson *et al.* (1995) acknowledged that this uncertainty may have affected the statistics of compound chondrules in their studies. To correct for this source of error, they multiplied their thin-section counts by a factor of 3, though the actual value of the correction factor is unknown (Wasson *et al.*, 1995). This value was originally estimated by Gooding (1979) by dividing the percent of compound chondrules found by removing whole chondrules from meteorites by the percent identified in thin-section. However, considering all uncertainties it could actually range from 2 to 4. Thus, a detailed understanding of the biases associated with identifying a compound chondrule in thin-section is needed in order to interpret thin-section statistics.

In this chapter, some of the issues surrounding compound chondrule formation are reexamined. In the next section, the problems of identifying compound chondrules in thin-sections are quantitatively discussed, and theoretical correction factors needed for estimating the population of compound chondrules from such studies are derived. These factors are applied to the compound chondrule statistics of Wasson *et al.* (1995) in section 3 to reevaluate the occurence rate of compound chondrules. In section 4, a new model for chondrule collisional evolution is developed and applied to conditions plausible for chondrule formation. In section 5, some implications for this work are discussed in the context of chondrule formation.

5.2 Thin-section Studies

Three types of compound chondrules were identified by Wasson *et al.* (1995) based on their geometries in thin-section: adhering, consorting, and enveloping. Adhering and consorting compounds are those in which the contact angle (angular distance

along the primary chondrule in contact with the secondary) between the components never reaches more than 180°. Enveloping chondrules are those which appear to have contact angles greater than 180°. Consorting compounds and adhering compounds are similar and are distinguished by the apparent ratio of diameters of the primary and secondary chondrules in thin-section. For the purposes of this work, no distinction is made between adhering and consorting chondrules as the methods used can be applied to both.

5.2.1   Adhering Chondrules

First, consider two spheres joined together such that they would be defined as adhering chondrules (Figure 5.1). The primary is defined as a sphere with radius a, and the secondary is characterized by a mean radius b (mean radius is used here because the secondary shape may not be spherical). For simplicity, the chondrules are assumed to be symmetric about the line which connects their centers. Following Wasson *et al.* (1995), the contact angle, ϕ, is defined as the angular distance along the primary that is in contact with the secondary. The corresponding angle, γ, is defined as the angular distance along the secondary that is deformed by the primary. For this case, ϕ is defined as the maximum contact arc, that is, the contact arc perpendicular to the line of centers. The chord which connects the two ends of the contact (the length of the contact) is defined as s and is equal to:

$$s = 2a \sin \left(\frac{\phi}{2} \right) \tag{5.1}$$

If a thin-section slices through this compound chondrule, an angle, β, will be formed between the plane of the thin-section and the line of centers of the chondrule. The maximum length of the compound chondrule is then:

$$h = a + b + \left(a \cos \left(\frac{\phi}{2} \right) + b \cos \left(\frac{\gamma}{2} \right) \right) \tag{5.2}$$
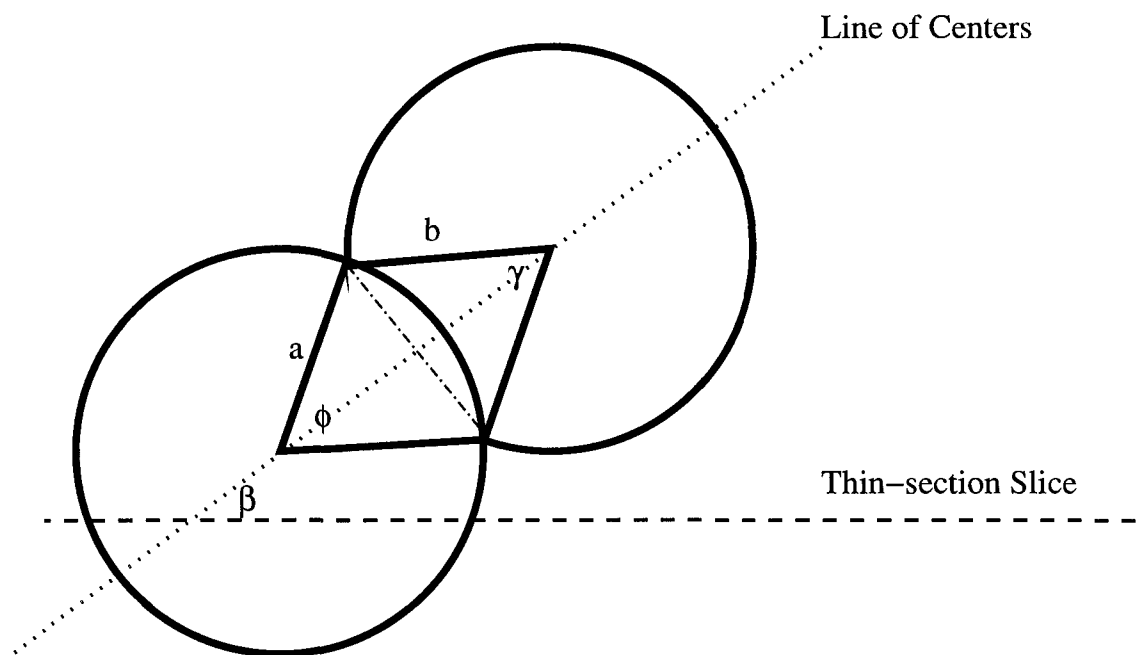
Figure 5.1: The geometry and defined terms for the calculations involving adhering compound chondrules.

Projected onto a line perpendicular to the thin-section, the height is (assuming $a \approx b$):

$$h_{proj} = a + max\left(a, b + \left(a\cos\left(\frac{\phi}{2}\right) + b\cos\left(\frac{\gamma}{2}\right)\right)\sin\beta\right) \qquad (5.3)$$

The projection of the contact chord onto a line perpendicular to the thin section is $s\cos\beta$. If a thin-section slices through this area of contact, it will be identified as an adhering compound chondrule; if it does not contain the contact area, it will not be identified as such. Therefore, assuming the thickness of the thin-section is small compared to the total height of the chondrule, the probability that the area of contact is also contained in that thin-section is the height of the contact divided by the height of the compound:

$$P\left(\phi, \beta\right) = \frac{2a\sin\left(\frac{\phi}{2}\right)\cos\beta}{a + b + \left(a\cos\left(\frac{\phi}{2}\right) + b\cos\left(\frac{\gamma}{2}\right)\right)\sin\beta} \qquad (5.4)$$

In order to calculate the probability that a given compound chondrule will be identified in a thin-section cut with an arbitrary orientation, we average over all β:

$$P\left(\phi\right) = \frac{\int_0^{\frac{\pi}{2}} P\left(\phi, \beta\right)d\beta}{\int_0^{\frac{\pi}{2}} d\beta} \qquad (5.5)$$

which we find to be (assuming explicitly that $a=b$):

$$P\left(\phi\right) = \frac{2}{\pi}\ln\left(1 + \cos\left(\frac{\phi}{2}\right)\right)\tan\left(\frac{\phi}{2}\right) \qquad (5.6)$$

Considering those contact arcs which measure between 0 (which would be two spheres tangent to one another) and π (the same angular range that Wasson *et al.* (1995) defined for adhering chondrules), the probability that the two chondrules would be identified as compounds in the thin-section by

$$P = \frac{\int_0^\pi P\left(\phi\right)d\phi}{\int_0^\pi d\phi} \qquad (5.7)$$

which is roughly 25%. In other words, when a thin-section slice intersects a compound chondrule, there is a 75% chance that it will not be identified as such, which

means that thin-section statistics would have to be multiplied by 4 to extend to the population of whole chondrules. This assumes that there is no preferred contact angle, i.e., that it is equally probable for any contact angle to exist (this issue is discussed in section 3).

5.2.2 Enveloping chondrules

Compound chondrules may also occur as enveloping chondrules, where one chondrule is surrounded by another (Figure 5.2). Assuming that the inner chondrule has a radius b and the outer chondrule extends some radius, a, from the center of the compound chondrule, then the probability that a thin section cut will intersect both chondrules is the diameter of the inner chondrule divided by the diameter of the outer chondrule:

$$P(a, b) = \frac{2b}{2a} \qquad (5.8)$$

which reduces to the ratio of their effective radii. Averaging over all possible ratios, the total probability of being able to identify an enveloping chondrule is

$$P = \frac{\int_0^1 \frac{b}{a} \, d\left(\frac{b}{a}\right)}{\int_0^1 d\left(\frac{b}{a}\right)} \qquad (5.9)$$

or 50%, implying that the correction factor for these types of compounds is 2. This is an approximate value, however, because if the inner chondrule is only slightly cut by the thin-section, it may mistakenly be identified as a relict grain.

5.3 Application to Compound Statistics

Wasson *et al.* (1995) identified and described 80 compound chondrules which comprised about 0.8% of all chondrules observed in thin-section. Of those, 72 were classified either as consorting or adhering chondrules. As mentioned above, these authors multiplied by a factor of three to account for biases due to observing objects in thin-section. This factor was applied for all compound chondrules regardless of
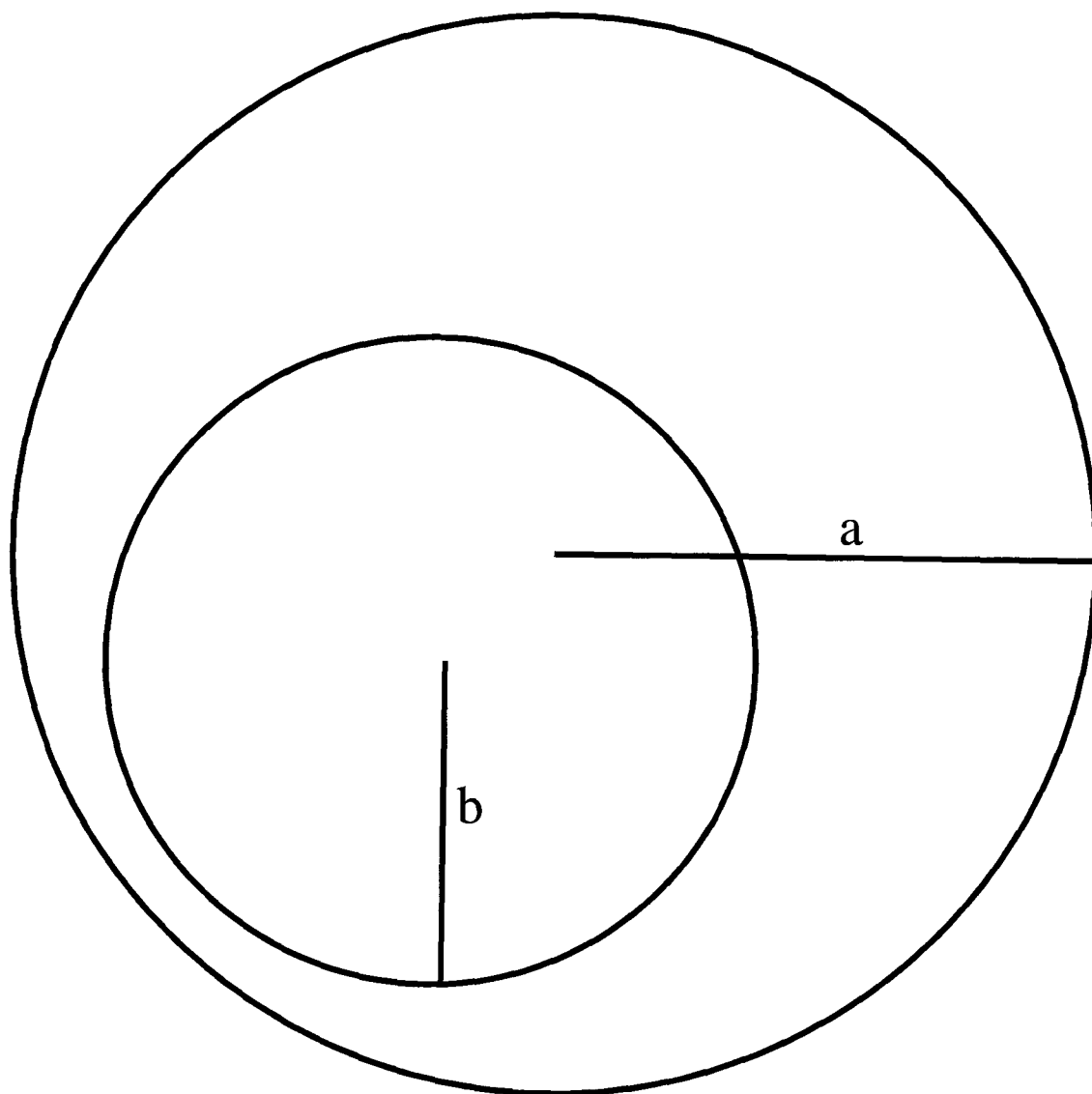
Figure 5.2: The geometry and defined terms for the calculations involving 0 compound chondrules.

contact geometry. However, equation (4.6) suggests that the probability of identifying a compound chondrule in thin-section is dependent on the contact angle between the primary and secondary. This warrants further investigation.

Figure 5.3 shows the distribution of contact angles for adhering chondrules measured by Wasson *et al.* (1995). Above, it was found that if there were no preferred distribution of contact angles, the correction factor for extrapolating thin-section counts to the total chondrule population would be a factor of 4 (close the value of 3 used by previous studies). However, Figure 5.3 suggests that there is a preference for low ($\phi \leq 90°$) contact angles among adhering chondrules. According to equation (5.6), these low angles have a relatively low probability of being observed in thin-section. Therefore, the geometries of compound chondrules must be considered in correcting for underestimates.

However, the contact anble observed for adhering chondrules in thin-section are likely not equal to the maximum contact arc that could have existed. For this to be the case, the thin-section would have to intersect the compound chondrule exactly at the center of the contact between the two components. In reality, the thin-section cut is likely to intersect the contact area at any point with equal probability. If we assume the contact area is a circle with radius $s/2$, then the thin-section will, on average, cut the contact at a distance $s/4$ from the center of the arc. The contact arc at this point can be related to the maximum contact arc by the following formula:

$$\sin\left(\frac{\overline{\phi}}{2}\right) = \frac{\sqrt{3}}{2}\sin\left(\frac{\phi_{max}}{2}\right) \tag{5.10}$$

where $\overline{\phi}$ is the average contact angle of a thin-section cut and ϕ_{max} is the maximum contact angle that could be cut from a compound chondrule if it were cut along its line of centers. Thus, Figure 5.3 may only represent a histogram of the average contact angle, $\overline{\phi}$, rather than the maximum contact angle for which equation (6) was derived. Applying the above relation to each of the contact angles in Figure 5.3 gives the modified distribution in Figure 5.4. While the distribution has moved to the right (towards higher contact angles), the tendency for small contact angles
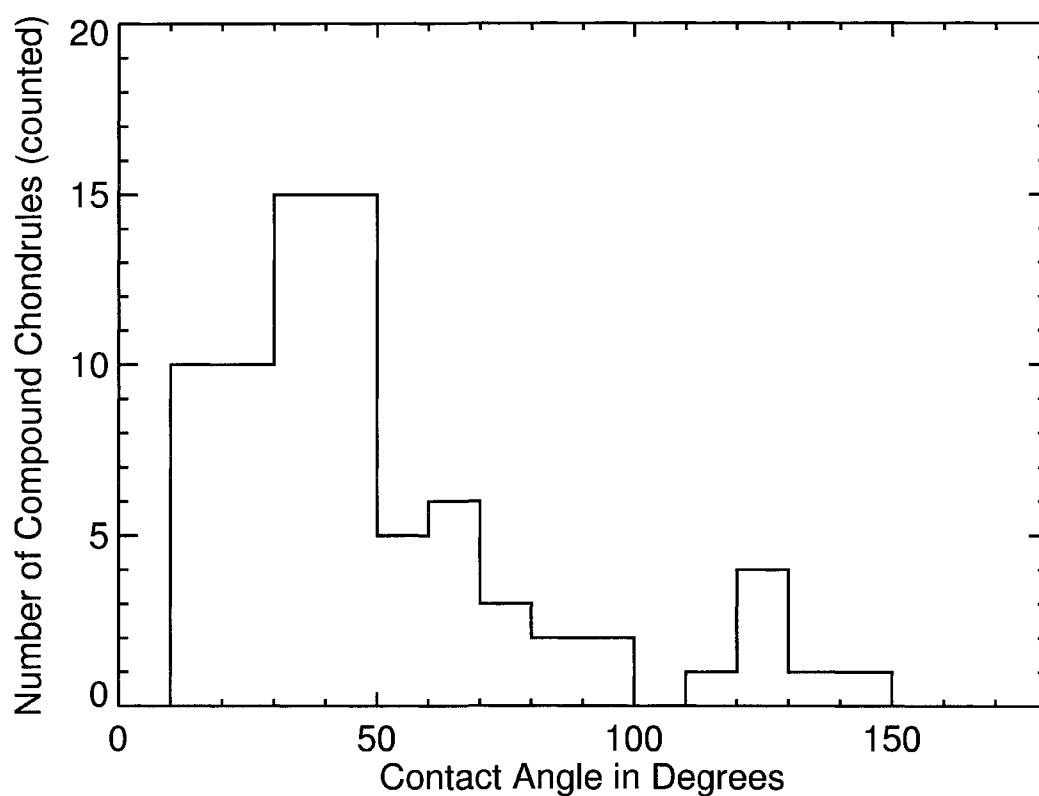
Figure 5.3: Plotted is a histogram which shows the distribution of contact angles for the adhering and consorting compound chondrules observed in thin-section by Wasson *et al.* (1995). The angles are distributed in 10° bins.

is still noticeable.

Figure 5.5 shows the "corrected" distribution of contact angles based upon the measurements of Wasson *et al.* (1995). This distribution was obtained by taking the histogram of Figure 5.4 and applying a correction factor (found by calculating the probability of detecting a compound chondrule using equation (5.6) and then taking the inverse) to each individual bin. The bins are 10 degrees wide, and the correction factor was evaluated for the middle angle of each bin. This procedure was repeated with bins 1, 5 and 20 degrees wide and the results did not change significantly.

Figure 5.5 shows that the distribution of the contact angles is dramatically changed by considering the angular dependence of the correction factors. Summing up the corrected values from each bin yields a total number of compound chondrules ~520, implying that ~5.2% of all chondrules are adhering compounds. Because only a small number of enveloping chondrules have been observed, they are a minor component of the population. To be conservative, due to the simple geometries used in deriving the equations in Section 5.2, it is estimated that ~5% of all chondrules are compounds. The shape of the distribution shown in Figure 5.5 will be discussed below.

While this reinterpretation of the data gives a different result than that of Wasson *et al.* (1995), it compares favorably with the findings of Gooding and Keil (1981). These authors found that 9 of 216 ($\approx$4.2%) whole chondrules removed from meteorites were compounds. The results of this study are within one standard deviation, 1.4%, of this value. This point is worth noting because the biases that are corrected for in this work would not exist in a study of whole chondrules. Gooding and Keil (1981) also studied chondrules in thin-section and identified 1.4% of their sample ($\approx$1600 chondrules) as being compounds. Because no geometries were reported along with these statistics, their results can not be compared with the findings of this work.
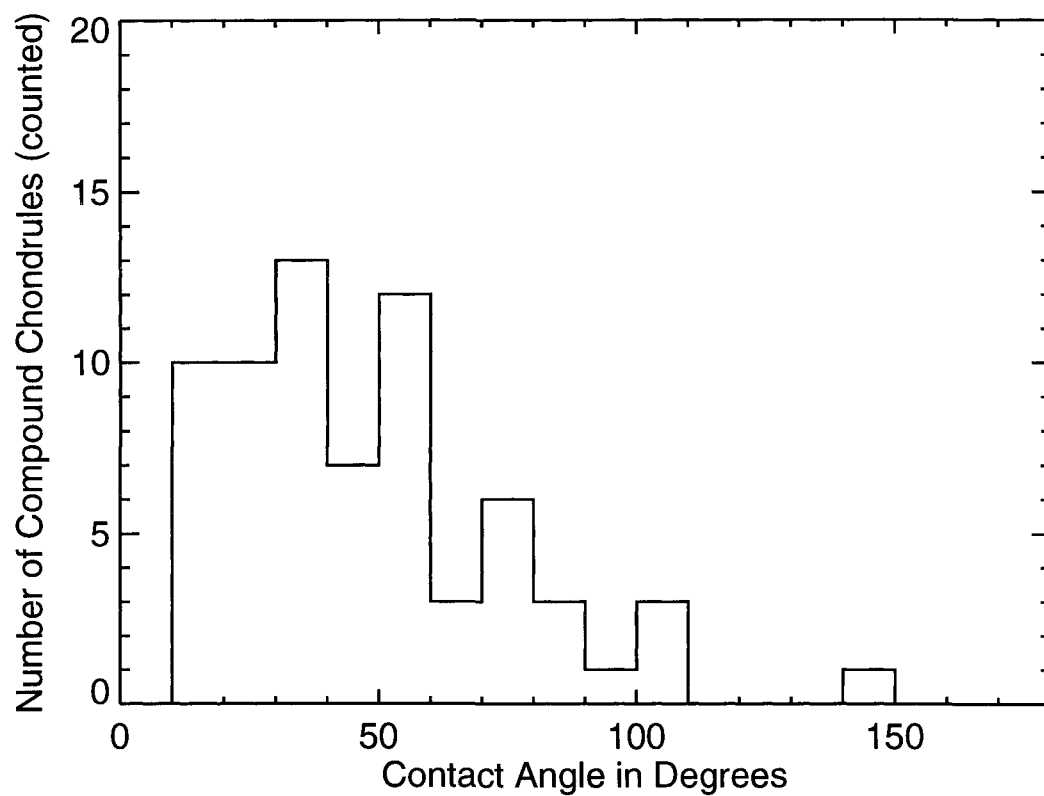
Figure 5.4: Same distribution of contact angles as in Figure 3, but modified to account for the likelihood of a thin-section slice cutting through a random section of the contact of a compound chondrule.
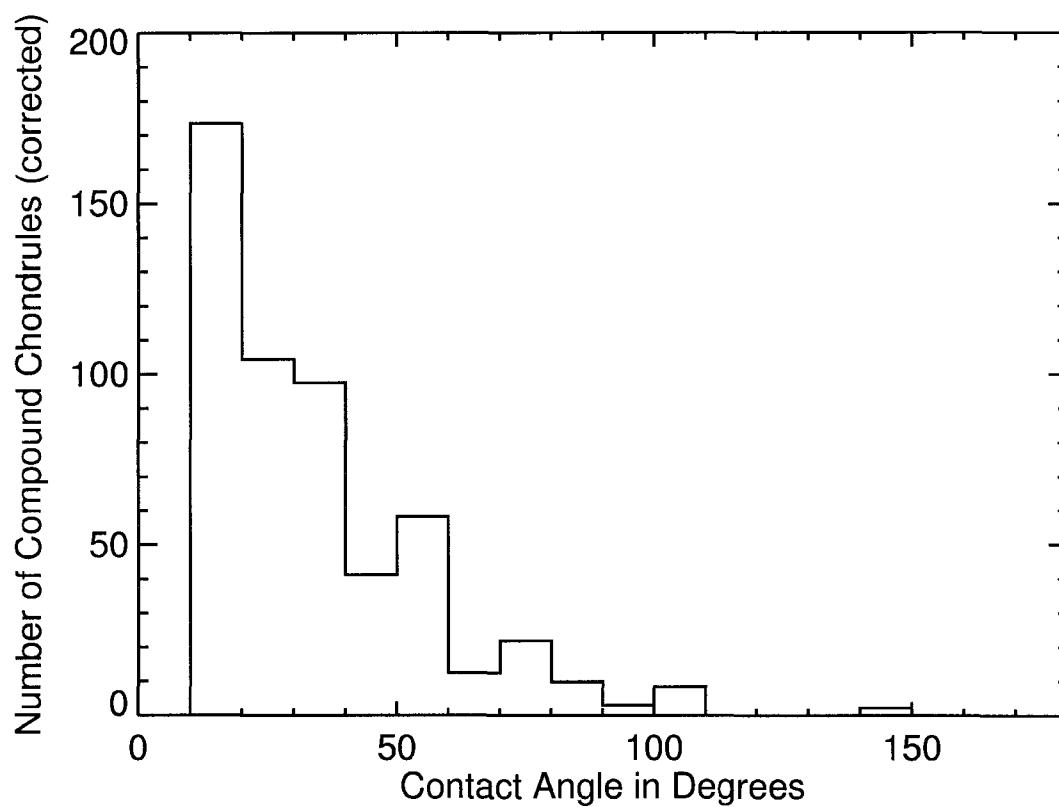
Figure 5.5: Shown is the same data as in Figure 3 after the correction factor (found using equation (4)) was applied to each bin.

Because Wasson *et al.* also documented the textures of the components in the compounds they observed, the compound chondrules can be grouped into the following categories: porphyritic-porphyritic (PP), non-porphyritic-non-porphyritic (NN), and mixed (M) (there were 3 compounds not included in this analysis because the textures of individual compound components were not unique). By making histograms for each of these categories and correcting for biases as described above, it is found that of all compound chondrules, 71% are NN, 25% are M, and 4% are PP. In addition, 92% of all secondaries (the most deformed component of the compound chondrule) are non-porphyritic, whereas 8% are porphyritic. These statistics will be further discussed below.

5.4   A More General Model for Chondrule Collisions

Having identified the fraction of chondrules that are compounds, a collisional model is needed to provide insight into the environment in which they may have formed. Even if most compound chondrules formed by the method proposed by Wasson *et al.* (1995), collisions among chondrules may have occurred. In fact, these authors argued that such collisions are likely responsible for sibling chondrules (those they believed formed in the same heating event). Therefore, a comprehensive model for chondrule collisional evolution is needed to understand how compound chondrules could form in this manner.

Gooding and Keil (1981) used principles from the kinetic theory of gases to calculate a collision rate for chondrules. They found the collisional probability to be:

$$P = \sqrt{2}\ \pi\ \overline{v}\ d^2\ n_c\ t_{plas} \tag{5.11}$$

where $\overline{v}$ is the average relative speed of the chondrules, d is the chondrule diameter, n_c is the number density of the chondrules, and t_{plas} is the period of time during which chondrules are plastic, or the time during which the chondrules are at temperatures above their solidus. Note that this equation does not allow predictions to be

made about the number of collisions that would produce multiple compound chondrules, 3 or more chondrules fused together. Such an outcome is possible, especially if $t_{plas} \approx 1000$s of seconds as suggested by recent studies (Desch and Connolly, 2002; Ciesla and Hood, 2002). To fully investigate the collisional history of chondrules, the principles of kinetic theory for a multi-species gas must be applied to extend the model of Gooding and Keil (1981).

The number of collisions per unit volume per unit time between two species, A and B, is (Vincenti and Kruger, 1965):

$$Z = \frac{n_A n_B}{\sigma} \pi d_{AB}^2 \bar{v}_{AB} \tag{5.12}$$

where n_A and n_B are the number densities of species A and B, $d_{AB} = (d_A + d_B)/2$ where d_A and d_B are the diameters of the respective species, $\bar{v}_{AB}$ is the average relative velocity of A with respect to B, and σ is a correction factor: If A=B then σ=2; otherwise σ=1. (Note that this factor was not included in the analysis of Gooding and Keil (1981).) For gas molecules:

$$\bar{v}_{AB} = \left(\frac{8kT}{\pi m_{AB}} \right)^{\frac{1}{2}} \tag{5.13}$$

where k is Boltzmann's constant, T is the temperature of the gas, and m_{AB} is defined as

$$m_{AB} = \frac{m_A m_B}{m_A + m_B} \tag{5.14}$$

where m_A and m_B are the masses of a molecule of A and B respectively. For the purposes of this study, $\bar{v}$ is defined as the average velocity of a single chondrule, and the average velocities of agglomerates scale with mass in the same manner as the gas molecules above. Therefore, when two agglomerates composed of i and j chondrules respectively are considered, the relative velocity of the two will be:

$$\bar{v}_{ij} = \sqrt{\frac{i+j}{i \times j}} \bar{v} \tag{5.15}$$

In this model, the effective diameters of the agglomerates scale as the geometric mean of their most extreme axes, i.e., the axes that the agglomerates would

have if all the constituent chondrules were collinear. Thus for an agglomerate made up of i chondrules, its effective diameter would be:

$$d_i = i^{\frac{1}{3}} d_1 \qquad (5.16)$$

where d_1 is the diameter of a single chondrule.

This model allows an initial number density of single chondrules to be set and then calculates the number of collisions that will occur for every time step through the period under consideration. At the end of each time step, the new size distribution is calculated and the process is repeated. The time step is chosen such that changes to the size distribution are small over that interval.

Figure 5.6 shows the results of some model runs for different concentrations of particles. A solar composition (concentration factor = 1) is defined as that where all solids are in the form of chondrules with a mass ratio of solids to gas of 0.005. The gas density was assumed to be 10^{-8} g cm^{-3} (reasonable for a post-shock region of the solar nebula). A chondrule mass density of 3.0 g cm^{-3} and a mean chondrule diameter of 0.6 mm (a value used so that the results can be compared to work of other authors) have been assumed, which gives a solar number density for the chondrules, n_c, of 1.5×10^{-7} cm^{-3}. The relative velocity of the chondrules with respect to one another, $\bar{v}$, is assumed to be 100 cm s^{-1}. This velocity is roughly that expected for chondrule sized objects in a solar nebula with a turbulence parameter, α, of order 10^{-4} (Cuzzi et al., 1998). Higher velocities likely would have resulted in disruption of the chondrules rather than fusing. In fact, Kring (1991) argued, based on surface tension calculations, that chondrules would be disrupted rather than fused if collisions took place at velocities greater than 130 cm s^{-1}.

Figure 5.6 plots the fraction of double chondrules (2 chondrules fused together) that result in clusters of given concentrations after 10^4 seconds have elapsed (the assumed plasticity time). This is approximately how long the chondrules remained plastic in the model runs presented in Desch and Connolly (2002). This value for the plasticity time is used because Desch and Connolly (2002) explored a
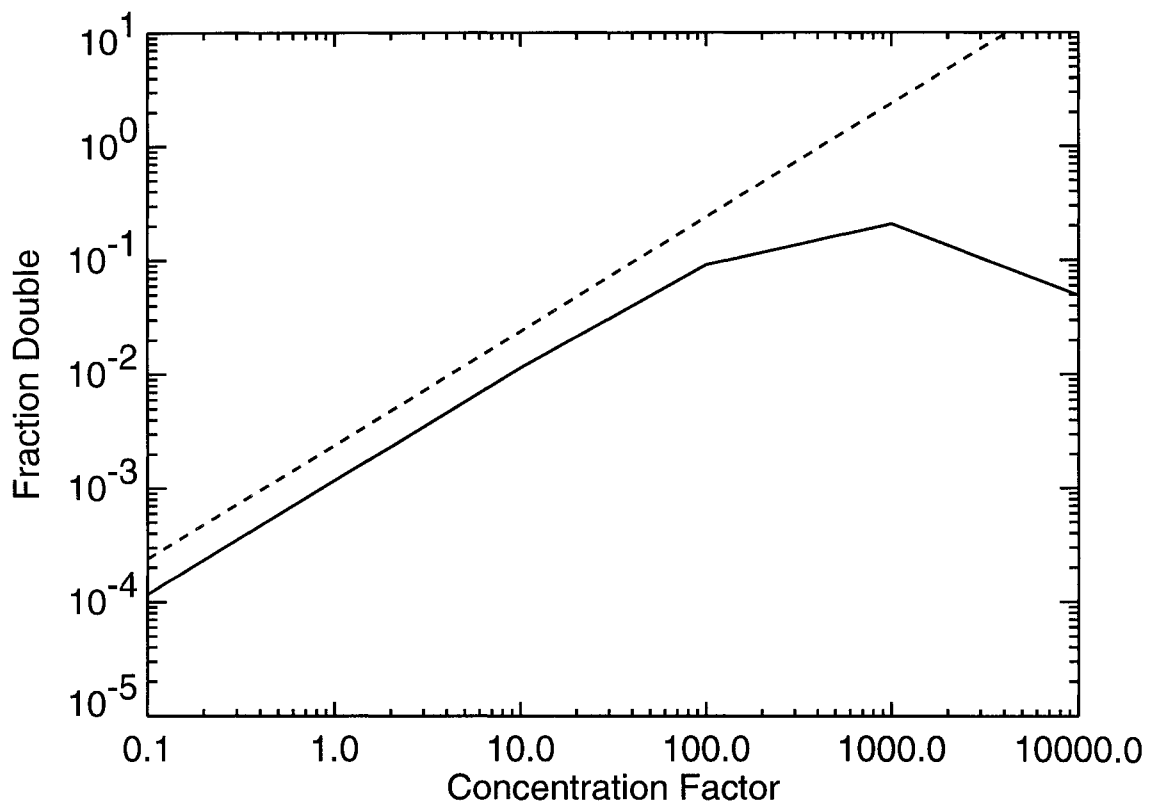
Figure 5.6: The fraction of double chondrules predicted for different concentrations of chondrules. The chondrules were assumed to have diameters of 0.6 mm, were plastic for 10000 seconds, and had mean relative velocities of 100 cm/s. Our model (solid line) predicts fewer doubles than does that of Gooding and Keil (dashed line).

large range of nebular conditions and found that this was the average plasticity time for chondrules and made specific predictions on the concentration of chondrules in the nebula. It should be pointed out that the plasticity time decreased with an increased concentration of particles.

The solid line represents the results of the model presented here, while the dashed line represents the predictions made by the equation given in Gooding and Keil (1981). The difference in the two models at low concentrations is a factor of 2, which comes from the correction factor Vincenti and Kruger (1965) introduce (the σ term in the collision frequency equations). As concentrations get higher, the difference grows. This is because at higher densities, the double chondrules are susceptible to collisions as well, and therefore are being destroyed as well as created. Also, the Gooding and Keil model was meant to predict a small number of collisions so that the number density of chondrules, n_c, would not change significantly as the system evolved. This is valid for the smaller concentrations due to the small frequency of collisions, but breaks down at higher concentrations of chondrules.

Another way of comparing the two models is shown in Figure 5.7, which plots the fraction of single chondrules left in a population after the system evolves as described for Figure 5.6. This method is better because it does not distinguish between chondrule aggregates composed of different numbers of the original chondrules. For low concentrations, the two models agree fairly well, but for concentration factors greater than 10, the Gooding and Keil (1981) model starts to underestimate the number of single chondrules remaining. In other words, at high concentrations (those greater than 10× solar), the Gooding and Keil (1981) model overestimates the number of compound chondrules that would be produced.

Table 5.1 shows more results of this new collisional model. For different concentration factors the percentage distribution of single, double, triple, and quadruple chondrules are listed. The percentages are defined as the number of objects composed of the corresponding number of individual chondrules divided by the number of agglomerates in a given volume. Thus a double chondrule is counted as a
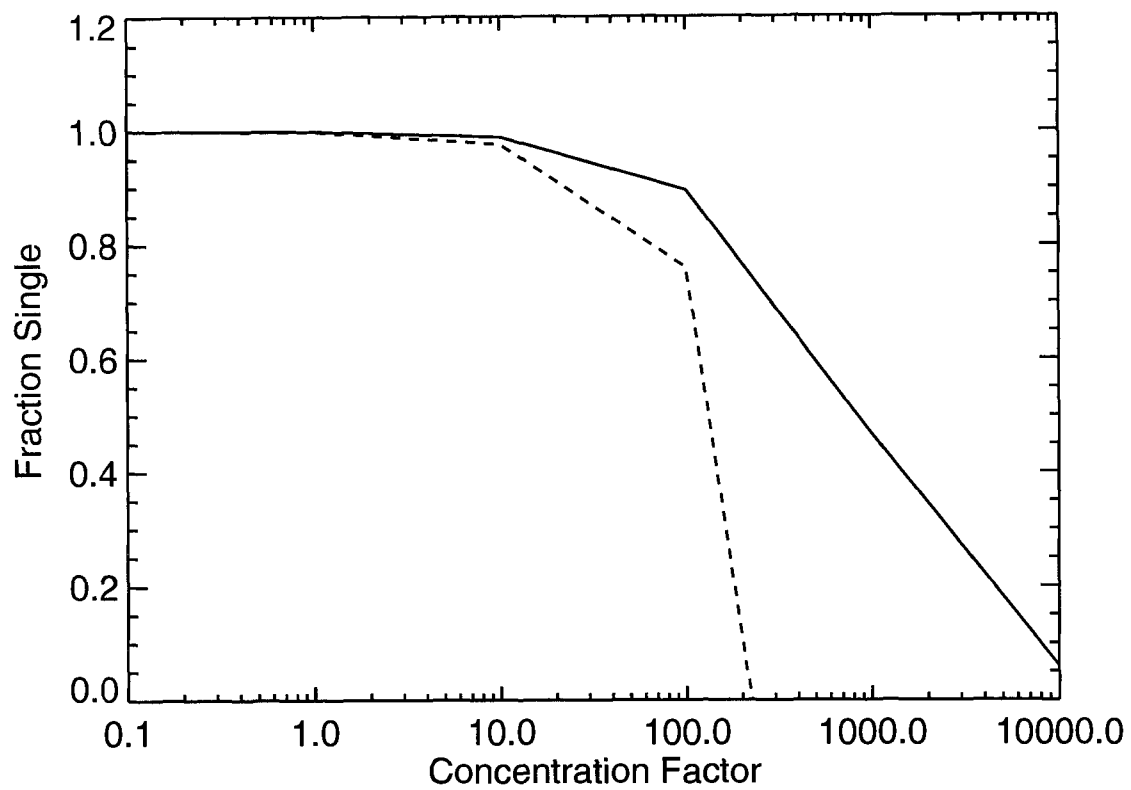
Figure 5.7: The fraction of single chondrules remaining for the cases examined in Figure 6. Our model (solid line) closely matches that of Gooding and Keil (dashed line) for small concentrations, but quickly diverges at high concentrations.

solitary double, not as two chondrules compounded together. The initial conditions in these simulations were the same as those described above. In order for 5% of all chondrules to be compounds, the concentration of chondrules must have been approximately 45 times the solar value. For cases with concentration factors above the canonical solar case, a small percentage of agglomerates will contain three or more of the original single chondrules. Thus compound chondrules are not limited to just two chondrules fused together in the collisional model. Identification of such objects in meteorites would support the hypothesis that compound chondrules formed via collisions.

5.5   Discussion

In deriving the formula for the probability of identifying an adhering compound chondrule in thin-section, a success was defined as when the thin-section cut through the projected length of the contact between the two components. It should be pointed out that if the thin-section was cut through the same compound chondrule nearly perpendicular to the line of centers such that it passed through the compound where the secondary chondrule was in contact with the primary, as shown in Figure 5.8, it could also be identified a compound chondrule. If this were the case, however, the thin-section slice would make it appear as an enveloping chondrule, not an adhering one. The probability of this is low, particularly for small contact angles, but only a tiny fraction (7.5%) of those chondrules identified in thin-section by Wasson *et al.* (1995) were of this type. Therefore, it could be possible that some, if not all, enveloping chondrules identified in thin-section do not come from compounds in which one chondrule surrounds another, but rather from adhering compounds which were sliced in a manner such that the primary appears surrounded by the secondary. Statistics of enveloping chondrules from whole chondrules removed from meteorites are needed to further investigate this possibility.

If compound chondrules did not form by the collisions of plastic chondrules,
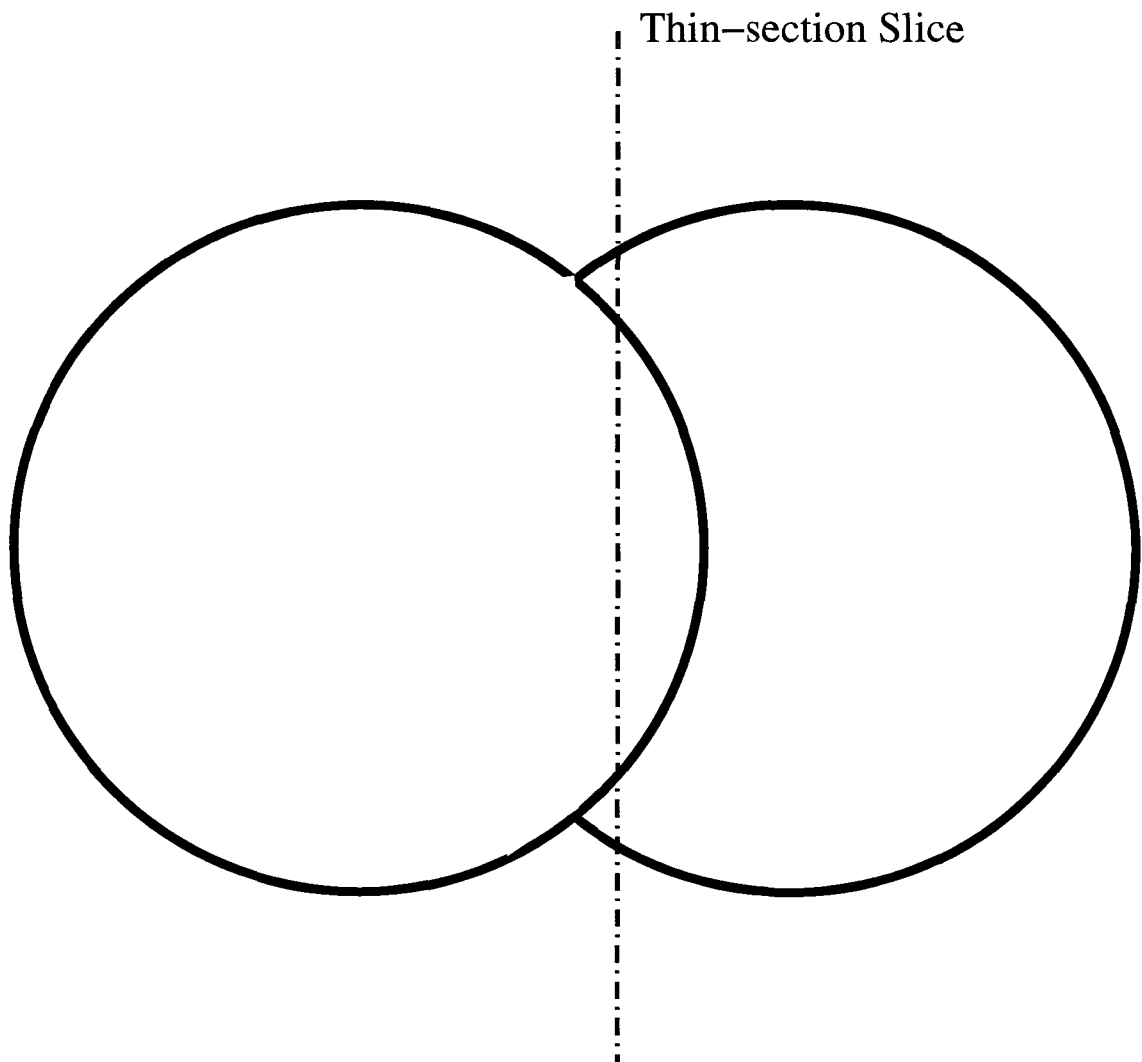
Thin–section Slice

Figure 5.8: A possible manner by which an adhering compound chondrule would be sliced by a thin-section. If cut in this manner, the compound would look like an enveloping compound and not an adhering compound.

but rather by the melting of loose aggregates on the surface of a primary chondrule as proposed by Wasson *et al.* (1995), then the results of this work can still provide some insight into the nebular environment at the time of their formation. Firstly, the higher frequency of compound chondrules suggests that more chondrules would have accreted porous aggregates between chondrule forming events than previously believed. Secondly, the strong preference in Figure 5 for small contact angles between adhering chondrules is likely a result of the way they formed, though it is unclear why melting of porous aggregates would lead to such a distribution.

If compound chondrules are the result of collisions among plastic chondrules, much can be inferred about the environment that chondrules formed in and the mechanism by which they formed. For example, in the context of the shock model of Chapter3, the cooling rates for chondrules behind shock waves were found to be greater for higher concentrations of chondrules (see also Desch and Connolly, 2002). This agrees well with the observation that non-porphyritic chondrules (those that have cooled rapidly) have a higher fraction of compound chondrules than do porphyritic ones. However, this needs to be reexamined, as discussed above, because porphyritic chondrules are not believed to melt as completely as non-porphyritic chondrules (Yu and Hewins, 1998). This more solid state would likely make the porphyritic chondrules more rigid, and therefore, less likely to stick or deform when collisions took place. Such an idea is supported by the data taken by Wasson *et al.* (1995). The average contact angle in adhering chondrules is significantly smaller when the secondary has a porphyritic texture. Also, of the 15 compound chondrules observed in which one of the adhering components is porphyritic and the other is not, the secondary is non-porphyritic in 11 of them. These two observations suggest that porphyritic chondrules do not deform as easily as non-porphyritic chondrules. Therefore, it may be possible that some porphyritic chondrules may have experienced collisions, but not formed compounds. If this were the case, then porphyritic chondrules may have experienced more collisions than compound chondrule statistics would suggest.

If this were not the case, then the discrepancy between the frequency of compound chondrules with non-porphyritic textures and those with porphyritic ones would provide information about how chondrules were formed. Specifically, if as described above, 71% of all compound chondrules are NN, then 3.5% of all chondrules are NN-compounds. According to Gooding and Keil (1981) 16% of all chondrules are non-porphyritic. Therefore, ~22% of all non-porphyritic chondrules are compounds. Based on the collisional model developed above, this would require non-porphyritic chondrules to form in regions of the nebula where chondrules were concentrated, on average, 200 times above the solar value. Likewise, if 4% of all compound chondrules are PP, then 0.2% of all chondrules are PP-compounds. Because 84% of all chondrules are porphyritic (Gooding and Keil, 1981), 0.23% of all porphyritic chondrules are compounds, implying that they formed in regions of the nebula where chondrules were concentrated, on average, at about the canonical solar value.

It is important to note that 25% of all compound chondrules (1.3% of all chondrules) have both porphyritic and non-porphyritic textures in their components. The textures of chondrules are representative of their thermal histories. Therefore, if these compound chondrules were formed by the collision of individual chondrules, those individual chondrules reached different peak temperatures and/or cooled at different rates. This could be achieved in two different manners: 1) the chondrules formed in different heating events, and the secondary formed in a region of the nebula in close proximity to cooler chondrules such that it could collide with one while still plastic, or 2) the chondrules were formed in the same heating event and the differences in thermal histories are due to differences in how they were processed. Those models which have produced thermal histories of silicate particles consistent with those inferred with chondrules (Chapter 3, Desch and Connolly, 2002) require very large formation regions of chondrules which suggests that the former possibility is not likely. However, it should be pointed out that the shock waves in these models produce a single thermal history for the particles, and therefore predict that all the chondrules formed in a shock wave would have the same or

similar textures. Investigation of how different chondrule textures can be formed in the same shock wave are needed. This could be due to the finite extent of a particular concentration of chondrules in the nebula or the different physical properties of the different chondrule precursors (emissivity, absorptivity, heat capacity, mass, grain size distribution).

As discussed above, considering the distribution of contact angles for adhering chondrules in Figure 5.5, a preference for small contact angles ($\phi < 90°$) is strongly noticeable. This also can be explained by the shock wave model. In the shock wave model, chondrules are hottest immediately behind the shock front and cool as they drift away from the shock front. Chondrules will deform most easily during collisions when they have low viscosity, which would correspond to when they are at higher temperatures. That is, chondrules will deform most (have higher contact angles) immediately behind the shock front. At lower temperatures, the deformation would be less and result in lower contact angles in compound chondrules. In the shock model, the number density of chondrules increases dramatically shortly after passing through the shock front before settling on a roughly constant (higher) value as the chondrules drift from the shock front (Chapter 3). Therefore, collisions would be much more frequent among chondrules while they were at the lower temperatures and therefore less deformable. The distribution in Figure 4 thus could be a direct result of this compression and cooling.

The concentrations reported here depend strongly on the assumption that the post shock region had a gas density of 10^{-8} g cm^3 during the time that chondrules were warm enough to deform plastically. Again, if the density of the gas during this time period was lower, this would lead to requiring higher concentrations of particles. Likewise, if the gas density were higher in this region, then the relative concentrations would be lower. Thus, if the density of the post-shock gas was 2×10^{-8} g cm^{-3}, the required enhancement of chondrules would be ~ 25 times greater than the canonical solar value, close to the value predicted by Desch and Connolly (2002).

The density of the gas behind a shock is determined by its density far upstream from the shock and the velocity (Mach number) of the shock. In order to produce a higher gas density behind the shock, the nebula must have been more dense (massive) or the shocks must have been stronger than those that have been studied (Desch and Connolly, 2002; Ciesla and Hood, 2002) Passage through a shock front increases the gas density by no more than a factor of 6 (very fast shocks), and those considered thus far increase the density by a factor of 3-4. To double this enhancement, if possible, would require a shock with a velocity much greater than those studied and thus, different shock sources than those studied. However, while this would increase the gas density, it would also increase the gas temperature, which would likely lead to temperatures for chondrules much higher than the range of peak temperatures deduced by experiments. Therefore it is unlikely that faster shocks could lead to significantly higher gas densities and still produce chondrules.

If the initial gas density of the chondrule forming region were two times greater than has been studied, this suggests either chondrule formation took place closer to the proto-sun or the solar nebula was more massive than has been studied. The former possibility is limited, as closer to the sun would imply higher temperatures, and chondrule precursors originally had to be below the temperature at which troilite formed (< 650 K in the canonical nebula). Also, if this were the case, chondrules would have to be transported back out to the asteroid belt region after their formation. If the nebula were instead more massive, this would support the hypothesis that chondrules formed in a gravitationally unstable disk of the type described by Boss (2002). However, if the disk is roughly two times more massive than had been studied, this would significantly change the ambient temperature and pressure or radial distance at which chondrules formed (c.f. Boss, 1996). It should be pointed out that Desch and Connolly (2002) investigated shocks caused by a gravitationally unstable disk and concluded that the post shock region would have a gas density $\sim 10^{-8}$ g cm^{-3} immediately behind the shock. Thus, it is unlikely that the post-shock gas density was much higher than what has been considered here.

The result that 5% of chondrules are compounds implies that chondrules formed, on average, in regions of the nebula where chondrules were more concentrated than previously believed. Based on the model presented in this paper, the average concentration of particles was ~45 times greater than that expected for those conditions behind a shock wave in the canonical solar nebula. This number could prove to be conservatively low because it was assumed that all solids were in the form of chondrules. If some fraction of the mass of solids was present as dust in addition to chondrules, as is expected (Hood and Ciesla, 2001), or if the mass density of chondrules is higher than the assumed 3 g cm^{-3}, a higher concentration factor would be needed. For example, using the numbers of Desch and Connolly (2002), who assumed that 75% of the solids existed as chondrules and the density of the chondrules was 3.3 g cm^{-3}, the average concentration factor would be ~60 rather than 15, as found by those authors. Likewise, if the sticking efficiency of plastic chondrules is less than 1, as might be expected as chondrules cool and become more rigid, or if the time that chondrules are plastic is less than 10^4 seconds, then a larger concentration of chondrules would be required. Models for chondrule formation other than the shock model would have to enhance solids to much higher relative concentrations (all concentrations discussed have assumed that the nebular gas was compressed by a shock wave). Such enhancements would be difficult (Weidenschilling, 2002).

Many mechanisms have been suggested for concentrating solids in the solar nebula, among them are turbulent concentration, gravitational settling to the midplane, and collisional disruption of planetesimals (c.f. Hood and Ciesla, 2001). The latter mechanism has not been studied quantitatively, so expected concentrations produced in this way are unknown. Desch and Connolly (2002) found that the compound chondrule population matches well with the predicted time particles spend in turbulent concentrations according to Cuzzi *et al.* (2001). However, these authors argued that chondrules formed in areas of the nebula with an average concentration factor of 15, based on a compound chondrule population of 2.4%, not 5%. The average concentration factor of 45 found by this study could still result

from turbulent concentrations; however, as mentioned above, this is only a lower limit. If the average concentration factor is much higher, this would likely be the result of gravitational settling to the midplane.

The results of this chapter depend strongly on the detailed data of Wasson *et al.* (1995). Future thin-section investigations of compound chondrules should be as comprehensive as the study carried out by those authors in order to maximize the information that can be deduced. While much still needs to be studied, the frequency and distribution of contact angles for compound chondrules appear to be explained best by the collisions of a group of chondrules as they cool and become spatially concentrated. While other mechanisms can not be definitively ruled out, this does offer support to the hypothesis that shock waves were the dominant chondrule forming mechanism in the solar nebula.

5.6 Summary

Thin-section studies of compound chondrules have been performed by previous authors, though interpretations of their results have proven difficult. The uncertainty in where the thin-section cut intersects the compound can lead the observer to believe that it was not a compound at all. Simple geometric models were used to correct for this uncertainty and were applied to previous thin-section studies. These corrections showed that compound chondrules may be more common than previously believed, and the different compound structures are easily explained by the shock wave model for chondrule formation. Future studies using techniques such as X-ray tomography may allow further interpretation of compound chondrules without being subject to the biases and uncertainties inherent with those of thin-sections.

Table 5.1: Distribution of chondrule agglomerates after 10000 seconds of collisional evolution

Concentration Factor	Single	Double	Triple	Quadruple
1	99.88 %	0.12	0.00	0.00
10	98.84	1.15	0.01	0.00
20	97.70	2.24	0.06	0.00
30	96.60	3.28	0.12	0.00
40	95.51	4.27	0.21	0.01
50	94.45	5.21	0.32	0.02
60	93.41	6.11	0.44	0.03
70	92.40	6.96	0.58	0.05
80	91.41	7.78	0.73	0.07
90	90.44	8.56	0.89	0.10
100	89.49	9.30	1.07	0.13

CHAPTER 6

Formation of Fine-Grained Phyllosilicates in Shock Waves

6.1 Introduction

Chondrules are often found in meteorites surrounded by fine-grained rims (FGRs) composed of similar material as that found in the chondrite matrix (Jones *et al.*, 2000). These rims range in thickness from 10s to 100s of microns thick and have been interpreted as dust that accreted onto the chondrules at low temperatures between their formation and incorporation into their respective parent bodies (Metzler and Bischoff, 1996). The thickness of the rims generally increase with chondrule size, which has led some authors to suggest that this dust was accreted close to the sites where the chondrules formed (Morfill *et al.*, 1998).

The textures and chemistry of FGRs have been studied in detail for most chondrite groups. In general, these rims are composed of silicates, metals, and sulfides (Metzler and Bischoff, 1996). Among the most studied FGRs are those found in the CM carbonaceous chondrites. These meteorites are of particular interest to planetary science because they are rich in both water and organic molecules, making them prime candidates for the source of Earth's prebiotic material. The majority of their water is contained within phyllosilicates which are found in the FGRs of the chondrules that they contain. The presence of hydrated grains in their rims makes these FGRs stand out from the anhydrous ones found in most other chondrites.

The phyllosilicates in the CM FGRs typically occur as extremely small grains (10–100 nm), and are often in direct contact with anhydrous minerals, suggesting that these phyllosilicates had formed before they were accreted into the

chondrule rims (Metzler *et al.*, 1992; Lauretta *et al.*, 2000). The most abundant phase in these rims is chrysotile, $Mg_3Si_2O_5(OH)_4$, which occurs as small (< 20 nm) crystals with cylindrical or fibrous morphologies. The second most abundant phase is cronstedtite, $(Fe^{+2,+3})_3(Fe^{+3},Si)_2O_5(OH)_4$, which occurs as relatively large, platy grains up to 500 nm long and 100 nm wide. Some cronstedtite is coherently intergrown with tochilinite, $FeS \cdot Fe(OH)_2$ (Lauretta *et al.*, 2000).

While phyllosilicates (e.g. serpentine, brucite) were found to be thermodynamically stable in the canonical solar nebula, the reaction that would form them is believed to have been too slow under these conditions for them to have formed during the lifetime of the solar nebula (Fegley and Prinn, 1989). In order to form phyllosilicates in the nebula, anhydrous grains would have had to been exposed to H_2O pressures that were enhanced by many orders of magnitude over that which was found in the canonical solar nebula. One place that this may have occurred was in a giant planet subnebula (Fegley and Prinn, 1989). Metzler *et al.* (1992) argued that while the phyllosilicates may have formed in this environment, the large gravity associated with the giant planet subnebula would not allow the minerals to be accreted in smaller bodies.

To resolve this issue, a complex history for the origin of fine-grained phyllosilicate minerals was proposed by Metzler *et al.* (1992). In this model, silicates accreted with water ice to form an uncompacted planetesimal. The ice then melted, and the conditions in the planetesimal were such that liquid water was stable. This water reacted with anhydrous silicates to form the phyllosilicates. This planetesimal was then catastrophically disrupted, and the phyllosilicates were dispersed into the nebula. Chondrules and other coarse-grained components then encountered this debris which accreted onto their surfaces forming FGRs. The chondrules and FGRs then accreted together to form the CM parent body.

In this chapter, an alternative origin for the formation of phyllosilicates in the solar nebula is presented. As stated above, the formation of such minerals would be possible in a region of the nebula where the water vapor pressure was many orders

of magnitude above the canonical solar value. Such increases in pressure may have been a natural result of chondrule forming shock waves. If shocks could increase the water vapor pressure to the values needed for rapid silicate hydration, they could then be responsible for the formation of chondrules and the grains which are found in their rims.

6.2 Kinetics of Hydration

The chemical reaction used in this study is the hydration of forsterite to serpentine and brucite:

$$2Mg_2SiO_4 + 3H_2O \rightarrow Mg_3Si_2O_5(OH)_4 + Mg(OH)_2$$
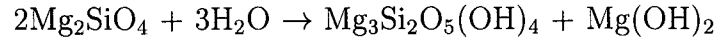
Chemical equilibria studies have shown that the products of this reaction were stable in the solar nebula at temperatures below 225 K (Fegley and Prinn, 1989). The time scale for this reaction to go to completion were calculated using using Simple Collision Theory (SCT) (Fegley and Prinn, 1989). SCT allows the collision rate between the reactants (the gaseous water molecules and the forsteritic grains) and the energies of each of these collisions to be claclulated. For those collisions which had energies equal to or greater than the activation energy of the reaction, the reaction proceeded in the forward direction. The time scale for completion of this reaction is the amount of time it takes for all of the forsterite to be hydrated.

SCT calculations are done as follows (Fegley and Prinn, 1989). The collision rate (molecules per cm^2 per second) of water molecules on the surface of the grains is given by

$$\sigma_{H_2O} = 10^{25.4} \frac{P_{H_2O}}{(m_{H_2O}T_g)^{\frac{1}{2}}} \tag{6.1}$$

where P_{H_2O} is the water vapor pressure in bars, m_{H_2O} is the molecular weight of water in g/mol, and T_g is the temperature of the gas.

The total number of collisions per unit volume per second is therefore

$$\nu_{H_2O} = \sigma_{H_2O} \times A_{forsterite} \tag{6.2}$$

where $A_{forsterite}$ is the total surface area of the forsterite grains per cm^3. The time that it takes for all of the water molecules to collide with all of the forsterite grains is

$$t_{coll} = \frac{n_{H_2O}}{\nu_{H_2O}} \tag{6.3}$$

where n_{H_2O} is the number of water molecules per cm^3. The number of these collisions which take place with an energy greater than the activation energy, E_a, is given by

$$f_{H_2O} = \nu_{H_2O} \exp\left(\frac{-E_a}{RT_g}\right) \tag{6.4}$$

where R is the ideal gas constant. The time scale for the reaction to go to completion is then given by

$$t_{chem} = \beta\, t_{coll} \exp\left(\frac{E_a}{RT_g}\right) \tag{6.5}$$

where β is the molar ratio of forsterite to water.

Fegley and Prinn (1989) used an activation energy of 70 kJ/mol in their original study. Their results are reproduced in Figure 6.1. The time scales for the hydration of forsterite grains with diameters of 10 nm, 100 nm, 1 μm, 10 μm, and 100 μm are shown on the curves for a range of temperatures. This calculation assumes a standard nebula total pressure of 10^{-5} bars with a solar composition of water vapor. The different sized grains have different time scales due to the varying surface area to volume ratios. A higher surface area allows for more total collisions, which allows the reaction to occur more rapidly.

The time scales of interest are those at the point at which serpentine is stable, in this case at 225 K. Even for the smallest grains, 10 nm, the time scale for hydration is 10^{16} seconds (3×10^8 years) which is much longer than the expected lifetime of the solar nebula and therefore the gas would have dissipated before the reaction was completed.
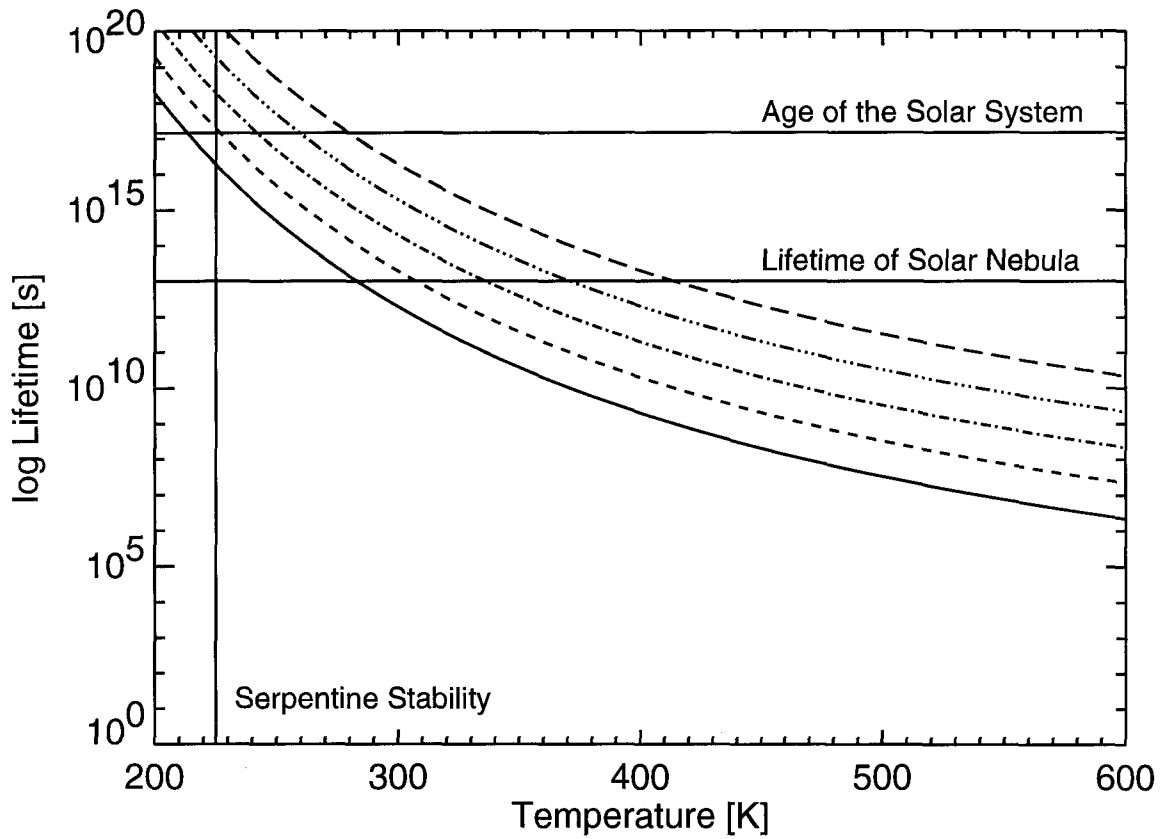
Figure 6.1: Above are the time scales for complete hydration of forsteritic grains in the canonical solar nebula. The different curves are for, starting with the lowest, 10 nm diameter grains, 100 nm, 1 micron, 10 microns, and 100 microns, where the different time scale for formation of these grains are due to their different surface area to volume ratios. The expected lifetime of the solar nebula and the age of the solar system are shown for comparison. This figure follows that shown in Fegley and Prinn (1989).

The activation energy used in this work is the same as that used by Fegley and Prinn (1989). This activation energy is based on the amount of energy required to convert MgO to Mg(OH)$_2$. Based on experimental studies of forsterite hydration, it has been suggested that this activation energy is too high (Wegner and Ernst, 1983; Sears and Akridge, 1998). However, these experiments were done under much different conditions than those expected for the solar nebula. In the work presented here, the activation is assumed to be 70 kJ/mol with the understanding that if the actual activation energy of this reaction is lower then the hydration reaction would occur much more rapidly.

6.3 Water Vapor and Ice in the Solar Nebula

Above the condensation point of water, the water vapor pressure in the canonical solar nebula would be (Supulver and Lin 2000):

$$P_{H_2O} = 5.1 \times 10^{-4} \ P_{H_2} \tag{6.6}$$

Water ice began to form in the nebula in regions where the equilibrium water vapor pressure is below the actual water vapor pressure. The distance from the sun where this began to take place depended on the temperature and pressure structures of the solar nebula, and likely migrated during its lifetime (Cassen, 1994).

Cyr *et al.* (1998) looked extensively at the distribution of water vapor in the inner part of the solar nebula. Her model traced the diffusion of water vapor from the inner nebula to the condensation front, and then tracked the resulting ice particles as they migrated inwards due to gas drag and began to sublimate. The inner nebula would lose its water in $\sim 10^5$ years if the ice particles did not drift inwards. This is much shorter than the time between nebular formation and the onset of chondrule formation ($>10^6$ years) (Amelin *et al.*, 2002). Therefore, if the inward migration of ice particles was slowed by some mechanism (e.g. transient heating, rapid accretion into large bodies), the amount of ice found at the snow line would be much larger than expected under canonical solar nebular conditions.

In addition to diffusive redistribution of water vapor, there are other mechanisms that would operate that could lead to different concentrations of water vapor or ice in the nebula. Over time, the solids that formed in the nebula would settle to the midplane as discussed by Weidenschilling (1988). This could lead to enhancements of solids by factors up to 100 or more. In fact, this mechanism has been studied at a heliocentric distance of 30 AU and was able to create concentrations at the midplane with a solids/gas mass ratio of $\sim 10^3$ (approximately 10^5 times the solar value). In addition, as discussed by Cuzzi *et al.* (2001), turbulence in the nebular gas may concentrate particles by factors of 1000 (or more) above the canonical solar value. Thus the concentrations of water vapor/ice could have varied by orders of magnitude in different locations throughout the solar nebula.

6.4   Model for Shock Waves in Icy Regions of the Nebula

The model used in this study is a modification of the one used in Chapter 3. It was modified to include a second solid species made entirely of water ice. The water ice particles are heated in the same manner as the silicate particles, except mass loss by evaporation is taken into account. This loss affects the momentum and energy of the ice particles as discussed below.

The energy and momentum of the silicate particles are described by the same equations as those in Chapter 3. Therefore the equations that describe their evolution can be written:

chondrule continuity

$$\frac{d}{dx}\left(\rho_{chon}v_{chon}\right) = 0 \tag{6.7}$$

chondrule momentum

$$\frac{d}{dx}\left(\rho_{chon}v_{chon}^2\right) = F_{D,chon} \tag{6.8}$$

chondrule energy

$$\frac{d}{dx}\left[\left(C_{chon}T_{chon} + \frac{1}{2}v_{chon}^2\right)\rho_{chon}v_{chon}\right] = Q_{g,chon} + Q_{p,chon} - Q_{chon,rad}$$
$$+ F_{D,chon}v_{chon} \qquad (6.9)$$

where ρ_{chon} is the mass density of the chondrules in the suspension, v_{chon} is the velocity of the chondrules with respect to the shock front, $F_{D,chon}$ is the drag force per unit volume due to the chondrules passing through the gas, C_{chon} is the heat capacity of the chondrules, T_{chon} is the temperature of the chondrules, $Q_{g,chon}$ is the rate of energy transfer per unit volume of the gas to the chondrules due to collisions, $Q_{p,chon}$ is the rate of energy gained per unit volume by the chondrules from the radiation of surrounding particles, and $Q_{chon,rad}$ is the rate of energy loss per unit volume by the chondrules due to radiation.

The water ice particles are described by similar equations, except that water molecules are allowed to escape to the gas phase. The rate at which this happens is equal to the sublimation rate minus the condensation rate. These were calculated using the equations given by Supulver and Lin (2000) who applied the experimental results of Haynes *et al.* (1992). The sublimation rate is given by:

$$J_{sublime} = -0.63 P_{eq}\left(\frac{\mu}{2\pi kT_{ice}}\right)^{\frac{1}{2}} \qquad (6.10)$$

and the condensation rate is given by:

$$J_{condense} = \left(1.04 - \frac{T_{ice}}{500}\right)\left(\frac{\mu}{2\pi kT_g}\right)^{\frac{1}{2}} P_{vap} \qquad (6.11)$$

where P_{eq} is the equilibrium vapor pressure of water, μ is the molecular mass of the water vapor, k is the Boltzmann constant, and T_{ice} is the temperature of the ice, T_g is the temperature of the gas, and P_{vap} is the effective vapor pressure of water. Combining these, we can find the equation for mass loss:

$$\frac{dm_{ice}}{dt} = 4\pi a^2\left(J_{condense} + J_{sublime}\right) \qquad (6.12)$$

Using the notation of Chapter 3, the equations that show how the ice particles evolve can be written as:

ice particle mass loss

$$\frac{dm_{ice}}{dx} = \frac{1}{v_{ice}}\frac{dm_{ice}}{dt} \tag{6.13}$$

ice particle continuity

$$\frac{d}{dx}\left(\rho_{ice}v_{ice}\right) = \frac{\rho_{ice}}{m_{ice}}v_{ice}\frac{dm_{ice}}{dx} \tag{6.14}$$

ice particle momentum

$$\frac{d}{dx}\left(\rho_{ice}v_{ice}^2\right) = F_{D,ice} + \frac{\rho_{ice}}{m_{ice}}v_{ice}^2\frac{dm_{ice}}{dx} \tag{6.15}$$

ice particle energy

$$\frac{d}{dx}\left[\left(C_{ice}T_{ice} + \frac{1}{2}v_{ice}^2\right)\rho_{ice}v_{ice}\right] = Q_{g,ice} + Q_{p,ice} - Q_{ice,rad}$$
$$+F_{D,ice}v_{ice} + L\frac{\rho_{ice}}{m_{ice}}v_{ice}\frac{dm_{ice}}{dx}$$
$$+\frac{1}{2}n_{ice}v_{ice}^3\frac{dm_{ice}}{dx}$$
$$+C_{ice}T_{ice}\frac{\rho_{ice}}{m_{ice}}v_{ice}\frac{dm_{ice}}{dx} \tag{6.16}$$

where ρ_{ice} is the total mass density of ice particles suspended per unit volume, v_{ice} is the velocity of the ice particle with respect to the shock front, $F_{D,ice}$ is the drag force per unit volume of the gas on the ice particle, C_{ice} is the heat capacity of the ice, T_{ice} is the temperature of the ice particle (assumed to be isothermal), $Q_{g,ice}$ is the heating rate per unit volume of the ice particle due to collisions with the gas, $Q_{p,ice}$ is the heating rate per unit volume of the ice particles due to absorption of radiation from all particles in the suspension, $Q_{ice,rad}$ is the rate of heat loss per unit volume by the particles due to radiation, and L is the latent heat of vaporization of the ice.

As the ice particles evaporate, their mass is lost to the surrounding gas. The equations that describe the evolution of the gas must be modified to take this into account. Therefore the equations describing the evolution of the gas are:

molecular hydrogen continuity

$$\frac{d}{dx}\left(n_{H_2}v_g\right) = -\eta_{H_2} \tag{6.17}$$

atomic hydrogen continuity

$$\frac{d}{dx}\left(n_H v_g\right) = 2\eta_{H_2} \tag{6.18}$$

water vapor continuity

$$\frac{d}{dx}\left(\rho_{H_2O}v_g\right) = -\frac{\rho_{ice}}{m_{ice}}v_{ice}\frac{dm_{ice}}{dx} \tag{6.19}$$

gas momentum equation

$$\frac{d}{dx}\left[\left(\rho_{H_2} + \rho_H + \rho_{H_2O}\right)v_g^2 + P_{Total}\right] = -F_{D,chon} - F_{D,ice} - \frac{\rho_{ice}}{m_{ice}}v_{ice}^2\frac{dm_{ice}}{dx} \tag{6.20}$$

gas energy equation

$$\frac{d}{dx}\left[\left(\rho_{H_2}C_p^{H_2} + \rho_H C_p^H \rho_{H_2O}C_p^{H_2O}\right)v_gT_g + \frac{1}{2}\left(\rho_{H_2} + \rho_{H_2O}\right)v_g^3\right] =$$
$$-Q_{g,ice} - Q_{g,chon} - Q_{g,diss} - F_{D,ice}v_{ice} - F_{D,chon}v_{chon}$$
$$-\frac{1}{2}\frac{\rho_{ice}}{m_{ice}}v_{ice}^3\frac{dm_{ice}}{dx} + C_p^{H_2O}T_{ice}\frac{\rho_{ice}}{m_{ice}}v_{ice}\frac{dm_{ice}}{dx} \tag{6.21}$$

where ρ_{H_2}, ρ_H and ρ_{H_2O} are the mass densities of the hydrogen molecules, the hydrogen atoms and the water molecules in the gas, P_{Total} is the total pressure of the gas, and $C_p^{H_2}$, C_p^H and $C_p^{H_2O}$ are the specific heats (at constant pressure) for the hydrogen molecules, hydrogen atoms, and water vapor molecules in the gas, and $Q_{g,diss}$ is rate of energy loss from the gas per unit volume due to hydrogen dissociation. This model assumes that the water vapor and hydrogen molecules in

the gas are coupled together enough such that they have the same velocity, v_g and temperature, T_g.

All calculations are done in the free molecular flow approximation, and the drag force and heat exchange terms are calculated as discussed in Chapter 3. Because the gas consists of hydrogen molecules, hydrogen atoms and water vapor, the exchange terms, $Q_{g,chon}$ and $Q_{g,ice}$ were calculated for all gaseous species, assuming that they were at the same temperature, T_g, and velocity v_g and then summed together. The radiation due to the presence of two different species of different temperatures and optical properties (ice and chondrules) were handled in the same manner as by Desch and Connolly (2002), though it was found that the thermal radiation emitted from the ice particles before vaporization could be ignored.

6.5   Model Results

For the results presented here, all silicate and ice particles were treated originally as 1 millimeter diameter isothermal spheres. The silicates were assumed to have the same properties as in Chapter 3: a heat capacity of 10^7 erg g^{-1} K^{-1}, a latent heat of melting of 4.5×10^9 erg g^{-1} spread over the temperature range 1400 to 1900 K, wavelength averaged emissivities of 0.9, and mass densities of 3.3 g cm^{-3}. The ice particles were assumed to be pure and had a particle density of 1 g cm^{-3} with thermal properties as described by Moses (1992): heat capacity of 4.2×10^7 erg g^{-1} K^{-1}, latent heat of melting was 3.35×10^9 erg g^{-1} (melting temperature of 273 K), latent heat of vaporization was 2.8×10^{10} erg g^{-1} and 2.5×10^{10} erg g^{-1} for the solid and liquid phases respectively. Because the ice particles changed in size as they sublimated, the optical properties of the particles would change as well. In all cases considered, the temperature of the ice particles never got above 270 K. Therefore, the peak wavelengths (as determined by Wien's Law) that the ice particles would be emitting at were never shorter than 10 μm and never longer

than 20 μm (corresponding to a temperature of 150 K, the lowest temperature considered in this model). This is the same general range of wavelengths considered byMoses (1992), who used real and imaginary indices of 1.4 and 0.4 to calculate the emissivities of the ice particles. We used these indices and Equation (3) of Rizk *et al.* (1991) to calculate the emissivity of the ice particles when their radii were less than 60μm (when the radii were comparable to the peak wavelength they would radiate at); otherwise their emissivity was assumed to be 1. This approximation was valid since the resulting vapor pressure of water did not depend significantly on the optical properties used for the ice particles. (To test this, cases where the emissivity of the water ice was assumed to be 1 regardless of the radii of the ice particles were run, and the resultant vapor pressure varied by a very small fraction of a percent.)

The hydrogen molecules were assumed to have a ratio of specific heats of 7/5 and a mean molecular mass of 3.34×10^{-24} g while the hydrogen atoms were assumed to have a ratio of specific heats of 5/3 and a mean molecular mass of 1.67 $\times 10^{-24}$ g. The water molecules were assumed to have a ratio of specific heats of 9/7 and a mean molecular mass of 3.01×10^{-23} g. In all cases it was assumed that the final temperature of the suspension would be the same as the initial temperature far upstream from the shock. These temperatures represent the boundary conditions assumed for the radiative transfer treatments.

The velocity of the shock here is chosen to be 5 km/s in the cases presented here. The reason for this is that icy regions of the nebula would be located further out from the sun than those regions that have thus far been considered for chondrule formation. In all proposed shock generating mechanisms, the velocity of the shock with respect to the nebular gas decreases with increasing distance from the proto-sun (Weidenschilling *et al.*, 1998; Boss, 2000). In addition, solid ice is chosen to be enhanced over the equilibrium value by a factor of 700. This factor was chosen such that the peak temperature of the chondrules would be just above 1900 K (as was done in Chapter 3). The dependence of the results of this chapter on this number

will be discussed below.

Figure 6.2 shows the temperature profile of the silicate particles in this simulation. The sharp increase in temperature approximately 15 hours upstream of the shock represents the point where the ice particles have vaporized. Further upstream of this point, the ice particles still exist and dominate the opacity of the nebula. Once the particles are completely vaporized, the silicates heat up rapidly due to the increased intensity of the radiation. As the shock front approaches, they are warmed even more to approximately 1400 K before crossing it. At that point, gas drag dominates the heating and the particles reach a peak temperature of 1980 K, before beginning to cool.

The cooling profile of the particles is shown in Figure 6.3. The profile follows the general trend discussed in Chapter 3, where the cooling is rapid initially before reaching a more gradual rate through the end of crystallization. In this particular case, the cooling rate of the particles as they approach the solidus temperature of 1400 K is 10 K/hr. Thus the peak temperature and cooling history of these particles is consistent with the thermal histories inferred for chondrules.

Figure 6.4 shows the thermal profile of the gas in this model. The increase in temperature approximately 250,000 km upstream of the shock again represents the point where the ice particles vaporized. At that point, the gas gets heated due to conduction from the silicates, and continues to be heated until passing through the shock front. Immediately behind the shock, the gas cools rapidly due to hydrogen dissociation, before cooling more gradually back to 150 K. The distance over which this occurs is roughly 300,000 km (0.002 AU) which is smaller than the shocks predicted by Boss (2000).

Figure 6.5 shows the pressure profiles of the gas in this system. The solid line represents the water vapor pressure. Initially, this water vapor pressure was at the equilibrium value at 150 K ($\sim 8 \times 10^{-11}$ bars). As the water ice began to vaporize, the water pressure increased to 5.5×10^{-6} bars, before being further
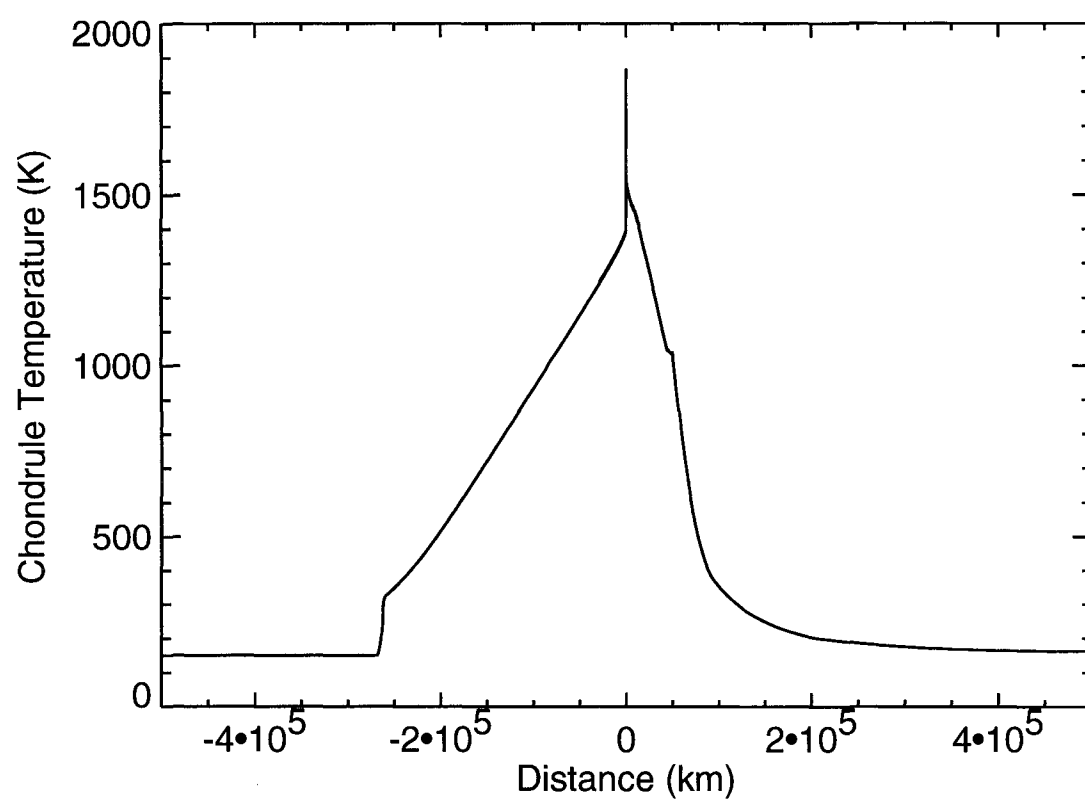
Figure 6.2: The thermal evolution of the silicate particles in this model.
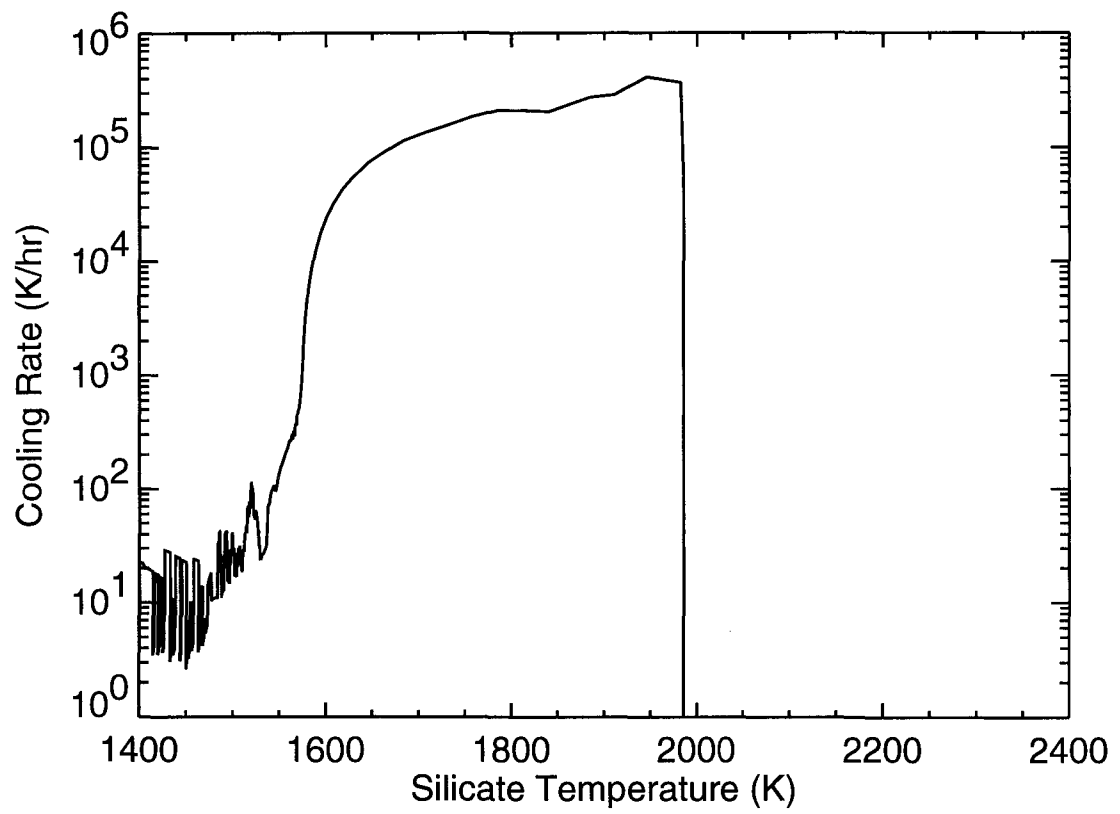
Figure 6.3: The cooling profile of the silicates in this model. Crystallization is assumed to occur between 1400 and 1900 K.

compressed as the gas warmed immediately before the shock front. The dotted line on the graph represents the total pressure of the system. The gas is further compressed by the shock wave, where the water vapor pressure reaches a value of $\sim 5.8 \times 10^{-4}$ bars, and remains at that value as the system cools. This pressure is over 5 orders of magnitude higher than what would be found in the canonical solar nebula at temperatures above the condensation temperature of water ice.

6.6 Hydration of Silicates

Once the water vapor pressure behind the shock is known, it was used to calculate the stability temperature of serpentine. Using the HSC Chemistry v5.0 software package, produced by Outokumpu Research Oy, thermodynamic equilibrium using a Gibbs energy minimization equilibrium solver. The systems considered were composed of H, He, C, N, O, Mg, Si, S, and Fe. In all cases, the elements were considered to exist in a solar ratio, with H and O being added for proper ice enhancements. The species considered in these calculations included 127 different gaseous molecules as well as Fe metal, forsterite, fayalite, enstatite, ferrosilite, troilite, chrysotile, greenalite, wustite, magnetite, hematite, brucite, Fe(II) hydroxide, Fe(III) hydroxide, graphite, SiC, cohenite, siderite, magnesite, sinoite, and water ice. Thermodynamic data for cronstedtite, which is the most abundant Fe-bearing phase in phyllosilicate-rich accretionary rims, was not available. Thus, greenalite, whose thermodynamic data is available (Rasmussen *et al.*, 1998), was used to represent the Fe-bearing phyllosilicate material.

Under the conditions predicted above, the only solids stable above a temperature of 460 K are forsterite, fayalite, and enstatite. Troilite becomes stable at 460 K, followed by greenalite at 380 K and chrysotile at 350 K. Water ice condenses at 240 K. Note that Fe-metal is not stable under any of the conditions studied here. However, it is likely that many, if not all, metal grains in primitive meteorites originated in chondrule melts, which are decoupled from the surrounding gas phases
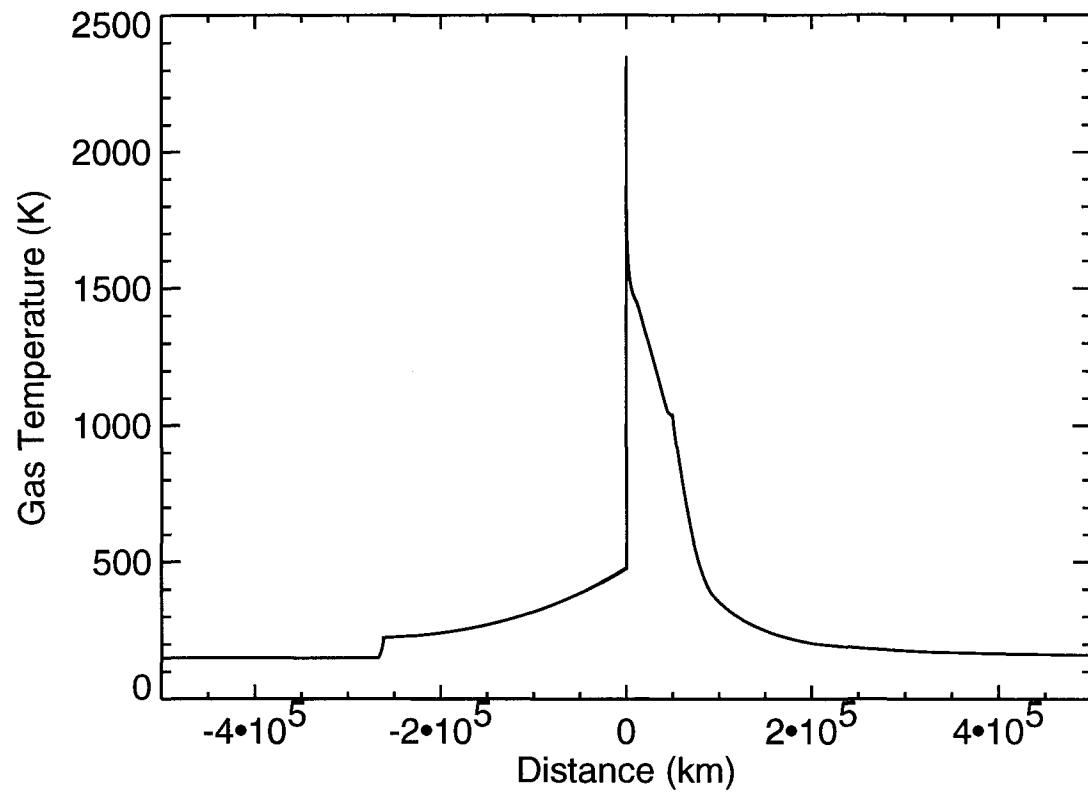
Figure 6.4: The temperature profile of the gas in the model presented. The system relaxes back down to its original temperature after traveling approximately 300,000 km beyond the shock front.
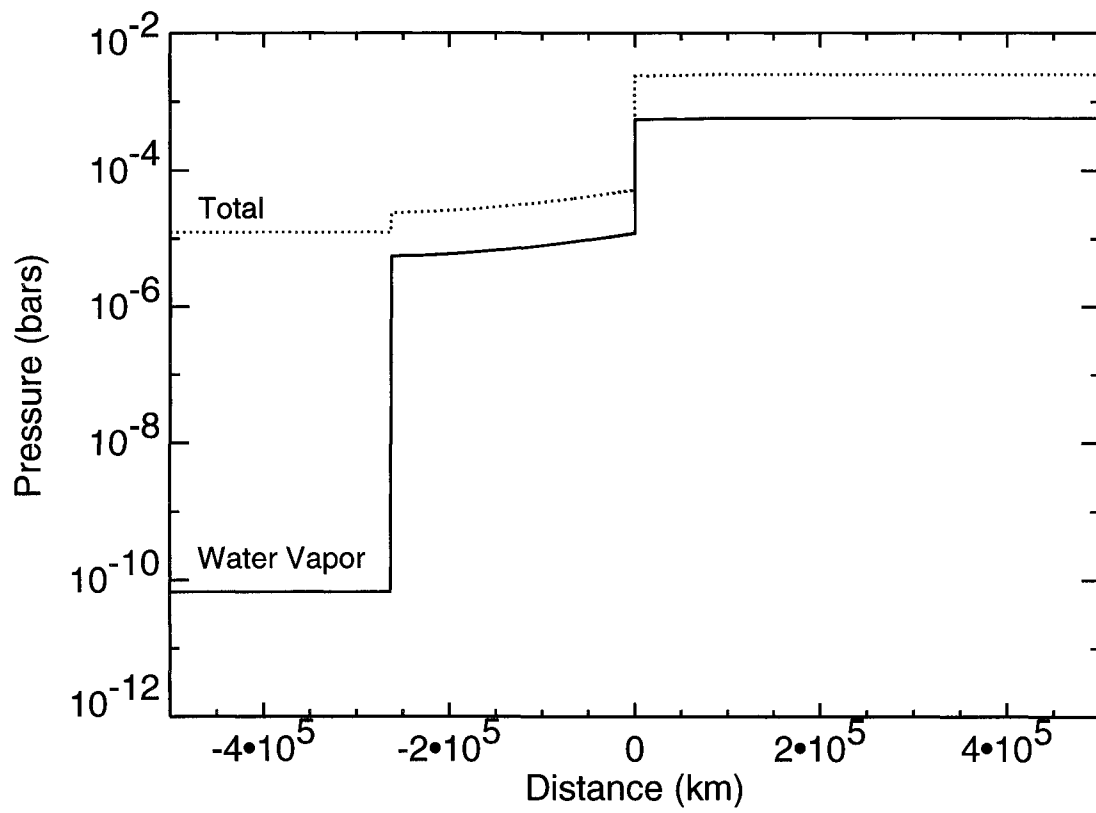
Figure 6.5: The water vapor and total gas pressure profiles in the shock. The maximum value of the water vapor pressure is 5.8×10^{-4} bars.

(Connolly *et al.*, 1994a; Lauretta *et al.*, 2001). If metal grains migrated to the exteriors of the chondrule melts, they would quickly react with the gas and begin to oxidize, such that a 100 μm Fe grain would become magnetite in less than 5 hours. This explains the absence of metal grains in the exteriors of chondrules in CM chondrites. Tochilinite was not included as a solid species because thermodynamic data for this phase are not available, but it would probably form in place of troilite due to the high water vapor pressure.

As discussed by (Fegley and Prinn, 1989), the increase in the partial pressure of water has two major effects on the formation of phyllosilicates. The rate of phyllosilicate formation increases because it is proportional to the water vapor pressure, which determines the collision rate of water molecules with the surfaces of the grains. In addition, the temperature at which phyllosilicates become stable increases. These two factors result in a significant increase in the rate of phyllosilicate formation, which is shown in Figure 6.6.

At 380 K, using an activation energy of 70 kJ/mole, the time scale for a 10 nm grain of fayalite (Fe_2SiO_4) to hydrate to greenalite is 15 hours, or ~0.6 days. At 350 K, the time scale for a 10 nm grain of forsterite to hydrate to chrysotile is 3.8 days. These hydration reactions will proceed as long as there is water vapor to impact the surface of the olivine grains. Thus, once water ice begins to condense, phyllosilicate formation ceases. The cooling history of the gas is shown in Figure 6.7. The time interval between phyllosilicate formation and ice condensation is 12 days, which is long enough to form 10 nm grains of chrysotile and 100 nm grains of greenalite, the same sized grains observed in chondrule rims in CM chondrites. Thus this model produces conditions that would allow for both the types and sizes of minerals found in these FGRs to be formed.
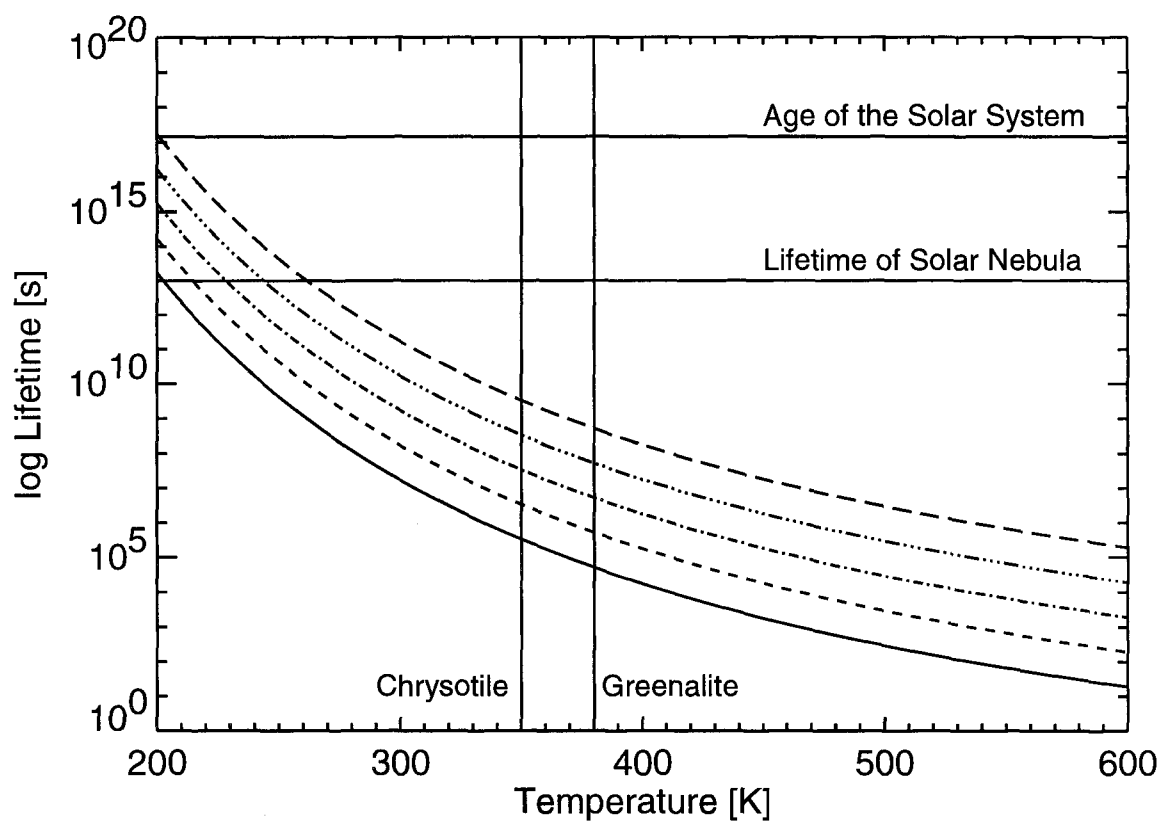
Figure 6.6: Same as that shown in Figure 6.1, using the maximum water vapor pressure found behind the shock in the above model. In this case the stability temperatures of both the Fe and Mg bearing phyllosilicate minerals are considered.
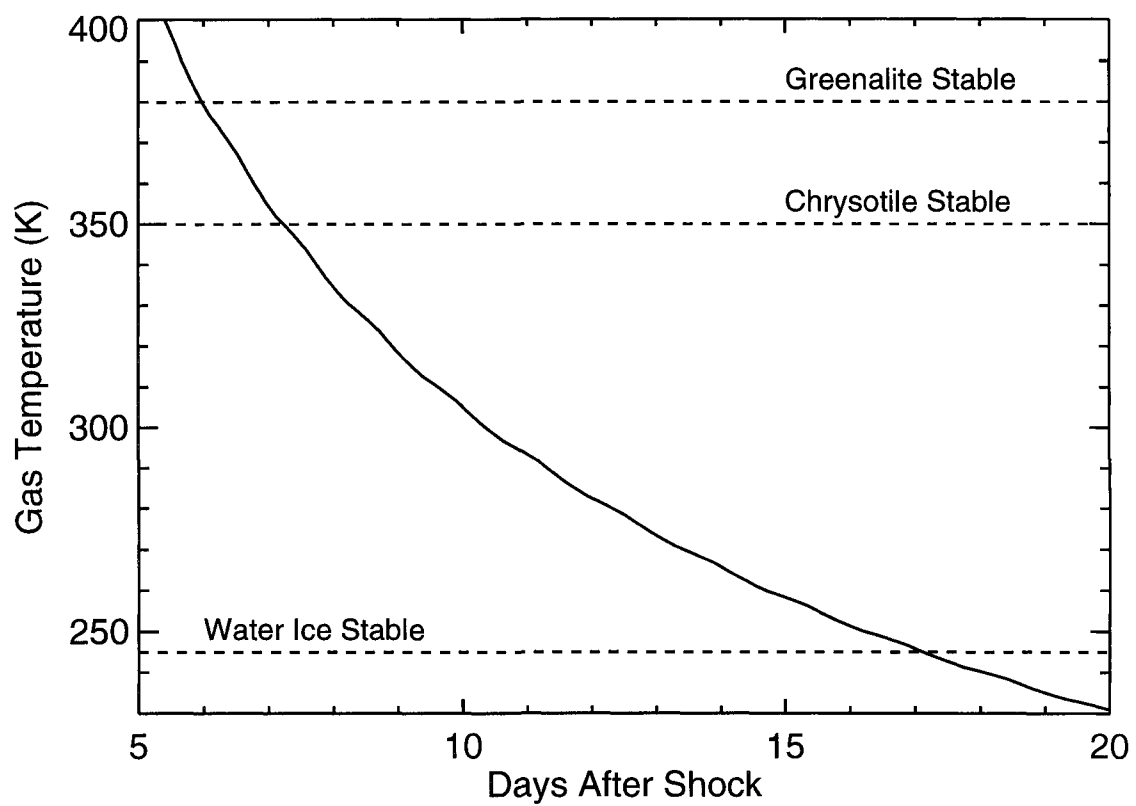
Figure 6.7: The cooling profile of the gas in the shock wave considered. There is a period of approximately 12 days between when the water vapor can begin to react with the grains to form phyllosilicates and ice condensation begins.

6.7 Discussion

This work has shown that shock waves in icy regions of the nebula could have produced conditions which allowed for rapid hydration of silicates, which had previously been thought to be impossible. In addition, the conditions predicted by this model allows the size distribution of grains observed in CM chondrites to be produced (Lauretta *et al.*, 2000; Chizmadia and Brearley, 2003).

In order for this to occur, however, the shock wave must encounter a region of the nebula where ice was enhanced over the canonical solar value. Such a scenario is possible due to the diffusive redistribution of water vapor to the snow line (Cyr *et al.*, 1998), gravitational settling of particles to the nebular midplane (Weidenschilling, 1988, 1997), or turbulent concentration (Cuzzi *et al.*, 2001). In fact, a combination of these mechanisms may lead to even further enhancements than had previously been calculated. It should also be pointed out that such enhancements are not needed on a large scale for the nebula, but rather only locally. Such enhancements likely occurred during the planetesimal building stage of the nebula.

In addition, it should be pointed out that this study was performed as a "worst case scenario." The activation energy assumed, 70 kJ/mol, may be higher than the actual activation energy (Wegner and Ernst, 1983). Chizmadia and Brearley (2003) reported that the phyllosilicates observed in the chondrule rims in the Y-791198 CM2 carbonaceous chondrite are amorphous. Amorphous material would have a much lower activation energy than the crystalline material assumed in the model presented here (Joseph Nuth, personal communication). In addition, if the small grains are due to condensation of material behind the shock, they would have large surface area to volume ratios. This would hasten the reaction because the larger the surface area to volume ratio, the faster the reaction proceeds, and much of the hydration would occur as a surface reaction, requiring a much lower activation energy due to the open lattice sites on the edge of the grain Rietmeijer (1999).

Thus, the results of this work are likely valid in regions of the nebula with lower concentrations of ice.

The results of this work do not only explain the observed mineralogy of the CM chondrites by offering a method by which phyllosilicates can be formed in the nebula, but also shows how the problems with further aqueous alteration on the CM parent body can be reconciled. Models of aqueous alteration on the CM parent body have shown that the formation of phyllosilicates will cause the internal temperature of the body to rise above 400 K, over temperatures over 100 K higher than it is thought the CM chondrites had experienced (Cohen and Coker, 2000). If a significant amount of hydration took place in the nebula, as predicted in this model, then less heat will be produced inside the parent body. The predicted differences between models of the CM parent body and mineralogies of the CM meteorites can thus be reconciled. A sustained lower temperature on aqueously altered parent bodies allows for the survival, and possible delivery to earth, of organic materials.

In addition to showing how water can be incorporated into solid bodies and delivered to the terrestrial planets, this work also has implications for the distribution of water vapor in the solar nebula. The dehydration of the phyllosilicates considered here requires a significantly higher activation energy to occur, on the order of 400-700 kJ/mol (Wegner and Ernst, 1983; Rietmeijer, 1999). Thus, once these solids have formed, they could migrate very close to the sun before becoming completely dehydrated. Thus these minerals could transport water vapor further inward than ice as studied by Cyr *et al.* (1998).

The results of this work are not limited to chondrule formation in regions of the nebula where water ice was drastically enhanced. The level of hydration observed in FGRs may be a result of chondrule and rim formation in regions of the nebula with different ice enhancements. Pre-accretionary hydration of grains in FGRs likely took place for chondrules found in CM, CR, and possibly CI chondrites, whereas those around chondrules in other carbonaceous chondrite groups are largely anhydrous (Bischoff, 1998). Those chondrules with anhydrous rims may simply be

the result of shock waves operating in regions of the nebula that were depleted (or at least not enhanced) in water vapor or ice. As discussed above, the distribution of water ice throughout the solar nebula varied with heliocentric distance and with time producing environments with varying rock/water ratios. The existence of aqueously altered meteorites implies that the formation of chondrules and eventually meteorite parent bodies may have extended out to where Jupiter is currently located.

6.8   Summary

While shock waves have been considered to be likely chondrule forming mechanisms, what effects they might have on the chemistry of the nebula had not been considered. Here it has been shown that in icy regions of the nebula, shock waves can both form chondrules and create conditions that allow for the rapid hydration of the silicate grains found in chondrule rims. Thus, shock waves may not only have been responsible for the thermal processing of a majority of solids found in primitive meteorites, but they also could have provided the energy and conditions to allow chemical reactions to take place that would have been inhibited in the canonical solar nebula. This study represents the first coupling of a physical model for a nebular process with a chemical kinetic model for the formation of meteoritic material.

CHAPTER 7

Conclusions and Future Work

In this dissertation, the shock wave model for chondrule formation has been further developed and the predicted properties of chondrules from this model have been compared to those actually observed. Nebular shock waves can thermally process chondrules in a manner that is consistent with the experimentally inferred rates, including their rapid heating and allow them to cool at rates between 10 to 1000 K/hour. The predicted cooling histories also would allow the volatiles observed in chondrules to be retained (Yu and Hewins, 1998). In addition to thermal processing, the shock wave model allows the observed properties of compound chondrules to form through the collisions of molten chondrules behind the shock front. Finally, shock waves may also create conditions that allow for the chemical processing of minerals that are observed in chondrule fine-grained rims. The fact that the predictions of the model are consistent with our petrologic and chemical observations of the chondrites offers further support that shock waves were the dominant chondrule forming mechanism which operated in the nebula.

Despite this support, there are still a number of questions that must be answered. In this section, those issues are discussed and examples of future studies that may help clarify these issues are proposed.

7.1 Source of the Shock Waves

In the work presented in this paper, no particular source of the shock waves has been assumed. A number of shock wave generating mechanisms have been proposed,

though, much like chondrule formation mechanisms, none is without fault. One of the goals of this work has been to characterize what shock wave conditions would be necessary to produce chondrules, and from there the different mechanisms could be tested to see if they produced such shocks.

Among the first proposed shock generating mechanisms was the accretion shock, or the shock that would be produced as material accreted onto the solar nebula from the interstellar cloud from which the solar system formed. The material that fell onto the nebula would encounter the nebular gas at supersonic speeds, and the solids suspended in that material would be subjected to shock heating (Ruzmaikina and Ip, 1994). A problem with this shock generating mechanism is that it requires material to be heated as it is accreted onto the solar nebula. This would only happen once, and thus material would not be reprocessed. This reprocessing is necessary in order to explain the relict grains found inside chondrules (Wasson, 1996).

Some authors have argued that the early, massive, stage of the solar nebula would have large shock waves fueled by gravitational instabilities. These instabilities could take the form of massive clumps (Boss, 2000, 2002) or spiral density waves (Wood, 1996) and these dense zones may have grown to become Jupiter. A problem with this mechanism is that these shocks would likely only operate in the early ($<$ 10^6 years) solar nebula. Recent work by Amelin *et al.* (2002) found that chondrules formed 2.5 +/- 1.3 million years after CAIs formed. CAIs are also believed to have formed in the solar nebula, therefore the shock waves which formed chondrules would have to operate in the more quiescent stage of the nebula. This would also pose a problem for the accretion shock discussed above, as the accretion of material onto the solar nebula would likely have slowed considerably at this point. However, if the solar nebula was gravitationally unstable later in its evolution, then these would still be possible sites of chondrule formation.

Another shock wave generating mechanism that has been proposed has been planetesimals which orbit the sun with supersonic velocities (Hood, 1998;

Weidenschilling *et al.*, 1998). Weidenschilling *et al.* (1998) found that planetesimals could get trapped in resonances with Jupiter, which would cause their eccentricities to rise to values around 0.3. At these eccentricities, the planetesimals would move through the nebular gas at velocities ranging from 5 to 10 km/s. Hood (1998) showed that the bow shocks created by planetesimals moving with this speed would be strong enough to melt chondrules. However, as this work has shown, keeping the chondrules suspended in warm gas is needed in order to allow chondrules to cool slowly. In the planetesimal bow shock model, the shock waves would only be as thick as the planetesimal which formed them, roughly tens to hundreds of kilometers (Hood, 1998). Chondrules would move through this thickness of shocked gas in a matter of seconds to minutes, and thus may cool too rapidly. It has been suggested that if the shock waves also created a zone of hot, densely concentrated, dust (micron-sized or smaller particles), then this dust would help to keep the chondrules warm (Hood and Ciesla, 2001). However, the calculations that have been done for this case require the chondrules and dust to initially be at the same temperature everywhere and have no relative velocity with one another, which are not valid assumptions in the shock wave model. Such a state may be reached far behind the shock front, (>100 km), but this would require large planetesimals to create shocks of this size. In addition, these simulations required concentrations of dust about 100 times the canonical solar value in order to allow proper cooling rates of chondrules in a zone $\sim$100 km thick. While large concentrations of millimeter sized particles are possible, smaller particles are difficult to concentrate at such high values (Cuzzi *et al.*, 2001; Weidenschilling, 2002). Thus, planetesimal bow shocks are not likely candidates for forming chondrules.

A final mechanism that may produce shock waves is the interaction of either a growing or fully formed Jupiter with the inner nebula. Such interactions can cause density waves in the inner nebula to form as Jupiter is accreting material (Bryden *et al.*, 1999) or as it is migrating (Rafikov, 2002). The boundaries of these density waves would be shock fronts, and thus possible sites where chondrules would form. Detailed hydrodynamical modeling of such density waves are needed in order to

characterize these shocks.

While many of the proposed shock generating mechanisms seem to have their faults, some of these faults may be due to our incomplete understanding of these mechanisms. Mayer *et al.* (2002) presented similar calculations as those previously done by Boss (2002), but with a very high resolution in their smooth particle hydrodynamic (SPH) code. These new results have increased our understanding on the possibility of giant planet formation by gravitational instabilities. Thus, more detailed modeling of the different shock wave generating mechanisms are needed in order to fully evaluate those mechanisms as being responsible for chondrule formation.

7.2 Further Developments of the Shock Wave Model

While the model presented within this thesis has provided insight into how chondrules may have been formed by shock waves within the solar nebula, a number of simplifying assumptions were made. In order to fully understand how chondrules would be formed by shock waves, these effects must be further investigated.

7.2.1 Chemical Reactions in the Gas

Iida *et al.* (2001) presented a model for the chemical evolution of the nebular gas behind a shock wave. The chemistry of the gaseous species will be important in determining the post-shock gas density and pressure. Also, considering what reactions take place for a variety of possible chondrule forming scenarios (various initial pressures, dust concentration, etc.) may affect the chemistry of the solids within the nebula as well.

7.2.2 Gas Opacity

In this work, the silicates have been assumed to be the dominant source of opacity for the gas. This is the general assumption made for most treatments of the solar nebula (eg. Cassen, 1994). However, in regions of the solar nebula where water vapor is significantly enhanced, the opacity of the gas may become important. Thus, a more detailed model should consider the effects of gas opacity on the heating and cooling of the chondrules.

7.2.3 Size Distribution of Solids

In the work presented in this thesis, the solids suspended in the nebula were generally considered to be of a uniform size. While such a scenario may have existed due to the turbulent concentration selectively working on a particular sized particle (Cuzzi *et al.*, 2001), other models of nebular evolution suggest that multiple sizes of particles would be present during a chondrule forming event. Because different sized particles would have different stopping distances (distances over which they lose their relative velocity with respect to the gas), this could be the reason that chondrules are sorted by size amongst the chondrites (Harold C. Connolly and Love, 1998).

In addition, for very small particles, the emissivities would be much smaller than for the chondrules (Rizk *et al.*, 1991). This would cause the particles to be heated to very high temperatures and vaporize. If a significant amount of vaporization were to take place, then the gas would be enhanced in mass and help maintain slow cooling rates for the particles. The kinetics of vaporization were studied by Miura *et al.* (2002), but they did not consider the case of many particles being processed at a time.

7.3 Experimental Thermal Processing of Chondrules

The thermal histories of chondrules predicted by the shock wave model as discussed in this work include periods of "flash heating" during the melting process and periods of cooling which include both rapid and slow cooling rates. As discussed, these thermal histories match, in general, what has been inferred for actual chondrules. The way by which these histories have been inferred has been by producing synthetic chondrules in the laboratory.

However, the conditions used in the above experiments were not exactly like those predicted here. In the cooling experiments of Yu and Hewins (1998), those who most closely resemble the cooling histories found in the work here, the time that the samples are heated through their melting temperatures are as high as hundreds of seconds to minutes. The heating times found in this work are only a few seconds, much less than considered by experiments. Experiments which heat and cool chondrules as predicted in this work are needed in order to ensure that the proper chondrule textures would be produced.

7.4 Vaporization of Minerals

Many chondrules contain primary S and Na which implies that the high temperatures that chondrules reached were not maintained for long periods of time. In the results presented here, the chondrules reached and maintained temperatures above the canonical condensation temperatures of S and Na for time periods up to a few hours long. Thus it is unclear whether this time period would be too long for S and Na to be retained.

Recent studies have determined the rates at which S and Na would have vaporized in the solar nebula (Tachibana and Tsuchiyama, 1998; Shirai *et al.*, 2000). Modeling the vaporization of these species in a similar way as done with water in Chapter 6 of this work will help evaluate whether the thermal profiles predicted in

the shock wave model would allow for their retention. Because larger concentrations of solids lead to shorter thermal processing times, requiring the retention of S and Na may help to constrain the concentration of solids in the chondrule forming environment.

7.5 Compound Chondrules

As discussed in Chapter 4 of this work, compound chondrules should provide information about the concentration of solids during the chondrule formation event. Thus it is important to know the frequency of compound chondrules and their distribution among textural types. The uncertainties in using thin-sections to study compounds make them less than desirable for such a study. Processes such as X-ray tomography provide a non-destructive method by which these objects can be studied in three-dimensions without the problems that thin-sections create. Development of such methods are needed in order to fully understand what information compound chondrules can provide about the chondrule formation event and environment.

7.6 Summary

The work presented here has provided insight into how chondrules would be formed by nebular shocks. The thermal and collisional evolution of chondrules along with the mineralology of at least some of their rims can be explained by shock waves provided:

1. the shocks move with velocities between ~ 5 and 10 km/s

2. the chondrule precursors are not concentrated in the nebula more than 300 times the canonical solar value

3. the shocks are greater than 1000 km in thickness

4. the shocks operated during the later quiescent stage of the nebula

Such shocks may have been created due to density waves in the inner solar nebula due to the formation or orbital migration of Jupiter.

Linking chondrule formation to the formation of Jupiter may have important astrophysical and astronomical implications. The Space Infrared Telescope Facility (SIRTF) and Next Generation Space Telescope (NGST) will be observing disks around young stars over the next decade. Giant planets seem to be relatively common objects in the galaxy, and thus, it is possible such objects would be forming in the disks that will be observed. If large scale, high energy events such as the shock waves described in this work are a consequence of the formation of such objects, then they may influence the observations that are made. Thus the SIRTF and NGST observations that will be made may add to our understanding of how chondrules formed.

REFERENCES

Adachi, I., Hayashi, C., and Nakazawa, K. (1976). The gas drag effect on the elliptical motion of a solid body in the primordial solar nebula. *Progress of Theoretical Physics*, **56**, 1756–1771.

Amelin, Y., Krot, A. N., Hutcheon, I. D., and Ulyanov, A. A. (2002). Lead Isotopic Ages of Chondrules and Calcium-Aluminum-Rich Inclusions. *Science*, **297**(5587), 1678–1683.

Beckwith, S. V. W., Sargent, A. I., Chini, R. S., and Guesten, R. (1990). A survey for circumstellar disks around young stellar objects. *Astronomical Journal*, **99**, 924–945.

Bischoff, A. (1998). Aqueous alteration of carbonaceous chondrites: evidence for preaccretionary alteration–A review. *Meteoritics and Planetary Science*, **33**, 1113–1122.

Boss, A. P. (1996). A concise guide to chondrule formation models. In *Chondrules and the Protoplanetary Disk* (R. H. Hewins, R. H. Jones, and E. R. D. Scott, editors), pages 257–263.

Boss, A. P. (1998). Evolution of the Solar Nebula. IV. Giant Gaseous Protoplanet Formation. *Astrophysical Journal*, **503**, 923–933.

Boss, A. P. (2000). Possible Rapid Gas Giant Planet Formation in the Solar Nebula and Other Protoplanetary Disks. *Astrophysical Journal*, **536**, L101–L104.

Boss, A. P. (2002). Evolution of the Solar Nebula. V. Disk Instabilities with Varied Thermodynamics. *Astrophysical Journal*, **576**, 462–472.

Boss, A. P. and Vanhala, H. A. T. (2000). Triggering Protostellar Collapse, Injection, and Disk Formation. *Space Science Reviews*, **92**, 13–22.

Browning, L., McSween, H. Y., and Zolensky, M. E. (2000). On the origin of rim textures surrounding anhydrous silicate grains in CM carbonaceous chondrites. *Meteoritics and Planetary Science*, **35**, 1015–1023.

Bryden, G., Chen, X., Lin, D. N. C., Nelson, R. P., and Papaloizou, J. C. B. (1999). Tidally Induced Gap Formation in Protostellar Disks: Gap Clearing and Suppression of Protoplanetary Growth. *Astrophysical Journal*, **514**, 344–367.

Cassen, P. (1994). Utilitarian models of the solar nebula. *Icarus*, **112**, 405–429.

Cassen, P. (2001). Nebular thermal evolution and the properties of primitive planetary materials. *Meteoritics and Planetary Science*, **36**, 671–700.

Chizmadia, L. J. and Brearley, A. J. (2003). Mineralogy and Textural Characteristics of Fine-grained Rims in the Yamato 791198 CM2 Carbonaceous Chondrite: Constraints on the Location of Aqueous Alteration. In *Lunar and Planetary Institute Conference Abstracts*, No. 1419.

Ciesla, F. J. and Hood, L. L. (2002). The Nebular Shock Wave Model for Chondrule Formation: Shock Processing in a Particle-Gas Suspension. *Icarus*, **158**, 281–293.

Clayton, R. N. (1981). Isotopic variations in primitive meteorites. *Royal Society of London Philosophical Transactions Series A*, **303**, 339–349.

Clayton, R. N. and Mayeda, T. K. (1983). Oxygen isotopes in eucrites, shergottites, nakhlites, and chassignites. *Earth and Planetary Science Letters*, **62**, 1–6.

Cohen, B. A. and Coker, R. F. (2000). Modeling of liquid water on CM meteorite parent bodies and implications for amino acid racemization. *Icarus*, **145**, 369–381.

Collison, A. J. and Fix, J. D. (1991). Axisymmetric models of circumstellar dust shells. *Astrophysical Journal*, **368**, 545–557.

Connolly, H. C., Hewins, R. H., Ash, R. D., Zanda, B., Lofgren, G. E., and Bourot-Denise, M. (1994a). Carbon and the formation of reduced chondrules. *Nature*, **371**, 136–139.

Connolly, H. C., Hewins, R. H., Atre, N., and Lofgren, G. E. (1994b). Compound chondrules: an experimental investigation. *Meteoritics*, **29**, 458.

Connolly, H. C., Jones, B. D., and Hewins, R. H. (1998). The flash melting of chondrules: an experimental investigation into the melting history and physical nature of chondrule precursors. *Geochimica Cosmochimica Acta*, **62**, 2725–2735.

Cuzzi, J. N., Hogan, R. C., Paque, J. M., and Dobrovolskis, A. R. (2001). Size-selective Concentration of Chondrules and Other Small Particles in Protoplanetary Nebula Turbulence. *Astrophysical Journal*, **546**, 496–508.

Cyr, K. E., Sears, W. D., and Lunine, J. I. (1998). Distribution and Evolution of Water Ice in the Solar Nebula: Implications for Solar System Body Formation. *Icarus*, **135**, 537–548.

Desch, S. J. and Connolly, H. C. (2002). A model of the thermal processing of particles in solar nebula shocks: Application to the cooling rates of chondrules. *Meteoritics and Planetary Science*, **37**, 183–207.

Desch, S. J. and Cuzzi, J. N. (2000). The Generation of Lightning in the Solar Nebula. *Icarus*, **143**, 87–105.

Drake, M. J. (1979). Geochemical evolution of the eucrite parent body - Possible nature and evolution of asteroid 4 Vesta. In *Asteroids*, pages 765–782.

Eisenhour, D. D. (1996). Determining chondrule size distributions from thin-section measurements. *Meteoritics and Planetary Science*, **31**, 243–248.

Fegley, B. J. and Prinn, R. G. (1989). Solar nebula chemistry - Implications for volatiles in the solar system. In *The Formation and Evolution of Planetary Systems*, pages 171–205.

Gibbard, S. G., Levy, E. H., and Morfill, G. E. (1997). On the Possibility of Lightning in the Protosolar Nebula. *Icarus*, **130**, 517–533.

Gombosi, T. I., Nagy, A. F., and Cravens, T. E. (1986). Dust and neutral gas modeling of the inner atmospheres of comets. *Reviews of Geophysics*, **24**, 667–700.

Gooding, J. L. (1979). *Petrographic properties of chondrules in unequilibrated H-, L-, and LL-group chondritic meteorites*. Ph.D. thesis, University of New Mexico.

Gooding, J. L. and Keil, K. (1981). Relative abundances of chondrule primary textural types in ordinary chondrites and their bearing on conditions of chondrule formation. *Meteoritics*, **16**, 17–43.

Grossman, J. N. (1988). The formation of chondrules. In *Meteorites and the Early Solar System* (J. F. Kerridge and M. S. Matthews editors) , pages 680–696.

Harold C. Connolly, J. and Love, S. G. (1998). The Formation of Chondrules: Petrologic Tests of the Shock Wave Model. *Science*, **280**(5360), 62–67.

Haynes, D. R., Tro, N. J., and George, S. M. (1992). Condesnsation and evaporation of H_2O on ice surfaces. *Journal of Physical Chemistry*, **96**, 8502–8509.

Hewins, R. H. (1997). Chondrules. *Annual Review of Earth and Planetary Sciences*, **25**, 61–83.

Hollenbach, D. J., Yorke, H. W., and Johnstone, D. (2000). Disk Dispersal around Young Stars. *Protostars and Planets IV* (V. Mannings, A. P. Boss, S. S. Russell, editors), 401–428.

Hood, L. L. (1998). Thermal processing of chondrule and CAI precursors in planetesimal bow shocks. *Meteoritics and Planetary Science*, **33**, 97–107.

Hood, L. L. and Ciesla, F. J. (2001). The scale size of chondrule formation regions: Constraints imposed by chondrule cooling rates. *Meteoritics and Planetary Science*, **36**, 1571–1585.

Hood, L. L. and Horanyi, M. (1991). Gas dynamic heating of chondrule precursor grains in the solar nebula. *Icarus*, **93**, 259–269.

Hood, L. L. and Horanyi, M. (1993). The nebular shock wave model for chondrule formation - One-dimensional calculations. *Icarus*, **106**, 179–189.

Hood, L. L. and Kring, D. A. (1996). Models for multiple heating mechanisms. In *Chondrules and the Protoplanetary Disk* (R. H. Hewins, R. H. Jones, and E. R. D. Scott, editors), 265–276.

Horanyi, M., Morfill, G., Goertz, C. K., and Levy, E. H. (1995). Chondrule formation in lightning discharges. *Icarus*, **114**, 174–185.

Igra, O. and Ben-Dor, G. (1980). Parameters affecting the relaxation zone behind normal shock waves in a dusty gas. *Israeal Journal of Technology*, **18**, 159–168.

Iida, A., Nakamoto, T., Susa, H., and Nakagawa, Y. (2001). A Shock Heating Model for Chondrule Formation in a Protoplanetary Disk. *Icarus*, **153**, 430–450.

Jones, R. H. (1990). Petrology and mineralogy of Type II, FeO-rich chondrules in Semarkona (LL3.0) - Origin by closed-system fractional crystallization, with evidence for supercooling. *Geochimica Cosmochimica Acta*, **54**, 1785–1802.

Jones, R. H., Lee, T., Connolly, H. C., Love, S. G., and Shang, H. (2000). Formation of Chondrules and CAIs: Theory VS. Observation. In *Protostars and Planets IV* (R. H. Hewins, R. H. Jones, and E. R. D. Scott, editors), 927–946.

Kitamura, M. and Tsuchiyama, A. (1996). Collision of icy and slightly differentiated bodies as an origin for unequilibrated ordinary chondrites. In *Chondrules and the Protoplanetary Disk* (R. H. Hewins, R. H. Jones, and E. R. D. Scott, editors), 319–326.

Landau, L. D. and Lifshitz, E. M. (1987). *Fluid Mechanics*. Pergamon, New York.

Lauretta, D. S., Hua, X., and Buseck, P. R. (2000). Mineralogy of fine-grained rims in the alh 81002 cm chondrite. *Geochimica Cosmochimica Acta*, **64**, 3263–3273.

Lauretta, D. S., Buseck, P. R., and Zega, T. J. (2001). Opaque minerals in the matrix of the Bishunpur (LL3.1) chondrite: constraints on the chondrule formation environment. *Geochimica Cosmochimica Acta*, **65**, 1337–1353.

Lewis, J. S. (1972). Metal/silicate fractionation in the Solar System. *Earth and Planetary Science Letters*, **15**, 286–290.

Lofgren, G. E. (1996). A dynamic crystallization model for chondrule melts. In *Chondrules and the Protoplanetary Disk* (R. H. Hewins, R. H. Jones, and E. R. D. Scott, editors),187–196.

Lofgren, G. E. and Hanson, B. (1997). Formation of Compound Chondrules by Low-Velocity Collisions. *Meteoritics and Planetary Science*, **32**, 81–82.

Mayer, L., Quinn, T., Wadsley, J., and Stadel, J. (2002). Formation of Giant Planets by Fragmentation of Protoplanetary Disks. *Science*, **298**, 1756–1759.

Metzler, K. and Bischoff, A. B. (1996). Constraints on chondrite agglomeration from fine-grained chondrule rims. In *Chondrules and the Protoplanetary Disk* (R. H. Hewins, R. H. Jones, and E. R. D. Scott, editors), 153–161.

Metzler, K., Bischoff, A., and Stoeffler, D. (1992). Accretionary dust mantles in CM chondrites - Evidence for solar nebula processes. *Geochimica Cosmochimica Acta*, **56**, 2873–2897.

Mihalas, D. (1970). *Stellar Atmospheres*. Freeman, San Francisco.

Miura, H., Nakamoto, T., and Susa, H. (2002). A Shock-Wave Heating Model for Chondrule Formation: Effects of Evaporation and Gas Flows on Silicate Particles. *Icarus*, **160**, 258–270.

Morfill, G. E. (1985). Physics and Chemistry in the Primitive Solar Nebula. In *Birth and the Infancy of Stars* (R. Lucas, A. Omont, R. Stora,editors), 693–710.

Morfill, G. E., Durisen, R. H., and Turner, G. W. (1998). NOTE: an Accretion Rim Constraint on Chondrule Formation Theories. *Icarus*, **134**, 180–184.

Moses, J. I. (1992). Meteoroid ablation in Neptune's atmosphere. *Icarus*, **99**, 368–383.

Ozisik, M. N. (1977). *Basic Heat Transfer*. McGraw Hill, New York.

Podosek, F. A. and Cassen, P. (1994). Theoretical, observational, and isotopic estimates of the lifetime of the solar nebula. *Meteoritics*, **29**, 6–25.

Pollack, J. B., Hubickyj, O., Bodenheimer, P., Lissauer, J. J., Podolak, M., and Greenzweig, Y. (1996). Formation of the Giant Planets by Concurrent Accretion of Solids and Gas. *Icarus*, **124**, 62–85.

Radomsky, P. M. and Hewins, R. H. (1990). Formation conditions of pyroxene-olivine and magnesian olivine chondrules. *Geochimica Cosmochimica Acta*, **54**, 3475–3490.

Rafikov, R. R. (2002). Planet Migration and Gap Formation by Tidally Induced Shocks. *Astrophysical Journal*, **572**, 566–579.

Rasmussen, M. G., Evans, B. W., and Kuehner, S. M. (1998). Low-temperature fayalite, greenalite, and minnesotaite from the Overlook gold deposit, Washington; phase relations in the system $FeO-SiO_2-H_2O$. *Canadian Mineralogist*, **36**, 147–162.

Rietmeijer, F. J. M. (1999). Energy for dust modification in the solar nebula, and in the first-formed protoplanets and thier present-day survivors. In *Lunar and Planetary Institute Conference Abstracts*, 1065.

Rizk, B., Hunten, D. M., and Engel, S. (1991). Effects of size-dependent emissivity on maximum temperatures during micrometeorite entry. *Journal of Geophysical Research*, **96**, 1303–1314.

Rubin, A. E. (2000). Petrologic, geochemical and experimental constraints on models of chondrule formation. *Earth Science Reviews*, **50**, 3–27.

Ruzmaikina, T. V. and Ip, W. H. (1994). Chondrule formation in radiative shock. *Icarus*, **112**, 430–447.

Sanders, I. S. (1996). A chondrule-forming scenario involving molten planetesimals. In *Chondrules and the Protoplanetary Disk* (R. H. Hewins, R. H. Jones, and E. R. D. Scott, editors), 327–334.

Sears, D. W. G. and Akridge, D. G. (1998). Nebular or parent body alteration of chondritic material: Neither or both? *Meteoritics and Planetary Science*, **33**, 1157–1167.

Shirai, T., Tachibana, S., and Tsuchiyama, A. (2000). Evaporation Rates of Na from Na2O-SiO2 Melt at 1 atm. In *Lunar and Planetary Institute Conference Abstracts*, 1610.

Shu, F. H., Shang, H., and Lee, T. (1996). Toward an Astrophysical Theory of Chondrites. *Science*, **271**, 1545–1552.

Shu, F. H., Shang, H., Glassgold, A. E., and Lee, T. (1997). X-rays and Fluctuating X-Winds from Protostars. *Science*, **277**(5331), 1475–1479.

Supulver, K. D. and Lin, D. N. C. (2000). Formation of Icy Planetesimals in a Turbulent Solar Nebula. *Icarus*, **146**, 525–540.

Swindle, T. D., Davis, A. M., Hohenberg, C. M., MacPherson, G. J., and Nyquist, L. E. (1996). Formation times of chondrules and Ca-Al-rich inclusions: constraints from short-lived radionuclides. In *Chondrules and the Protoplanetary Disk* (R. H. Hewins, R. H. Jones, and E. R. D. Scott, editors), 77–86.

Tachibana, S. and Tsuchiyama, A. (1998). Incongruent evaporation of troilite (FeS) in the primordial solar nebula: an experimental study. *Geochimica et Cosmochimica Acta*, **62**, 2005–2022.

Tanaka, K. K., Tanaka, H., Nakazawa, K., and Nakagawa, Y. (1998). Shock Heating Due to Accretion of a Clumpy Cloud onto a Protoplanetary Disk. *Icarus*, **134**, 137–154.

Taylor, G. J., Scott, E. R. D., and Keil, K. (1983). Cosmic setting for chondrule formation. In *Chondrules and Their Origins* (E. A. King editor), 262–278.

Treiman, A. H., Gleason, J. D., and Bogard, D. D. (2000). The SNC meteorites are from Mars. *Planetary and Space Science*, **48**, 1213–1230.

Tsuchiyama, A., Nagahara, H., and Kushiro, I. (1981). Volatilization of sodium from silicate melt spheres and its application to the formation of chondrules. *Geochimica et Cosmochimica Acta*, **45**, 1357–1367.

Vincenti, W. G. and Kruger, C. H. (1965). *Introduction to Physical Gas Dynamics*. Krieger Publishing Company, Malabar, FL.

Wasson, J. T. (1993). Constraints on chondrule origins. *Meteoritics*, **28**, 14–28.

Wasson, J. T. (1996). Chondrule Formation: Energetics and Lenghth Scales. In *Chondrules and the Protoplanetary Disk* (R. H. Hewins, R. H. Jones, and E. R. D. Scott, editors), 45–54.

Wasson, J. T., Krot, A. N., Min, S. L., and Rubin, A. E. (1995). Compound chondrules. *Geochimica Cosmochimica Acta*, **59**, 1847–1869.

Wegner, W. W. and Ernst, W. G. (1983). Experimentally determined hydration and dehydration reaction rates in the system $MgO\text{-}SiO_2\text{-}H_2O$. *American Journal of Science Series*, **A283**, 151–180.

Weidenschilling, S. J. (1977). The distribution of mass in the planetary system and solar nebula. *Astrophysics and Space Science*, **51**, 153–158.

Weidenschilling, S. J. (1988). Formation processes and time scales for meteorite parent bodies. In *Meteorites and the Early Solar System* (J. F. Kerridge, and M. S. Matthews editors), 348–371.

Weidenschilling, S. J. (1997). The Origin of Comets in the Solar Nebula: A Unified Model. *Icarus*, **127**, 290–306.

Weidenschilling, S. J. (2000). Formation of Planetesimals and Accretion of the Terrestrial Planets. *Space Science Reviews*, **92**, 295–310.

Weidenschilling, S. J. (2002). Self-Consistent Models of the Dusty Subdisk in the Solar Nebula: Implications for Meteorites. In *33rd Annual Lunar and Planetary Science Conference*, , 1230.

Weidenschilling, S. J., Marzari, F., and Hood, L. L. (1998). The Origin of Chondrules at Jovian Resonances. *Science*, **279**, 681–684.

Whipple, F. L. (1950). Theory of micro-meteorites. I. In an isothermal atmosphere. *Proceedings of the National Academy of Sciences, USA*, **86**, 687–695.

Wood, J. A. (1985). Meteoritic constraints on processes in the solar nebula. In *Protostars and Planets II* (D. C. Black and M. S. Matthews editors), 687–702.

Wood, J. A. (1996). Processing of chondritic and planetary material in spiral density waves in the nebula. *Meteoritics and Planetary Science*, **31**, 641–645.

Wood, J. A. (2000a). Pressure and Temperature Profiles in the Solar Nebula. *Space Science Reviews*, **92**, 87–93.

Wood, J. A. (2000b). The Beginning: Swift and Violent. *Space Science Reviews*, **92**, 97–112.

Wood, J. A. and Morfill, G. E. (1988). A review of solar nebula models. In *Meteorites and the Early Solar System* (J. F. Kerridge, and M. S. Matthews, editors), 329–347.

Yu, Y. and Hewins, R. H. (1998). Transient heating and chondrite formation - Evidence from sodium loss in flash heating simulation experiments. *Geochimica Cosmochimica Acta*, **62**, 159–172.